CAPE SORELL-1 WELL

CAPE SORELL BASIN, OFFSHORE WESTERN TASMANIA

Reconstruction of thermal, burial and source rock maturation histories using AFTA® and organic maturity results with comments on sediment provenance

GEOTRACK REPORT #806

An exclusive research study carried out by Geotrack International Pty Ltd in conjunction with AGSO - Geoscience Australia

Report prepared by: I. R. Duddy
AFTA determinations by: C.E. O'Brien

Final Report October 2001

Geotrack International Pty Ltd ABN 16 006 821 209
37 Melville Road, Brunswick West, Victoria 3055, Australia Ph +613 9380 1077 facsimile +61 3 9380 1477
email mail@geotrack.com.au

CAPE SORELL-1 WELL

Reconstruction of thermal, burial and source rock maturation histories using AFTA® and organic maturity results with comments on sediment provenance

GEOTRACK REPORT #806

CONTENTS

CONTENTS continued

TABLES

CONTENTS continued

FIGURES

CAPE SORELL-1 WELL

Reconstruction of thermal, burial and source rock maturation histories using AFTA® and organic maturity results with comments on sediment provenance

GEOTRACK REPORT #806

EXECUTIVE SUMMARY

Introduction and Objectives

Apatite Fission Track Analysis (AFTA®) and organic maturity data, including Vitrinite Reflectance (VR) and VRF™ methods have been applied to samples from the **Cape Sorell-1 well,** offshore Western Tasmania, to provide a thermal history framework for understanding the burial and source rock maturation histories at this location. In addition, the AFTA results have important implications for the thermal and structural histories of the sediment provenance areas that provided detritus to the Cape Sorell Basin during the L. Cretaceous and E. Tertiary.

AFTA and VR are used to *identify*, *characterise* and *quantify* any episodes of elevated paleotemperatures which have affected the well section, with particular emphasis on determining the timing of major paleo-thermal episodes, the magnitude of paleotemperatures in each episode, and the way in which paleotemperatures vary with depth. This information is used to infer the origins of the various episodes of heating and cooling, and provides rigorous constraints for modelling of the structural and source rock maturation histories.

Summary Conclusions

AFTA results show that the L. Cretaceous to E. Tertiary section at Cape Sorell-1 is at, or near, maximum paleotemperatures at the present day, based on a present-day geothermal gradient of 27.6°C/km estimated from the corrected BHT data and sea-bed temperature of 17.3°C. On this basis the majority of the measured vitrinite reflectance data from the late Cretaceous section, including the new VR data and that determined by the VRF™ method, underestimate the true maturity levels, presumably due to various degrees of geochemical suppression. The AFTA-constrained thermal history predicts a VR level of ~0.66% in the 3200-3240 m source rock interval and a transformation ration of ~0.3 based on measured AGSO kinetics.

AFTA in the Maastrichtian (73 to 65 Ma) part of the Sherbrook Group show clear evidence for rapid uplift and erosion of the sediment provenance area during the time interval 90 to 65 Ma; that is immediately prior to deposition. There is also evidence from one deeper Sherbrook Group sample for sediment reworked from a Mesozoic volcanogenic sediment, possibly the E. Cretaceous Eumeralla Formation or the L. Triassic sediments known onshore Tasmania.

Geotrack International Pty Ltd ABN 16 006 821 209
37 Melville Road, Brunswick West, Victoria 3055, Australia Ph +613 9380 1077 facsimile +61 3 9380 1477
email mail@geotrack.com.au

Thermal History Reconstruction

1. Kinetic modelling of the AFTA results from seven samples indicate that the Early Tertiary and Late Cretaceous sediment at present depths between 1565 and 3450 m are at, or near, maximum paleotemperatures at the present day. Present temperatures over this depth interval range from ~57 to 109°C based on a present-day geothermal gradient of 27.6°C/km estimated from the corrected BHT data, and sea-bed temperature of 17.3°C.

2. Comparison of the AFTA thermal history constraints with maximum paleotemperatures derived from the new VR data from Keiraville Konsultants and existing VR and VRF™ data, indicates that the majority of the organic maturity data in the Late Cretaceous section, including the VRF results, underestimate the true maturity of the section revealed by AFTA. Paleotemperature estimates from AFTA and new VR data from Keiraville Konsultants are summarised in Table i, together with equivalent vitrinite reflectance (VRE) levels derived from the AFTA results in each sample. Paleotemperatures estimated from existing maturity data from various sources supplied by AGSO are summarised in Table ii.

3. There is evidence from AFTA age data in one sample, GC806-2, for a minor downwards revision of present temperature from ~96°C based on the present-day geothermal gradient of 27.6°C/km, to ~93°C, emphasising the sensitivity of AFTA to present temperatures in the range ~90 to 110°C. This lower temperature provides a revised present-day geothermal gradient of 26.7°C/km, but this has no significant influence on the conclusions concerning the organic maturity data.

4. Further kinetic modelling of the AFTA results was undertaken *assuming* that the VRF levels and the new measured VR results in the Late Cretaceous source rock section indicate the true maximum temperatures to which the drilled section was subjected. In this case, these organic maturity data would require a present-day geothermal gradient of only ~22°C/km for a sea-bed temperature of 17.3°C, but the AFTA data would now *require* post-depositional heating at maximum paleotemperatures similar to the present-day temperatures estimated from the original gradient of 27.6°C/km. Thus, there is a fundamental mismatch between the AFTA and VRF results which can only be reconciled if the organic reflectance data are affected by various degrees of geochemical suppression. VRE levels derived from the AFTA results in each sample from this alternative thermal history at listed in Table iii.

5. There is tentative, but systematic, evidence from the all VR data obtained from the shallow Wangeripp Group (~1200 to 1400 m) for maximum paleotemperatures significantly higher than the present-day temperatures estimated from the corrected gradient of 27.6°C/km. This heating in not reflected in the majority of the VR data from the deeper section of the well, and is therefore tentatively interpreted as resulting from a transient lateral heating episode due to passage of heated fluids localized within the Wangeripp Group. Some

supporting evidence for fluid movement comes from Alan Cook's observation of oil inclusions within quartz overgrowths in sample GC806-5.1 at ~885 m within the Wangeripp Group. No AFTA data are available from the 1200 to 1400 m interval for comparison, as insufficient apatite for analysis was recovered from sample GC806-6.

Maturation History Reconstruction

6. Predicted VR maturity with time based on the AFTA-derived thermal history for the well section is illustrated in Figure ii. Two maturation histories consistent with the AFTA thermal history reconstruction are illustrated: **Reconstruction 1** is based on a constant paleogeothermal gradient of 26.7°C/km, equivalent to the AFTA-revised present-day gradient estimated from the corrected BHT data and constant sea-bed temperature of 17.3°C. **Reconstruction 2** is based on a constant paleo heat-flow of 49mWm^{-2} derived from the corrected BHT data combined with a set of assumed thermal conductivities and lithologies for the drilled section and constant sea-bed temperature of 17.3°C.

7. In both histories shown in Figure ii, the maturity in all units increases progressively to the present-day, with the maximum rate of increase during the Late Paleocene-Eocene corresponding with rapid burial during this time interval. Minor differences in the maturation histories in the Early Paleocene result from compaction effects not considered in the geothermal gradient model, but these have no significant influence on the assessment of the rates of maturation within the general oil window.

8. The AFTA-constrained thermal history predicts a present-day VR level of ~0.66% R_o(max) within the source rock interval, between ~3200 and 3240 m.

9. Prediction of hydrocarbon generation based on kinetics from a kerogen analysis obtained from the source rock interval between ~3200 and 3240 m in well indicates:

   - a transformation ratio of ~0.30 is predicted for the 3200 and 3240 m source rock interval at the present-day.
   - a transformation ration of ~0.15 corresponding to a maturity of ~ 0.6% R_o(max) was reached at ~40 to 35 Ma (Late Eocene).
   - approximately 150 mg/gTOC total hydrocarbons should have been generated between ~40 Ma and the present day.
   - some expulsion should have occurred from this source rock interval.

10. Observations by Alan Cook during the course of the VR analyses suggest the presence of expelled oil, as common oil inclusions within calcite and more rarely within quartz

overgrowth in samples associated with the source rock interval, but also from the Wangeripp Group at ~885 m.

Burial History Reconstruction

11. There is no evidence from the AFTA thermal history reconstruction for any coherent post-depositional cooling episodes that can be attributed to significant episodes of uplift and erosion. On this basis, the entire drilled section at Cape Sorell-1 is considered to be at or near maximum burial at the present-day.

Sediment Provenance Information

12. The AFTA fission track age results from samples of Late Cretaceous age indicate derivation of most apatite, and presumably other detrital components of the sediments, from a provenance terrain rapidly uplift and eroded in during the interval ~90 to 65 Ma, i.e. coeval with the deposition of the Late Cretaceous Sherbrook Group section. Unpublished AFTA results from the Paleozoic Merrideth granite from onshore west-coast Tasmania is consistent with rapid cooling at this time, as are published fission track results from other Paleozoic rocks in the area (Dumitru et al., 1991).

13. The AFTA provenance results require kilometre-scale uplift and erosion of basement rocks adjacent to the Sorell Basin, presumably as a response to transpressional tectonics associated with a strike-slip margin developed between the west coast of Tasmania and Antarctica during the Late Cretaceous and Early Tertiary. Thus, an Antarctic provenance for some of the sediment is also possible.

14. AFTA results from sample GC806-2, including the broad range of Cl-content of the analysed apatites, indicate a contribution from an older source terrain, possibly including Triassic or Early Cretaceous volcanogenic sediments.

15. AFTA results from sample GC806-10 and –3 are dominated by the high present-temperatures at which they reside and provide no effective provenance information.

Recommendations for follow-up studies

16. Application of (U-Th)/He dating of apatite is recommended to complement the AFTA results in Cape Sorell-1. This may be particularly useful in confirming and revealing the timing of possible hot fluid movement suggested by VR results in the Wangeripp Group.

17. The important tectonic implications for the uplift history of the west Tasmania margin from the AFTA results in Cape Sorell-1 could be further investigated by carrying out further studies from onshore outcrops, other offshore wells (Whelk-1, Clam-1 & Prawn-1) and deep-sea dredge samples.

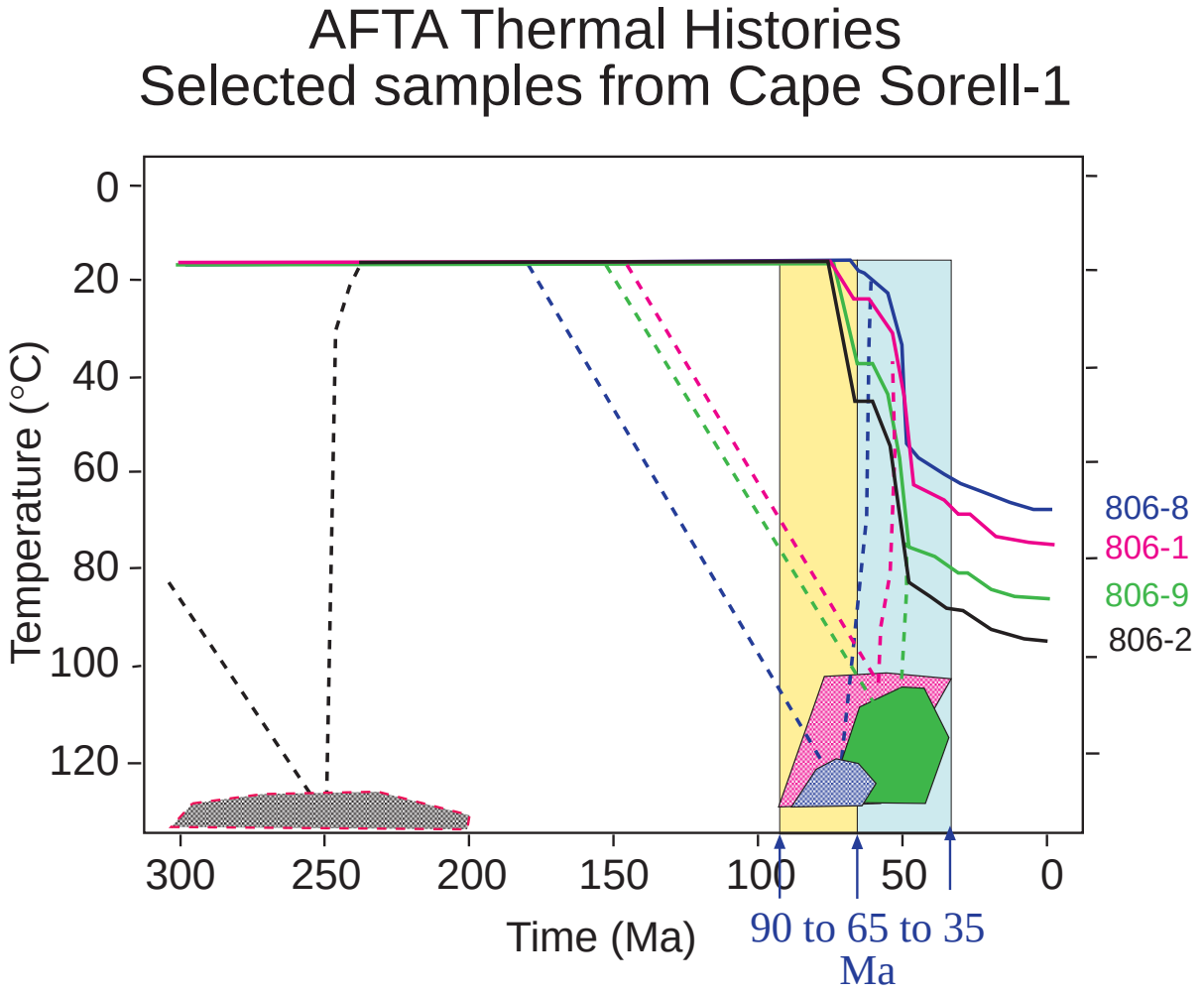

Figure i: Schematic illustration of the thermal histories derived from the AFTA results in individual samples from the **Cape Sorell-1 well, offshore Western Tasmania.** Thermal history constraints from individual AFTA samples are presented in Table i.

While the figure shows that the AFTA constraints in individual samples would allow heating to maximum paleotempertaure significantly higher than present temperatures after deposition, in the period between ~65 and 35 Ma, this is highly inconsistent with the VR results, which suggest maximum paleotemperatures even less than present temperatures. The results from samples 806-1, -8 &-9 can only be reconciled if AFTA records the thermal history of the rapidly cooled sediment source terrain (90 to 65 Ma) and the VR and VRF results show various degrees of geochemical suppression. AFTA results from sample 806-2 show evidence for an additional older provenance terrain, with cooling below 130°C at some tine between 300 and 200 Ma.

The coloured-coded boxes indicate time and temperature constraints obtained from AFTA in each sample and the yellow column, 90 to 65 Ma, indicates the time at which the sediment provenance region cooled derived from the overlap in timing constraints obtained from key samples.

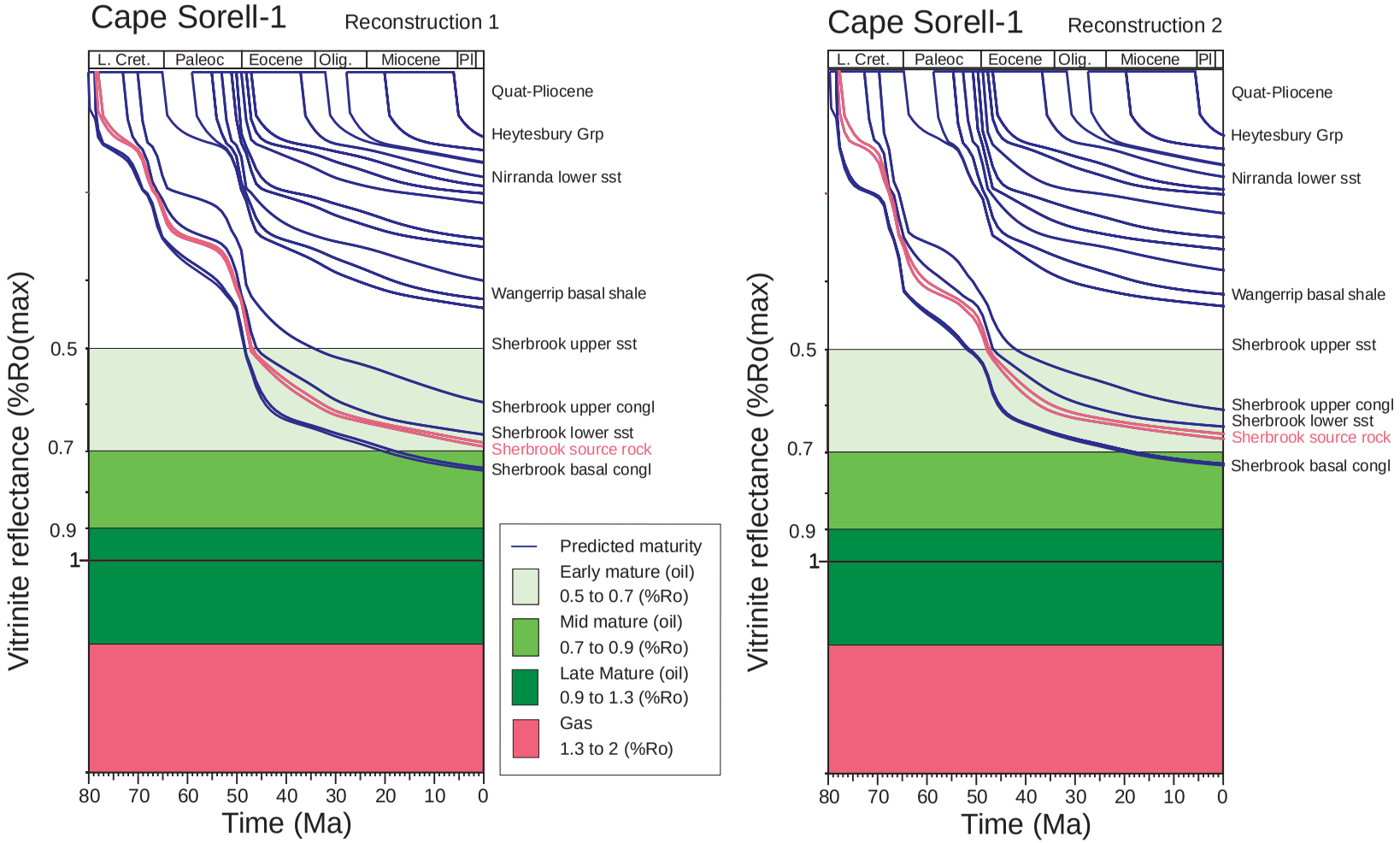

Figure ii: Maturation history reconstruction for the **Cape Sorell-1 well,** based on the thermal history reconstruction derived from the AFTA results (Table i), although it is emphasised that since the AFTA results indicate that maximum paleotemperatures are at the present-day, the results provide no additional constraints on the paleo-heat flow history. **Reconstruction 1** is based on a constant paleogeothermal gradient of 27.6°C/km estimated from the corrected BHT data and constant sea-bed temperature of 17.3°C with time. **Reconstruction 2** is based on a constant heat-flow of 49mWm^{-2} derived from the corrected BHT data combined with a set of assumed thermal conductivities and lithologies for the drilled section and constant sea-bed temperature of 17.3°C with time.

For both histories, vitrinite reflectance in the entire drilled section is predicted to have increased progressively to the present-day, with the source rock interval (~3200-3240 m) reaching a level of ~0.66% R_o(max). The maximum rate of increase in VR occurs in the Late Paleocene-Eocene as a response to a relatively high burial rate producing a high heating rate during this time interval. Minor differences between the two maturation histories in the Early Paleocene result from compaction effects not considered in the geothermal gradient model, but these have no significant influence on the assessment of the rates of maturation within the general oil window.

Table i: Paleotemperature analysis summary from AFTA and new VR results from the Cape Sorell-1 well, offshore western Tasmania (Geotrack Report #806)

				from AFTA and VR			
				Early episode(s)		Late episode	
Sample number	Mean depth	Stratigraphic age	Present temperature*1	Maximum paleotemperature*2	Onset of cooling	Maximum paleotemperature*2	Onset of cooling
(GC-)	(mKB)	(Ma)	(°C)	(°C)	(Ma)	(°C)	(Ma)
806-4.1	489	47-37	28	No VR			
806-5.1	855	50-49	38	60*3			
806-6	1294	53-50	50		No apatite		
806-6	1294	53-50	50	75*3			
806-7	1565	55-51	57	(<105	post-deposition)	(<90	30 to 0)
806-7	1565	55-51	57	58*3			
806-8	1990	70-65	69	(<125	post-deposition)	(<90	30 to 0)
806-8	1990	70-65	69	80*3			
806-1	2252	70-65	76	(<125	post-deposition)	(<100	30 to 0)
806-1	2252	70-65	76	No VR			
806-9	2694	73-65	88	(>105	deposition to 30)	(<105	30 to 0)
806-9	2694	73-65	88	No VR			
806-2	2954	73-70	96 (93)*4	(<100	post-deposition)	(<95	30 to 0)
806-2	2954	73-70	96	No VR			
806-10	3196	78-73	102	(<125	post-deposition)	(<115	30 to 0)
806-10	3196	78-73	102	90*3,*5			
806-10.1	3235	78-73	103	92*3,*5			
806-3	3450	80-78	109	(<125	post-deposition)	(<115	30 to 0)
806-3	3450	80-78	109	100*3,*5			

AFTA summary: The AFTA results are consistent with the entire section being at maximum temperatures at the present-day, although the results *would allow higher paleotemperatures* within in the listed limits. AFTA in the deeper samples (806-2, -10 & -3) also indicate that the "steady-state' present-day temperatures cannot be significantly lower than measured temperatures, indicating that the measured VR levels in associated samples are probably geochemically suppressed. VR in the shallower section (806-5.1 & -6) provide tentative evidence for transient heating, perhaps due to post-Eocene hot fluid flow, possibly associated with hydrocarbons.

N.B. Bracketed & italicised constraints indicate paleo-thermal episodes which are *allowed* by AFTA, but *not required*.

*1 Present temperature estimates for each sample are based on a mean annual sea-bed temperature of 17.3°C and a corrected present-day geothermal gradient of 27.6°C/km as described in Appendix A.

*2 All AFTA and VR paleotemperature estimates are derived assuming a heating rate of 0.2°C/Ma and a cooling rate of 5°C/Ma (see Section 2).

*3 Maximum paleotemperatures estimated from the vitrinite reflectance data using Burnham and Sweeney (1989).

*4 Present temperature revised slightly downwards on the basis of the AFTA age data in this sample – equivalent to a present-day geothermal gradient of 26.7°C/km compared to 27.6°C/km derived from the corrected BHT data.

*5 Maximum paleotemperatures estimated from measured VR is significantly less than present-temperature, which is interpreted on the basis of the AFTA results as due to probable "geochemical" suppression of the true VR levels - see text.

Table ii: Paleotemperature analysis summary from open-file VR and VRF™ data from the Cape Sorell-1 well, Tasmania (Geotrack Report #806)

Sample number (GC-)	Depth (m)	Stratigraphic unit	Stratigraphic age (Ma)	Present temperature (°C)	Measured VR*1 (%)	Analyst code*2 (FL)	Maximum Paleotemperature*3 (°C)
806-OF.1	1225	Wangerrip G	51-50	48	0.40	3	65
806-OF.2	1269	Wangerrip G	51-50	49	0.48	2	80
806-OF.3	1335	Wangerrip G	53-51	51	0.55	2	91
806-OF.4	1923	Sherbrook G	70-65	67	0.44	3	73
806-OF.5	2167	Sherbrook G	70-65	74	0.45	3	75
806-OF.6	2399	Sherbrook G	70-65	80	0.42	3	68
806-OF.7	2728	Sherbrook G	70-65	89	0.47	3	78
806-OF.8	3093	Sherbrook G	73-70	99	0.60	4	100
806-OF.9	3167	Sherbrook G	78-73	102	0.45	2	75
806-OF.10	3173	Sherbrook G	78-73	102	0.54	3	90
806-OF.11	3181	Sherbrook G	78-73	102	0.46	1	77
806-OF.12	3201	Sherbrook G	78-73	102	0.90	0	127
806-OF.13	3231	Sherbrook G	78-73	103	0.45	2	75
806-OF.14	3233	Sherbrook G	78-73	103	0.47	1	78
806-OF.15	3237	Sherbrook G	78-73	103	0.57	3	94
806-OF.16	3283	Sherbrook G	78-73	105	0.54	1	90
806-OF.17	3399	Sherbrook G	79-78	108	0.61	3	100
806-OF.18	3427	Sherbrook G	79-78	109	1.00	0	134
806-OF.19	3450	Sherbrook G	79-78	109	0.56	3	92
806-OF.20	3522	Sherbrook G	79-78	111	0.66	3	104

*1 VR data supplied by AGSO.

*2 AGSO Analyst source code:
FL0 = Amoco (1982)
FL1 = Armstrong et al. (1983)
FL2 = Ross (1982).
FL3 = Newman & Moore (2001) VRF™ data.
FL4 = Boreham et al. (2000).

*3 Maximum paleotemperatures estimated from the vitrinite reflectance data using Burnham and Sweeney (1989). All VR paleotemperature estimates are derived assuming a heating rate of 0.2°C/Ma and a cooling rate of 5°C/Ma (see Section 2).

Table iii: Equivalent VR levels (VRE) determined from the AFTA-derived maximum paleotemperature estimates from the Cape Sorell-1 well, offshore western Tasmania. (Geotrack Report #806)

Sample number	Depth average (range)	Stratigraphic age	Present temperature*1	Maximum paleotemperature*2 (± 95% confidence)	VRE*3 best-fit	VRE*3 ±95% confidence
(GC-)	(mKB)	(Ma)	(°C)	(°C)	(%)	(%)
806-6	1294	53-50	50		No apatite	
806-7	1565 (1500-1631)	55-51	57	72 (60 – 82)	0.43	0.39 – 0.49
806-8	1990 (1929-2051)	70-65	69	81 (75 – 90)	0.49	0.45 – 0.54
806-1	2252 (2198-2307)	70-65	76	90 (80 – 100)	0.54	0.48 – 0.60
806-9	2694 (2637-2752)	73-65	88	111 (90 – 118)	0.64	0.54 – 0.69
806-2	2954 (2899-3008)	73-70	96 (93)*4	101 (93 – 115)	0.62	0.61 – 0.65
806-10	3196 (3142-3249)	78-73	102	108 (102 – 118)	0.64	0.62 – 0.70
806-3	3450 (3399-3501)	80-78	109	104 (102 – 119)	0.66	0.62 – 0.71

*1 Present temperature estimates for each sample are based on a mean annual sea-bed temperature of 17.3°C and a corrected present-day geothermal gradient of 27.6°C/km as described in Appendix A.

*2 Maximum likelihood and ±95 confidence estimates of maximum paleotemperature from AFTA within the last 20 Ma. Derived assuming a heating rate of 0.2°C/Ma and a cooling rate of 5°C/Ma (see Section 2) – see text for further explanation.

*3 Equivalent vitrinite reflectance values determined from the AFTA-derived maximum paleotemperature estimates using Burnham and Sweeney (1989). Best-fit and ±95% confidence estimates for the VRE value determined from maximum likelihood and ±95% confidence estimates of maximum paleotemperature from AFTA – see text for further explanation.

*4 Present temperature revised slightly downwards on the basis of the AFTA age data in this sample – equivalent to a present-day geothermal gradient of 26.7°C/km compared to 27.6°C/km derived from the corrected BHT data.

CAPE SORELL-1 WELL

Reconstruction of thermal, burial and source rock maturation histories using AFTA® and organic maturity results with comments on sediment provenance

GEOTRACK REPORT #806

1. Thermal history reconstruction

1.1 Introduction

This exclusive research report carried out in conjunction with **AGSO – Geoscience Australia** presents the results of a thermal history reconstruction study on the **Cape Sorell-1 well**, **offshore western Tasmania.** The study is based on new AFTA® apatite fission track analysis of 7 samples, new vitrinite reflectance determinations on 7 samples and open-file VR and VRF™ determinations supplied by AGSO.

Stratigraphic details of the AFTA samples are summarised in Table A.1 (Appendix A), with AFTA results summarised in Tables B.1 and B.2 (Appendix B). Details of the new VR results are summarised in Table D.2 (Appendix D), with the open-file VR results summarised in Table D.3 (Appendix D).

1.2 Aims and objectives

The principle aim of this study was to use AFTA to determine the thermal history in the drilled section of the **Cape Sorell-1 well** with the specific objective of evaluating the present temperatures in the section estimated from the corrected BHT data. The implications of the constrained thermal history for the burial, structural and source rock maturation histories at this location are the discussed. During the course of the study, a specific kerogen kinetic analysis of a source rock sample from the well was supplied by AGSO, and this was used in conjunction with the AFTA-constrained thermal history to predict some aspects of the hydrocarbon generation history.

More specifically, key steps in this study are:

1) To use AFTA to determine the timing and magnitude of the maximum paleotemperature of key stratigraphic units;

2) To estimate the maximum paleotemperature from each VR value;

3) To integrate the maximum paleotemperatures estimated from AFTA and VR to provide a coherent reconstructed thermal history of the well section;

4) To identify the mechanism controlling heating and cooling in each paleo-thermal episode and to quantify the paleogeothermal gradient in each episode;

5) To derive a hydrocarbon source rock maturation history from the reconstructed thermal history;

6) To quantify the magnitude of uplift and erosion, if any, associated with each of the identified thermal episodes.

1.3 Data quality

AFTA data

Sufficient apatite suitable for analysis was provided by seven of the eight samples processed from **Cape Sorell-1.** Apatite yields suitable for fission track age determinations varied from excellent (>20 grains – the target for a determination) in two samples, good (15 to 19 grains) in one sample and fair (10 to 14 grains) in four samples, as summarised in Table A.1 (Appendix A). Track length data are of lesser quality, with less than 20 confined track length measurements obtained for all samples compared with the target of 100 measurements. Despite the relatively low numbers of track length measurements, the good quality of the apatite and the well-controlled fission track age data are such that reliable constraints have been placed on the thermal history, the true levels of source rock maturity and the timing of peak maturation in the drilled section.

VR data

Eleven cuttings samples from **Cape Sorell-1** were analysed for vitrinite reflectance by Alan Cook of Keiraville Konsultants, and of these, 7 contained sufficient *in situ* vitrinite for measurement. The quality of the vitrinite reflectance data obtained from the 7 samples is generally excellent, with 5 samples giving >25 measurements (25 being the target for a complete determination), 1 sample giving 14 measurements, and 1 sample giving 3 measurement fields on in-situ vitrinite (Table D.2, Appendix D). The lack of vitrinite in 4 samples and the low yields in another are attributed to the generally sandy lithologies of many of the samples available for analysis which were initially selected for AFTA determinations and not specifically for VR.

The new R_o(max) VR values obtained are considered to be very reliable because of the way in which the VR data are gathered, with primary in-situ vitrinite identified on petrographic grounds within polished sections (see Appendix D), and they are therefore considered to be accurate measurements of the organic reflectance. Despite the high quality of the determinations, there is clear evidence from the AFTA results

that the measured VR levels underestimate the true maturity of the Late Cretaceous source rock section, in particular.

In addition, existing vitrinite reflectance data from 5 data sets (Table D.3, Appendix D), including "corrected" VR measurements determined by the VRF™ method (Newman and Moore, 2001), were provided by AGSO for assessment on the basis of the AFTA-constrained thermal history. The VRF data are very similar to the uncorrected measurements obtained in this study at similar depths, and they are also interpreted to underestimate the true maturity of much of the Late Cretaceous section. On the other hand, a single equivalent VR level determined by Boreham et al. (2000) in the Late Cretaceous section on the basis of sterane-hopane geochemistry, is higher than associated R_o(max) and VRF values, and is much more consistent with AFTA. Other VR data sets are discussed in the text.

1.4 Report structure

The main conclusions of this report are provided in the Executive Summary. A summary of the paleotemperature estimates from individual AFTA and new VR samples based on the corrected present-day geothermal gradient of 27.6°C/km is provided in Table i. Table ii provides maximum paleotemperature estimates derived from the VR and VRF data supplied by AGSO. An alternative thermal history was also investigated assuming a lower present-day geothermal gradient of 22°C/km, with maximum paleotemperature estimates and equivalent VR values (VRE) derived from AFTA based on this analysis are presented in Table iii.

A schematic illustration of key features of the thermal history reconstruction derived from the AFTA results is presented in Figure i. Figure ii illustrates the reconstructed variation of maturity with time derived from the AFTA-constrained thermal history, for two models; a constant geothermal gradient model and a constant paleo-heat flow model.

Section 2 briefly explains the principles of interpretation of AFTA and VR data (with further details provided in Appendices C and D). Section 3 deals with a detailed interpretation of the AFTA and VR results in the Cape Sorell-1 well in terms of the thermal and burial histories, including comprehensive presentation of results in Tables and Figures. Predictions of the source rock maturation and hydrocarbon generation history, based on measured kerogen kinetics for a sample from the well, are discussed and illustrated in Section 4. Section 5 provides a brief discussion of the AFTA results in terms of implications for the thermal and tectonic histories of the provenance terrain of the Late Cretaceous and Early Tertiary sediments in Cape Sorell-1.

Recommendations for additional work that can assist in further elucidating the thermal and structural history of the region and lowering the risk in hydrocarbon exploration are given in Section 6.

Supporting information and data are provided in four Appendices (A, B, C and D). Details of all AFTA samples are presented in Table A.1 (Appendix A), together with the yields and quality of detrital apatite obtained after mineral separation. Sample preparation and analytical procedures for AFTA are described in Appendix B, followed by the presentation of all AFTA data, including raw track counts, fission track ages and the chlorine contents of dated grains. Appendix C outlines the principles employed in interpreting the AFTA data in terms of thermal history. Appendix D discusses the principles involved in integrating AFTA and VR data to provide a rigorous thermal history reconstruction.

2. Interpretation strategy

2.1 Thermal history interpretation of AFTA data

Basic principles

Interpretation of AFTA data in this report begins by assessing whether the fission track age and track length data in each sample could have been produced if the sample has never been hotter than its present temperature at any time since deposition. To this end, we consider a "Default Thermal History" for each sample, which forms the basis of interpretation. Default Thermal Histories throughout a well are derived from the stratigraphy of the preserved sedimentary section, combined with constant values for paleogeothermal gradient and paleo-surface temperature which are adopted from present-day values.

Using this history, AFTA parameters are predicted for each sample. If the measured data show a greater degree of fission track annealing (in terms of either fission track age reduction or track length reduction) than expected on the basis of this history, the sample must have been hotter at some time in the past. In this case, the AFTA data are analysed to provide estimates of the magnitude of the maximum paleotemperature in that sample, and the timing of cooling from the thermal maximum.

Because of the possible presence of tracks inherited from sediment source terrains, it is possible that track length data might show definite evidence that the sample has been hotter in the past (since deposition) while fission track ages are still greater than predicted from the Default Thermal History (which only refers to tracks formed after deposition). Similarly in samples in which all or most fission tracks were totally annealed in a paleo-thermal episode, and which have subsequently been cooled and then reburied, fission track age data might show clear evidence of exposure to higher temperatures in the past while track length data may be dominated by the present-day thermal regime and will not directly reveal the paleo-thermal effects. In circumstances such as these, evidence from either track length or fission track age data alone is sufficient to establish that a sample has been hotter in the past.

As AFTA data provide no information on the *approach* to a thermal maximum, they cannot independently constrain the heating rate and a value must therefore be assumed in order to interpret the data. The resulting paleotemperature estimates are therefore conditional on this assumed value. AFTA data do provide some control on the history after cooling from maximum paleotemperatures, through the lengths of tracks formed during this period.

Wherever possible, data from each sample are normally interpreted in terms of two episodes of heating and cooling, using assumed heating and cooling rates during each episode. The maximum paleotemperature is assumed to have been reached during the earlier episode. The timing of the onset of cooling and the peak paleotemperatures during the two episodes are varied systematically, and by comparing predicted and measured parameters the range of conditions which are compatible with the data can be defined. One additional episode during the cooling history is the limit of resolution from typical AFTA data. Alternatively, if the data can be explained by a single episode of heating and cooling, then a heating rate is assumed and the range of values of maximum paleotemperature and the time of cooling is defined as before.

If AFTA data show a lower degree of fission track annealing (age and/or length reduction) than expected on the basis of the Default Thermal History, this either suggests present temperatures may be overestimated or temperatures have increased very recently. In such cases, the data may allow a more realistic estimate of the present temperature, or an estimate of the time over which temperatures have increased.

AFTA data are predicted using a multi-compositional kinetic model for fission track annealing in apatite developed by Geotrack, described in more detail in Appendix C.

Specific to this report

For all samples analysed for this report, chlorine content has been determined in every apatite grain analysed (i.e., for both fission track age and track length measurement), as explained in more detail in Appendix A. For rigorous thermal history interpretation the age and length data have been grouped into 0.1 wt% Cl divisions (see Table B.3, Appendix B).

In this report, AFTA (and VR data) in all samples were interpreted using a heating rate of 0.2°C/Ma and a cooling rate of 5°C/Ma, rates chosen to reflect the preserved Neogene stratigraphy. All paleotemperature estimates are conditional on the assumed rates. However, it should be borne in mind that for the kinetics characterising both AFTA and VR, each order of magnitude change in heating rate has a systematic effect on the paleotemperature estimate of only ~10°C.

2.2 Thermal history interpretation of VR data

Basic principles

Interpretation of VR data follows similar principles to those used in interpreting the AFTA data (Section 2.1). If a measured VR value is higher than the value predicted from the Default Thermal History (making due allowance for analytical uncertainty),

the sample must have been hotter at some time in the past. In this case, VR data provide an independent estimate of maximum paleotemperature, which can be calculated using an assumed heating and cooling rates and timing information provided from AFTA data, if available (assumed, otherwise). If both AFTA and VR data are available from the same sample or well, then an identical heating rate must be used to obtain consistent paleotemperature estimates.

If a measured VR value is lower than expected on the basis of the Default Thermal History, either present temperatures may have been overestimated or temperatures have increased very recently. In such cases, the measured VR value may allow an estimate of the true present-day temperature. Alternatively the measured VR value may underestimate the true maturity for some other reason, e.g., suppression of reflectance in certain organic macerals, misidentification of true "in-situ" vitrinite, presence of caved material etc. Comparison of AFTA and VR data usually allows such factors to be identified, and where applicable they are discussed in the relevant section of text.

Vitrinite reflectance data (specifically $R_o$max values) are predicted using the distributed activation energy model describing the evolution of VR, with temperature and time developed by Burnham and Sweeney (1989) (see also Sweeney and Burnham, 1990).

Values of VR less than ~0.3% and greater than 5% cannot be assigned to a specific maximum paleotemperature with confidence, and such values are given maximum and minimum limits, respectively, appropriate to the particular heating rate used (see Appendix D). Further discussion of the methodology employed in interpreting VR data are given in Appendix D, which also briefly discusses the benefits of integrating AFTA and VR data.

Specific to this report

For this report, all VR values were interpreted using a heating rate of 0.2°C/Ma and a cooling rate of 5°C/Ma. These rates were used for consistency with the interpretation of the AFTA data, as specified in Section 2.1.

2.3 Comparison of paleotemperature estimates from AFTA and VR

Maximum paleotemperatures derived from AFTA and VR ($R_o$max) using the strategies outlined above are usually highly consistent. Estimates of maximum paleotemperature from AFTA (Tables i & iiii) are often quoted in terms of a range of paleotemperatures, as the data can often be explained by a variety of scenarios. Paleotemperature estimates from VR (Tables i and ii) are usually quoted to the nearest degree Celsius, as the value which predicts the exact measured reflectance. This is not meant to imply VR

data can be used to estimate paleotemperatures to this degree of precision. VR data from individual samples typically show a scatter equivalent to a range of between ±5 and ±10°C. Estimates from a series of samples are normally used to define a paleotemperature profile in samples from a well, or a regional trend in paleotemperatures from outcrop samples.

2.4 Paleogeothermal gradients

Basic principles

A series of paleotemperature estimates from AFTA and/or VR over a range of depths can be used to reconstruct a paleotemperature profile through the preserved section. The slope of this profile defines the paleogeothermal gradient. As explained by Bray et al. (1992), the shape of the paleotemperature profile and the magnitude of the paleogeothermal gradient provide unique insights into the origin and nature of the heating and cooling episodes expressed in the observed paleotemperatures.

Linear paleotemperature profiles with paleogeothermal gradients close to the present-day geothermal gradient provide strong evidence that heating was caused by greater depth of burial with no significant increase in basal heat flow, implying in turn that cooling was due to uplift and erosion. Paleogeothermal gradients significantly higher than the present-day geothermal gradient suggest that heating was due, at least in part, to increased basal heat flow, while a component of deeper burial may also be important as discussed in the next section. Paleogeothermal gradients significantly lower than the present-day geothermal gradient suggest that a simple conductive model is inappropriate, and more complex mechanisms must be sought for the observed heating. One common cause of low paleogeothermal gradients is transport of hot fluids shallow in the section. However, the presence of large thicknesses of sediment with uniform lithology dominated by high thermal conductivities can produce similar paleotemperature profiles and each case has to be considered individually.

A paleotemperature profile can only be characterised by a single value of paleogeothermal gradient when the profile is linear. Departures from linearity may occur where strong contrasts in thermal conductivities occur within the section, or where hot fluid movement or intrusive bodies has produced localised heating effects. In such cases a single value of paleogeothermal gradient cannot be calculated. However, it is important to recognise that the validity of the paleotemperatures determined from AFTA and/or VR are independent of these considerations, and can still be used to control possible thermal history models.

Estimation of paleogeothermal gradients in this report

Paleogeothermal gradients have not been estimated for this report as the section is interpreted to be at maximum temperatures at the present-day with no evidence for significant paleo-thermal episodes.

2.5 Eroded section

Basic principles

Subject to a number of important assumptions, extrapolation of a linear paleotemperature profile to a paleo-surface temperature allows estimation of the amount of eroded section represented by an unconformity, as explained in more detail in Section C.9 (Appendix C).

Specifically, this analysis assumes:

- The paleotemperature profile through the preserved section is linear;
- The paleogeothermal gradient through the preserved section can be extrapolated linearly through the missing section;
- The paleo-surface temperature is known; and,
- The heating rate used to estimate the paleotemperatures defining the paleogeothermal gradient is correct.

It is important to realise that any method of determining the amount of eroded section based on thermal methods is subject to these and/or additional assumptions. For example methods based on heat-flow modelling must assume values of thermal conductivities in the eroded section, which can never be known with confidence. Such models also require some initial assumption of the amount of eroded section to allow for the effect of compaction on thermal conductivity. Methods based on geothermal gradients, as used in this study, are unaffected by this consideration, and can therefore provide independent estimates of the amount of eroded section. But these estimates are always subject to the assumptions set out above, and should be considered with this in mind.

The analysis used to estimate paleogeothermal gradients is easily extended to provide maximum likelihood values of eroded section, for an assumed paleo-surface temperature, together with ±95% confidence limits. These parameters are quoted for the specific paleo-thermal episodes in which the paleotemperature profiles suggest that past heating may have been due, at least in part, to deeper burial. However, it is emphasised that such interpretations are not unique, and alternative interpretations are

always possible. For instance, where the eroded section was dominated by units with high thermal conductivities the paleogeothermal gradient through the missing section may have been much higher than in the preserved section, and extrapolation of a linear gradient will lead to overestimation of the eroded section.

The analysis used to estimate paleogeothermal gradients is easily extended to provide maximum likelihood values of eroded section for an assumed paleo-surface temperature, together with ±95% confidence limits.

However, it is emphasised that such interpretations are not unique and alternative interpretations are always possible. For instance, the paleogeothermal gradient through the missing section may have been much higher than in the preserved section where the eroded section was dominated by units with high thermal conductivities, and extrapolation of a linear gradient will lead to overestimation of the eroded section.

Estimation of eroded section in this report

As estimation of paleogeothermal gradients is not appropriate (or possible) in this report because the section is currently at maximum temperatures the methods described above for estimating the magnitude of removed section also cannot be applied.

3. Thermal history interpretation for the Cape Sorell-1 well

3.1 Sample details and geological background

Eight cuttings samples from the Early Tertiary and Late Cretaceous section intersected in the Cape Sorell-1 well were analysed by AFTA (Table A.1), with eleven associated samples submitted to Alan Cook of Keiraville Konsultants for VR analysis (Table D.2, Appendix D). Apatite yields varied from Excellent to none (Table A.1) and sufficient high quality AFTA data were obtained from seven of the eight samples enabling a very reliable assessment of the thermal history to be made.

Stratigraphic information for the **Cape Sorell-1 well** provided by AGSO – Geoscience Australia is listed in Table A.2 (Appendix A). Unless stated otherwise all depths referred to in this report are with respect to KB. The well was drilled in 94 m of water and intersected a more or less continuous section of Late Cretaceous to Recent sediments referred to the Heytesbury, Nirranda, Wangeripp and Sherbrook Groups with TD at 3523 m in sediments of Campanian age. Minor unconformities are identified between the Heytesbury and Nirranda Groups and the Wangeripp and Sherbrook Groups, as detailed in Table A.2.

A well-defined linear present-day geothermal gradient of 27.6°C/km was estimated from the corrected BHT values and present-day sea-bed temperature of 17.3°C supplied by AGSO (Table A.3, Appendix A).

3.2 Thermal history interpretation of Cape Sorell-1 AFTA data

Introduction

Fission track age and mean track length data in the seven cuttings samples analysed from this well are summarised in Table 3.1. The data are plotted as a function of depth and present temperature (derived from the present-day geothermal gradient of 26.7°C/km and a sea-bed temperature of 17.3°C, Table A.3, Appendix A) in Figure 3.1, where the fission track age data are contrasted with the variation of stratigraphic age through the section. The samples encompass a present depth between ~1500 and 3500 m over a present-day temperature range from ~57 to 109°C. Predicted AFTA parameters based on the Default Thermal histories for each sample are also plotted in Figure 3.1.

Interpretation of the AFTA data in terms of evidence that the samples may have been hotter in the past is summarised in Table 3.2. Following the strategy outlined in Section 2.1, estimates of the magnitude and timing of maximum paleotemperatures derived from the AFTA data in each sample are summarised in Table 3.3.

Evidence for elevated paleotemperatures from AFTA

Measured AFTA age data plotted in Figure 3.1 are consistent with, or older than, the ages predicted from the Default Thermal Histories (see Section 2.1) for the range of apatite Cl-compositions present in each sample, and therefore provide no evidence that the samples have been subjected to paleotemperatures higher than present-temperatures after deposition. Thus, as explained in Table 3.2, the AFTA data in all seven apatite-bearing samples from the Wangeripp and Sherbrook Groups, can be explained by a combination of inheritance of tracks from the source terrain(s) and the effects of the Default Thermal Histories, and do not *require* any additional post-depositional heating. More detailed kinetic modelling of the AFTA parameters in each sample enables more defined limits to be placed on the *allowed* magnitudes of post-depositional heating as explained below.

Timing and magnitude of maximum paleotemperatures from AFTA

Estimates of the *allowed* magnitude and timing of maximum paleotemperatures have been obtained by modelling the AFTA parameters for each sample through likely thermal history scenarios to determine the range of conditions giving predictions that are consistent with the measured data. The approach is described in more detail in Appendix C.

Thermal history solutions for each sample and further detailed comments are provided in Table 3.3. In all samples, the measured AFTA data would allow maximum paleotemperatures higher than the present temperatures after deposition within various limits. For example, results from sample GC806-7 (Wangeripp Group, present temperature 57°C), constrain paleotemperatures to less than 105°C at any time after deposition, and to less than 90°C at any time in the last 30 Ma (the 30 Ma limit was chosen arbitrarily to illustrate the general nature of the constraint). Similar limits are obtained from kinetic modelling of AFTA in the majority of the samples, although those from sample GC806-2 (2899 – 3008 m) are particularly instructive, as they place very tight limits on the present-day thermal conditions and the post-depositional thermal history. Modelling of the AFTA results in this sample require subtle downwards refinement of the present temperature from 96°C derived from the corrected present-day geothermal gradient of 27.6°C/km to 93°C in order to match the AFTA age data for the 0 to 0.1% Cl group, compositions which are particularly sensitive in this temperature range, as it is near the point of total fission track annealing. Furthermore, these data indicate that paleotemperatures must have been less than 100°C at any time since Maastrichtian deposition (@~73 to 70 Ma), and further constrain maximum paleotemperatures at 30 Ma to <98°C, declining to a maximum allowed paleotemperature of 93°C at the present-day. A present-day paleotemperature

of 93ºC at 2954 m (average depth of sample GC80-6-2) is equivalent to a linear geothermal gradient of 26.7°C/km for a sea-bed temperature of 17.3°C/km.

It should be noted that the AFTA results cannot provide an absolute minimum estimate of the present-day temperature in any sample, so a present-day geothermal gradient less than 26.7°C/km is possible. Indeed, a lower "steady state" present-day geothermal gradient is suggested by the majority of the vitrinite results from the Late Cretaceous section of the well (Section 3.3), and the influence of such a lower gradient of the AFTA results is investigated in more detail in Section 3.5.

Integration of the AFTA timing constraints obtained from individual samples indicates that the most likely situation is that the sampled section between ~1500 and 3500 m is at maximum post-depositional temperatures at the present-day due to burial under the influence of a present-day gradient of 26.7°C/km and a sea-bed temperature of 17.3°C.

Thermal history constraints derived from AFTA data in individual samples from **Cape Sorell-1 well** are summarised in Table i (Executive Summary).

3.3 Thermal history interpretation of Cape Sorell-1 VR data

Introduction

Mean R_o(max) vitrinite reflectance values from new analyses by Keiraville Konsultants are summarised in Table D.2 (Appendix D). Existing VR data (FL0 data set from Amoco, 1982; FL1 data set from Armstrong et al., 1983; FL2 data set from Ross, 1982), VRF™ (FL3 data set from Newman and Moore, 2001) and an equivalent VR value (VRE) from sterane-hopane geochemistry (FL4 data set Boreham et al., 2000) supplied by AGSO for the study are summarised in Table D.3 (Appendix D).

Evidence that samples have been hotter in the past from the VR data

New mean VR values ($R_o$max) range from ~0.36% to 0.60% over the depth range from ~850 to 3500 m encompassing the Wangeripp and Sherbrook Groups. These new data together with all existing VR, VRF and VRE values are plotted against depth (with respect to KB) in Figure 3.2 together with the VR profile calculated on the basis of the Default Thermal History (explained in Section 2.1), which is derived from the preserved stratigraphy in the **Cape Sorell-1 well** (Figure 3.3), a present-day geothermal gradient of 26.7°C/km (AFTA-revised) and a present-day sea-bed temperature of 17.3°C.

Inspection of the organic maturity data plotted in Figure 3.2 suggests a fairly complex pattern with increasing depth. VR data (for all data sets) in the upper Wangeripp Group plot above the Default History profile suggesting this section has experienced maximum paleotemperatures significantly higher than present temperatures at some time after deposition. On the other hand, VR data (new Ro(max) and FL3 data) from the basal Wangeripp Group and top of the Sherbrook Group plot close to the Default History profile suggesting that this part of the well is at maximum paleotemperatures at the present-day. The VRE level of 0.60% from 3093 m (FL4 dataset) derived from Sterane-Hopane geochemistry (Boreham et al., 2000) is quite consistent with the Default Thermal History, suggesting maximum paleotemperatures at the present-day.

Most VR data, including the new Ro(max) data and the VRF data (FL3 data set) in the Sherbrook Group section deeper than ~2300 m, including the source rock section around 3200 m, plot significantly below the Default History profile. Further, the FL1 (Armstrong et al., 1983) and FL2 (Ross, 1982) VR data from around 3200 m plot even further below the Default History profile. At *face value*, all VR measurements that plot below Default History profile suggest either, that the temperatures in this part of section have increased to their measured values only very recently (i.e. they are transiently high) or that the measured VR data are too low, and underestimate the true maturity. This anomaly is investigated further in Sections 3.4 and 3.5 in conjunction with the thermal history constraints provided by AFTA.

Finally, the two values near TD comprising the FL0 VR data set (Amoco, 1982) plot significantly above the Default History profile and are higher than all other data in the deeper section. These values are also inconsistent with AFTA for any allowed thermal history (see Sections 3.4 and 3.5) and they are therefore considered to be incorrectly determined.

Magnitude of maximum paleotemperatures from VR

Maximum paleotemperatures derived from the new R_o(max) VR data collected for the study (Table D.2, Appendix D) using the strategy outlined in Section 2.2, are summarised in Table i (Executive Summary) with maximum paleotemperatures derived from the existing VR, VRF and VRE data (Table D.3, Appendix D) summarised in Table ii (Executive Summary).

The VR-derived maximum paleotemperature estimates from the new R_o(max) data range from ~60°C in the Wangeripp Group at ~855 m to ~100°C in the Sherbrook group near TD (Table i). Maximum paleotemperatures derived from the FL 3 data set show a very similar range to the new data, whereas those derived from the FL 0 data set are much higher than all other data and those from the FL 1 and FL 2 data sets tend

to much lower than the other data sets at similar depths in the section near TD (Table ii). These trends in maximum paleotempertaure mirror the trends in the VR-depth plot described above, and are discussed further in the context of the AFTA thermal history constraints in Sections 3.4 and 3.5.

3.4 Thermal History Synthesis – integration of AFTA and VR results

Maximum paleotemperatures derived from the AFTA and the new R_o(max) VR data in this well are summarised in Table i (Executive Summary) while maximum paleotemperatures derived from the existing VR data sets are summarised in Table ii (Executive Summary). Paleotemperature constraints from AFTA and all VR results are plotted against depth in Figure 3.4, allowing the thermal history implications of all results to be assessed in a common framework.

Inspection of the paleotemperature-depth plot in Figure 3.4 reveals that the VR datasets display similar patterns to those described from the VR-depth plot in Figure 3.2, as would be expected. AFTA in individual samples are consistent with the present temperatures being the maximum since deposition, although allow (*but do not require*), maximum paleotemperatures higher than present temperatures within various limits as described in detail Table 3.3.

Maximum paleotemperatures allowed by AFTA in sample GC806-2 are only slightly higher than present temperatures, and are consistent with the maximum paleotemperature estimated from sterane-hopane geochemistry slightly deeper in the well (Figure 3.4). Both are consistent with the present-day temperature profile and provide strong evidence that this part of the Sherbrook Group is at, or near, maximum paleotemperature at the present-day.

While AFTA results from samples GC806-8 & -1 at the top of Sherbrook Group and from GC806-7 near the base of the Wangeripp Group *allow* maximum paleotemperatures significantly higher than present temperatures, maximum paleotemperatures from associated VR data (new R_o(max) and FL3 datasets) suggest that this part of the section is also at or near maximum paleotemperature at the present-day.

Maximum paleotemperatures estimated from all of the remaining VR results from the new R_o(max) data (GC806-3, -10 & -10.1) and the FL1, FL2 and FL3 data sets from the Sherbrook Group (all deeper than ~2300 m and including the recognised source rock interval at ~3200-3240 m) are systematically lower than present temperatures.

Maximum paleotemperatures lower than present temperatures can be interpreted in a number of ways :–

- the VR levels could be incorrectly measured.
- the VR levels could be measured correctly, but are suppressed
- the VR levels could be measured correctly, but the present temperatures have increased to the present value (26.7°C/km) in the very recent geological past. i.e. the present temperatures are transiently high, and a lower thermal gradient has operated in the past, at least over the last few 10's of millions of years.
- the present temperatures could be incorrectly measured.

Firstly, the corrected present-day temperatures supplied by AGSO are based on a number of measured values and define a well-constrained linear profile with a geologically reasonable geothermal gradient. On this basis, there is no reason to expect that it is incorrect. Furthermore, as explained in Section 3.5, lowering the geothermal gradient does not resolve the conflict between the AFTA and VR results.

The new R_o(max) data are considered to be of very high quality with determinations made on in situ vitrinite identified petrographically in whole rocks and therefore there is no reason to expect that they have not been measured correctly. The VRF values are similar to the new R_o(max) data and this is presumably also determined correctly (although the degree to which the original VR measurements have been corrected upwards by the VRF methodology is unknown to us, so just why the new R_o(max) measured data should agree with the VRF data is unclear). Most data from the FL1 and FL 2 data sets indicate even lower maximum paleotemperatures in the source rock interval, and thus these data probably have been measured incorrectly. (The FL0 data from this interval plot much higher than both the present temperatures and the AFTA-allowed maximum paleotemperatures (Figure 3.4), and these are also considered to have been measured incorrectly).

Thus, for the reliable new R_o(max) and VRF data suppression or a transient rise in present temperatures are the most likely explanations. Results from associated AFTA samples GC806-10 and –3, are again consistent with the present temperatures being the maximum post-depositional temperatures, but would allow higher temperatures, as shown. As discussed in detail in Section 3.5, remodelling of the AFTA results in these samples assuming a transient increase in temperature to the present level as suggested by these VR results, shows that such a model is not viable, and we therefore conclude that the all reliable VR measurements in the Sherbrook Group below ~3200 m are geochemically suppressed.

VR-derived maximum paleotemperature estimates from various data sets in the Wangeripp Group between ~ 855 and 1400 m are consistently higher than present

temperatures. No AFTA results are available from this depth interval, but this observation provides at least tentative evidence for an additional heating mechanism unrelated to burial in this part of the Wangeripp Group. Possible mechanisms include transient hot fluid flow within confined Wangeripp Group aquifers, or local intrusion of dykes or sills.

Finally, there is no evidence from AFTA or VR for any significant paleothermal episodes that can be related to either burial and uplift and erosion events, or to periods of elevated basal heat flow, although there is tentative evidence for a transient heating episode that has locally effected the Wangerrip Group around 1200 to 1400 m depth.

3.5 Testing an alternative thermal history model.

Introduction

Integration of the AFTA and VR results described in Section 3.4 strongly suggest that the Late Cretaceous section, including the key source rock interval at ~3200-3240 m, is at maximum temperatures at the present-day. In this scenario, even the reliably measured new R_o(max) VR data and the VRF determinations from the key source rock interval are interpreted to be geochemically suppressed, with no direct evidence from AFTA for a transient increase in present-day gradient. To further investigate whether AFTA would allow a transient increase in present-day gradient, and thus become compatible with the R_o(max) and VRF determinations as measured, we estimated a new present-day geothermal gradient assuming that the maximum paleotemperatures from these VR data (Table ii) indicate the real, "steady-state", present-temperatures. A gradient of 22°C/km for a sea-bed temperature of 17.3°C gives a good fit to these data in the section deeper than ~3200 m. This new present-day gradient in no longer compatible with the higher measured BHT values, unless the BHT values are a geologically recent, transient phenomena.

Thermal history constraints from AFTA assuming transient heating

In this scenario, the AFTA parameters for each sample have been modelled using Default Thermal Histories estimated from a paleogeothermal gradient of 22°C/km throughout most of the history, increasing to the measured present-day gradient of 26.7°C/km over the last 100,000 years. In effect, the transient effects of this recent increase in gradient are not felt by the AFTA data which only has had time to respond to the temperatures caused by the steady state gradient of 22°C/km.

In all samples, the measured AFTA data now require maximum paleotemperatures significantly higher than these lower present temperatures after deposition. This is in stark contrast to the situation based on the measured present-day gradient of 26.7°C/km, where the AFTA did not require, but allowed, higher paleotemperatures within certain limits.

The maximum paleotemperatures (±95% confidence limits) required by AFTA for each sample are listed in Table iii (Executive Summary). In all samples, AFTA is consistent with cooling from these paleotemperatures beginning at some time within the last 20 Ma. These new AFTA-derived maximum paleotemperatures are plotted together with the VR-derived maximum paleotemperatures in Figure 3.5. It is clear from this figure that the AFTA-derived maximum paleotemperatures are significantly higher than indicated by the VR data in the Sherbrook Group deeper than 3200 m. Furthermore, these required maximum paleotemperatures encompass the original present temperature estimated from the measured BHT data.

Thus, this remodelling clearly shows that the measured VR data from the deeper section cannot be reconciled with the AFTA data assuming a recent in temperatures, as AFTA predicts similar equivalent VR levels in each thermal history scenario investigated. AFTA-derived VRE levels are provided in Table 3.3 for the preferred thermal history and in Table iii (Executive Summary) for the "transient" history.

The unequivocal conclusion from this analysis is that the new R_o(max) VR data and the VRF determinations from the key source rock interval significantly underestimate the true maturity of the section, presumably due to geochemical suppression.

3.6 The preferred reconstructed thermal history for Cape Sorell-1

In summary, reconciliation of the maximum paleotemperatures determined from the AFTA and VR results with the present-day temperatures estimated from the corrected BHT data can be achieved if the Late Cretaceous section is at, or very near, maximum post-depositional temperatures at the present-day due to burial represented by the preserved stratigraphy and a constant paleogeothermal gradient similar to the AFTA-revised present-day gradient of 26.7°C/km. VR data in the Sherbrook Group deeper than ~3200 m are suppressed to varying degrees and do not indicate either the true maximum paleotemperatures experienced by the section, or the true maturity of the section. There is tentative evidence from VR data for a transient heating episode in the middle part of the Wangeripp group, due perhaps to hot fluid flow in a confined aquifer or local igneous intrusion.

The preferred thermal history for the **Cape Sorell-1 well** derived from this analysis is presented in Figure 3.6A. It is based on the preserved stratigraphy and a geothermal gradient of 26.7°C/km combined with a paleo-surface temperature of 17.3°C for the entire burial history. An equivalent thermal history based on the preserved stratigraphy and a constant basal heat flow of ~48 mWm^{-2} adopted from the present-day heat flow estimated from the corrected BHT data and a set of assumed thermal conductivites for a set of default lithologies (implemented in BasinMod™), is presented in Figure 3.6B. The histories are very similar, and only differ slightly in over the late ~40 Ma due to the effects of decompaction included in the heat flow model, but not in the gradient model.

3.7 Burial history reconstruction for Cape Sorell-1

As the preferred interpretation of the thermal history in Cape Sorell-1 involves maximum paleotemperatures at the present-day the results provide no evidence for any additional burial associated with any unconformities in the well. Therefore, the preserved stratigraphy in the well is considered to provide a valid representation of the actual burial history at this location, as illustrated by the burial history presented in Figure 3.2. This does not mean that the thermal history results preclude minor uplift and erosional episodes, but if such events did occur they have not resulted in thermal effects that can be measured with AFTA or VR data at the present-day.

Table 3.1: Summary of apatite fission track data - samples from Cape Sorell-1 (Geotrack Report #806)

Sample number	Average depth (m)	Present temperature*1 (°C)	Stratigraphic age (Ma)	Mean track length (µm)	Predicted mean track length*2 (µm)	Fission track age (Ma)	Predicted fission track age*2 (Ma)
Cape Sorell-1							
GC806-6	1294	50	53-50	-	-	-	-
GC806-7	1565	57	55-51	12.36 ± 0.28	13.1	92.2 ± 20.8	47
GC806-8	1990	69	70-65	11.76 ± 0.31	12.2	51.1 ± 6.3	54
GC806-1	2252	76	70-65	10.97 ± 0.50	11.4	47.9 ± 7.0	52
GC806-9	2694	88	73-65	12.05 ± 0.65	10.2	27.9 ± 5.9	39
GC806-2	2954	96	73-70	9.76 ± 0.79	11.1	74.2 ± 9.9	23
GC806-10	3196	102	78-73	10.34 ± 1.48	9.9	11.5 ± 8.2	7
GC806-3	3450	109	80-78	10.70 ± 0.43	9.1	24.7 ± 11.4	2

*1 See Appendix A for discussion of present temperature data.

*2 Values predicted from the Default Thermal History (Section 2.1); i.e. assuming that each sample is now at its maximum temperature since deposition. The values refer only to tracks formed after deposition. Samples may contain tracks inherited from sediment provenance areas. Calculations refer to apatites within the measured compositional range for each sample, as discussed in Appendix A.

Note: All depths quoted are TVD with respect to KB.

Table 3.2: Summary of thermal history interpretation of AFTA data in samples from the Cape Sorell-1 well, offshore western Tasmania (Geotrack Report #806)

Sample number	Do AFTA data require revision of present temperature?	Evidence of higher temperatures in the past from length data?	Evidence of higher temperatures in the past from fission track age data?	Conclusion
GC806-6 1294 m 53-50 Ma Paleocene	- 50°C	-	-	No apatite
GC806-7 1565 m 55-51 Ma Paleocene	No 57°C	Equivocal [Mean track length is ~0.7 µm shorter than expected on the basis of the Default Thermal History. Modelling the AFTA parameters through likely thermal history scenarios shows that measured lengths can be explained either by higher paleotemperatures after deposition or by inheritance of short tracks from the sediment source terrain.]	No [Central fission track age and all single grain ages are similar to, or older than, expected on the basis of the Default Thermal History.]	AFTA data from this sample shows no evidence that the sample has been hotter than present temperatures at any time since deposition, although a minor degree of additional heating is allowed, within certain limits.
GC806-8 1990 m 70-65 Ma Maastrichtian	No 69°C	Equivocal [Mean track length is ~0.4 µm shorter than expected on the basis of the Default Thermal History. Modelling the AFTA parameters through likely thermal history scenarios shows that measured lengths can be explained either by higher paleotemperatures after deposition or by inheritance of short tracks from the sediment source terrain.]	No [Central fission track age and all single grain ages are similar to, or older than, expected on the basis of the Default Thermal History.]	AFTA data from this sample shows no evidence that the sample has been hotter than present temperatures at any time since deposition, although a minor degree of additional heating is allowed, within certain limits.

Note: Interpretation of AFTA data is based on comparison of measured AFTA parameters with values predicted from "Default Thermal History" (Section 2.1); i.e., assuming that each sample is now at its maximum temperature since deposition. The predicted values for each sample are summarised in Table 3.1, and refer only to tracks formed after deposition. Samples may also contain tracks inherited from sediment provenance areas, which must be allowed for in interpreting the data. Calculations refer to apatites with the compositional range measured in each sample, as explained in Appendix A.

Table 3.2 (cont.): Cape Sorell-1 well, offshore western Tasmania (Geotrack Report #806)

Sample number	Do AFTA data require revision of present temperature?	Evidence of higher temperatures in the past from length data?	Evidence of higher temperatures in the past from fission track age data?	Conclusion
GC806-1 2252 m 70-65 Ma Maastrichtian	No 76°C	Equivocal [Mean track length is ~0.4 µm shorter than expected on the basis of the Default Thermal History. Modelling the AFTA parameters through likely thermal history scenarios shows that measured lengths can be explained either by higher paleotemperatures after deposition or by inheritance of short tracks from the sediment source terrain.]	No [Pooled fission track age is similar to that expected on the basis of the Default Thermal History.]	AFTA data from this sample shows no evidence that the sample has been hotter than present temperatures at any time since deposition, although a minor degree of additional heating is allowed, within certain limits.
GC806-9 2694 m 73-65 Ma Maastrichtian	No 88°C	Equivocal [Insufficient data for rigorous interpretation, only three track lengths measured].	No [Central fission track age and all single grain ages are similar to, or older than, expected on the basis of the Default Thermal History.]	AFTA data from this sample shows no evidence that the sample has been hotter than present temperatures at any time since deposition, although a minor degree of additional heating is allowed, within certain limits.

Note: Interpretation of AFTA data is based on comparison of measured AFTA parameters with values predicted from "Default Thermal History" (Section 2.1); i.e., assuming that each sample is now at its maximum temperature since deposition. The predicted values for each sample are summarised in Table 3.1, and refer only to tracks formed after deposition. Samples may also contain tracks inherited from sediment provenance areas, which must be allowed for in interpreting the data. Calculations refer to apatites with the compositional range measured in each sample, as explained in Appendix A.

Table 3.2 (cont.): Cape Sorell-1 well, offshore western Tasmania (Geotrack Report #806)

Sample number	Do AFTA data require revision of present temperature?	Evidence of higher temperatures in the past from length data?	Evidence of higher temperatures in the past from fission track age data?	Conclusion
GC806-2 2954 m 73-70 Ma Maastrichtian	Yes AFTA data are very sensitive to present-day temperatures >90°C. Kinetic modelling of the compositional groups present indicates that the present temperature of 96°C determined from the corrected BHT data is marginally too high and a maximum present-day temperature of ~93°C is more appropriate.	Equivocal [Relatively poor mean length based on 6 measurements. Mean track length is ~1.3 µm shorter than expected on the basis of the Default Thermal History. Modelling the AFTA parameters through likely thermal history scenarios shows that measured lengths can be explained either by higher paleotemperatures after deposition or by inheritance of short tracks from the sediment source terrain.]	No [Central fission track age and all single grain ages are similar to, or older than, expected on the basis of the Default Thermal History. Although as noted left, the fission track age data provide evidence that the present temperature may be slightly too high.]	AFTA data from this sample shows no evidence that the sample has been hotter than present temperatures at any time since deposition, and is dominated by the present temperature.
GC806-10 3196 m 78-73 Ma Campanian	No 102°C	Equivocal [Insufficient data for rigorous interpretation, only two track lengths measured].	No [Central fission track age and all single grain ages are similar to, or older than, expected on the basis of the Default Thermal History.]	AFTA data from this sample shows no evidence that the sample has been hotter than present temperatures at any time since deposition, and are dominated by the present temperature.

Note: Interpretation of AFTA data is based on comparison of measured AFTA parameters with values predicted from "Default Thermal History" (Section 2.1); i.e., assuming that each sample is now at its maximum temperature since deposition. The predicted values for each sample are summarised in Table 3.1, and refer only to tracks formed after deposition. Samples may also contain tracks inherited from sediment provenance areas, which must be allowed for in interpreting the data. Calculations refer to apatites with the compositional range measured in each sample, as explained in Appendix A.

Table 3.2 (cont.): Cape Sorell-1 well, offshore western Tasmania (Geotrack Report #806)

Sample number	Do AFTA data require revision of present temperature?	Evidence of higher temperatures in the past from length data?	Evidence of higher temperatures in the past from fission track age data?	Conclusion
GC806-3 3450 m 80-78 Ma Campanian	No 109°C	Insufficient data for rigorous interpretation [Only four track lengths measured].	No [Central fission track age and all single grain ages are similar to, or older than, expected on the basis of the Default Thermal History	AFTA data from this sample shows no evidence that the sample has been hotter than present temperatures at any time since deposition, and are dominated by the present temperature.

Note: Interpretation of AFTA data is based on comparison of measured AFTA parameters with values predicted from "Default Thermal History" (Section 2.1); i.e., assuming that each sample is now at its maximum temperature since deposition. The predicted values for each sample are summarised in Table 3.1, and refer only to tracks formed after deposition. Samples may also contain tracks inherited from sediment provenance areas, which must be allowed for in interpreting the data. Calculations refer to apatites with the compositional range measured in each sample, as explained in Appendix A.

Table 3.3: Estimates of timing and magnitude of elevated paleotemperatures from AFTA data in samples from the Cape Sorell-1 well, offshore western Tasmania (Geotrack Report #806)

Sample number Average depth	Stratigraphic age (Ma)	Present temperature*1 (°C)	Maximum paleo-temperature (°C)	Onset of cooling (Ma)	Maximum paleo-temperature (°C)	Onset of cooling (Ma)	Comments
GC806-6 1294 m	53 to 50 Paleocene	50	-	-	-	-	No apatite
GC806-7 1565 m	55 to 51 Paleocene	57	<105	Post-depn	<90	30 to 0	AFTA data in this sample can be explained by a combination of the Default Thermal History and the presence of tracks formed prior to deposition and therefore inherited from the sediment source terrains. The data set upper limits to the maximum post-depositional temperatures of <90°C within the last 30 Ma, and less than 105°C at any time after deposition. **Equivalent $R_o$max:** The Default Thermal History predicts a VR level of 0.39%, which is regarded as the most likely true maturity level at this depth, although the AFTA results would allow VR levels up to 0.69% (105°C). No measured VR data are available in this part of the well for comparison. **Provenance thermal history:** The fission track ages of individual grains are consistent with source areas with an age range between ~300 Ma and the Paleocene depositional age of this sample. Modelling of the AFTA results in the F-rich compositional group indicates that the source area for these detrital apatites cooled from >100°C at some time between 90 Ma and Paleocene deposition (95% confidence interval).

*1 Present temperature estimates were based on a sea-bed temperature of 17.3°C and linear gradient of 27.6°C/km. (See Appendix A.)

Table 3.3 (cont.): Cape Sorell-1 well, offshore western Tasmania (Geotrack Report #806)

Sample number Average depth	Stratigraphic age (Ma)	Present temperature*1 (°C)	Maximum paleo-temperature (°C)	Onset of cooling (Ma)	Maximum paleo-temperature (°C)	Onset of cooling (Ma)	Comments
GC806-8 1990 m	70-65 Ma Maastrichtian	69	<125	Post-depn	<90	30 to 0	AFTA data in this sample can be explained by a combination of the Default Thermal History and the presence of tracks formed prior to deposition and therefore inherited from the sediment source terrains. The data set upper limits to the maximum post-depositional temperatures of <90°C within the last 30 Ma, and less than 125°C at any time after deposition. **Equivalent $R_o$max:** The Default Thermal History predicts a VR level of 0.45%, which is regarded as the most likely true maturity level at this depth, although the AFTA-allowed maximum paleotemperature of 125°C would allow a VR level up to 0.88%. Measured open-file VR data bracketing this sample range from 0.44 to 0.45% (Table D.3, Appendix D), highly consistent with the Default Thermal History prediction. **Provenance thermal history:** Modelling of the AFTA results indicates that the source area for these detrital apatites cooled from >120°C at some time between 90 Ma and Maastrichtian deposition (95% confidence interval).

*1 Present temperature estimates were based on a sea-bed temperature of 17.3°C and linear gradient of 27.6°C/km. (See Appendix A.)

Table 3.3 (cont.): Cape Sorell-1 well, offshore western Tasmania (Geotrack Report #806)

Sample number Average depth	Stratigraphic age (Ma)	Present temperature*1 (°C)	Maximum paleo-temperature (°C)	Onset of cooling (Ma)	Maximum paleo-temperature (°C)	Onset of cooling (Ma)	Comments
GC806-1 2252 m	70-65 Ma Maastrichtian	76	<125	Post-depn	<100	30 to 0	AFTA data in this sample can be explained by a combination of the Default Thermal History and the presence of tracks formed prior to deposition and therefore inherited from the sediment source terrains. The data set upper limits to the maximum post-depositional temperatures of <100°C within the last 30 Ma, and less than 125°C at any time after deposition. **Equivalent R_0max:** The Default Thermal History predicts a VR level of 0.51%, which is regarded as the most likely true maturity level at this depth, although the AFTA-allowed maximum paleotemperature of up to 125°C would allow a VR level up to 0.88%. Measured open-file VR data bracketing this sample range from 0.45 to 0.42% (Table D.3, Appendix D), a little lower than the Default Thermal History prediction. **Provenance thermal history:** Modelling of the AFTA results indicates that the source area for these detrital apatites cooled from >100°C at some time between 80 Ma and Maastrichtian deposition (95% confidence interval).

*1 Present temperature estimates were based on a sea-bed temperature of 17.3°C and linear gradient of 27.6°C/km. (See Appendix A.)

Table 3.3 (cont.): Cape Sorell-1 well, offshore western Tasmania (Geotrack Report #806)

Sample number Average depth	Stratigraphic age (Ma)	Present temperature*1 (°C)	Maximum paleo-temperature (°C)	Onset of cooling (Ma)	Maximum paleo-temperature (°C)	Onset of cooling (Ma)	Comments
GC806-9 2694 m	73-65 Ma Maastrichtian	88	*>105*	*Depn to 30*	<105	30 to 0	AFTA data in this sample can be explained by a combination of the Default Thermal History and the presence of tracks formed prior to deposition and therefore inherited from the sediment source terrains. The data would allow however, maximum paleotemperatures >105°C between deposition and 30 Ma, and set an upper limit to the maximum post-depositional temperature of <105°C within the last 30 Ma. **Equivalent $R_o$max:** The Default Thermal History predicts a VR level of 0.58%, which is regarded as the most likely true maturity level at this depth, although the AFTA-allowed maximum paleotemperature of 125°C would allow a VR level up to 0.88%. Measured open-file VR data bracketing this sample range from 0.42 to 0.47% (Table D.3, Appendix D), significantly lower than the Default Thermal History prediction, suggesting a significant degree of geochemical suppression of the measured VR data. **Provenance thermal history:** Modelling of the AFTA results indicates that the source area for these detrital apatites cooled from >105°C at some time between 75 Ma and Maastrichtian deposition (95% confidence interval).

*1 Present temperature estimates were based on a sea-bed temperature of 17.3°C and linear gradient of 27.6°C/km. (See Appendix A.)
Note: Constraints in italics are *allowed*, but not required, by AFTA.

Table 3.3 (cont.): Cape Sorell-1 well, offshore western Tasmania (Geotrack Report #806)

Sample number Average depth	Stratigraphic age (Ma)	Present temperature*1 (°C)	Maximum paleo-temperature (°C)	Onset of cooling (Ma)	Maximum paleo-temperature (°C)	Onset of cooling (Ma)	Comments
GC806-2 2954 m	73-70 Ma Maastrichtian	96 Revised by AFTA to 93°C	<100	Post-depn	<98 (98 allowed only at 30 Ma)	30 to 0	AFTA data in this sample can be explained by a combination of the Default Thermal History and the presence of tracks formed prior to deposition and therefore inherited from the sediment source terrains. The data set a very tight upper limit to the maximum post-depositional temperatures of less than 100°C at any time after deposition, and a maximum of 98°C at 30 Ma declining to a maximum of 93°C at the present-day. **Equivalent R_0max:** The Default Thermal History predicts a VR level of 0.63%, which is regarded as the most likely true maturity level at this depth, although the AFTA-allowed maximum paleotemperature of up to 100°C would allow a VR level up to 0.65%. Measured open-file VR data bracketing this sample range from 0.47 to 0.60% (Table D.3, Appendix D), the highest value slightly lower than the Default Thermal History prediction, suggesting a minor degree of geochemical suppression of the measured VR data. **Provenance thermal history:** Inspection of the AFTA data suggests two groups of fission track ages in the F-rich compositional group suggesting two separate provenance ages. Modelling of the AFTA results indicates an older source area that cooled from >100°C at some time between ~375 and 200 Ma (95% confidence interval). The presence of second group of grains with Cl contents ranging from 0 to ~1.5 wt% is consistent with a detrital contribution from a Mesozoic volcanogenic source, possibly equivalent to the Eumeralla Formation or the Late Triassic volcanogenic sediment known to outcrop in Tasmania.

*1 Present temperature estimates were based on a sea-bed temperature of 17.3°C and linear gradient of 27.6°C/km. (See Appendix A.)

Table 3.3 (cont.): Cape Sorell-1 well, offshore western Tasmania (Geotrack Report #806)

Sample number Average depth	Stratigraphic age (Ma)	Present temperature*1 (°C)	Maximum paleo-temperature (°C)	Onset of cooling (Ma)	Maximum paleo-temperature (°C)	Onset of cooling (Ma)	Comments
GC806-10 3196 m	78-73 Ma Campanian	102	<125	Post-depn	<115	30 to 0	AFTA data in this sample are dominated by the present temperatures and can be explained by a combination of the Default Thermal History and the presence of tracks formed prior to deposition and therefore inherited from the sediment source terrains. The data set upper limits to the maximum post-depositional temperatures of <115°C within the last 30 Ma, and less than 125°C at any time after deposition. **Equivalent $R_o$max:** The Default Thermal History predicts a VR level of 0.66%, which is regarded as the most likely true maturity level at this depth, although the AFTA-allowed maximum paleotemperature of 125°C would allow a VR level up to 0.88%. The majority of measured open-file VR data bracketing this sample range from 0.45 to 0.54% (Table D.3, Appendix D), significantly lower than the Default Thermal History prediction, suggesting a significant degree of geochemical suppression of the measured VR data. One measured level of 0.9% is similar to the maximum value allowed by AFTA for a maximum paleotemperature of 125°C. **Provenance thermal history:** As the AFTA data in this sample are dominated by the present temperatures and little provenance information remains. However, one grain (0.59 wt%Cl) which is significantly older than expected from the Default History clearly indicate a provenance age older than ~100 Ma.

*1 Present temperature estimates were based on a sea-bed temperature of 17.3°C and linear gradient of 27.6°C/km. (See Appendix A.)

Table 3.3 (cont.): Cape Sorell-1 well, offshore western Tasmania (Geotrack Report #806)

Sample number Average depth	Stratigraphic age (Ma)	Present temperature*1 (°C)	Maximum paleo-temperature (°C)	Onset of cooling (Ma)	Maximum paleo-temperature (°C)	Onset of cooling (Ma)	Comments
GC806-3 3450 m	80-78 Ma Campanian	109	<125	Post-depn	<120	30 to 0	AFTA data in this sample are dominated by the present temperatures and can be explained by a combination of the Default Thermal History and the presence of tracks formed prior to deposition and therefore inherited from the sediment source terrains. The data set upper limits to the maximum post-depositional temperatures of <125°C within the last 30 Ma, and less than 120°C at any time after deposition. **Equivalent R_0max:** The Default Thermal History predicts a VR level of 0.71%, which is regarded as the most likely true maturity level at this depth, although the AFTA-allowed maximum paleotemperature of 125°C would allow a VR level up to 0.88%. Measured open-file VR data near this sample range from 0.56 to 0.66% (Table D.3, Appendix D), a little lower than the Default Thermal History prediction, suggesting some degree of geochemical suppression of the measured VR data. One measured of 1.0 % is similar to the maximum value allowed by AFTA for a maximum paleotemperature of 125°C. **Provenance thermal history:** As the AFTA data in this sample are dominated by the present temperatures and little provenance information remains. However, one grain (0.58 wt%Cl) which is significantly older than expected from the Default History clearly indicate a provenance age older than ~100 Ma.

*1 Present temperature estimates were based on a sea-bed temperature of 17.3°C and linear gradient of 27.6°C/km. (See Appendix A.)

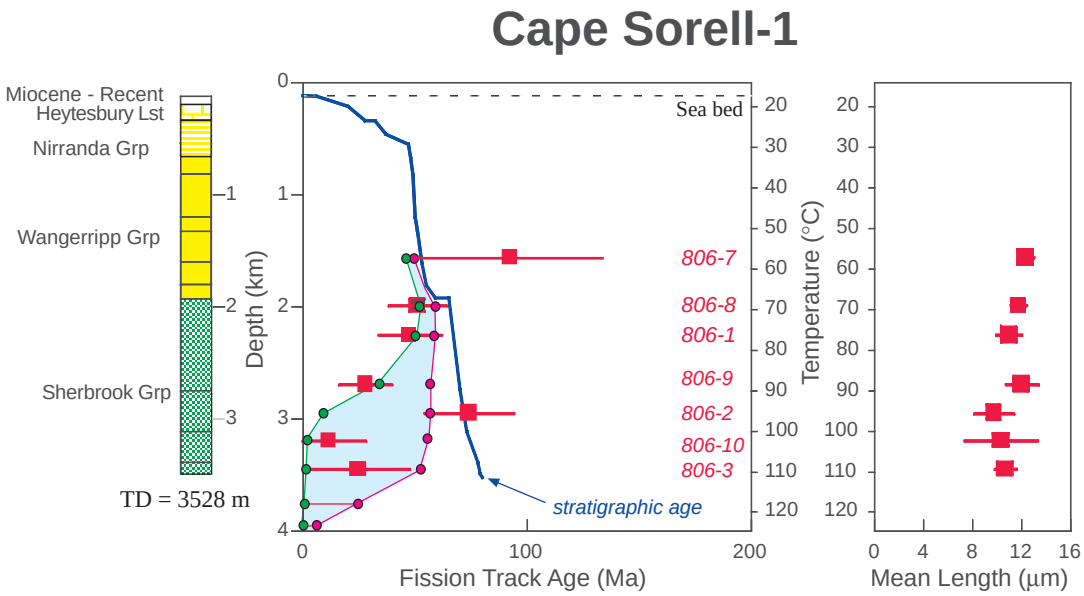

Figure 3.1: AFTA parameters plotted against sample depth and present temperature for samples from the **Cape Sorell-1 well, offshore Western Tasmania.** The variation of stratigraphic age with depth is also shown, as the solid line in the central panel. A present-day geothermal gradient of 27.6°C/km and sea-bed temperature of 17.3°C is used for the temperature scale.

The coloured area indicates the range of AFTA age parameters expected on the basis of the Default Thermal Histories in each sample, incorporating the range of apatite compositions present.

The measured fission track ages are similar to, or older than, the values expected from the Default Thermal Histories, consistent with the sampled section being at or very close to, maximum temperatures at the present-day.

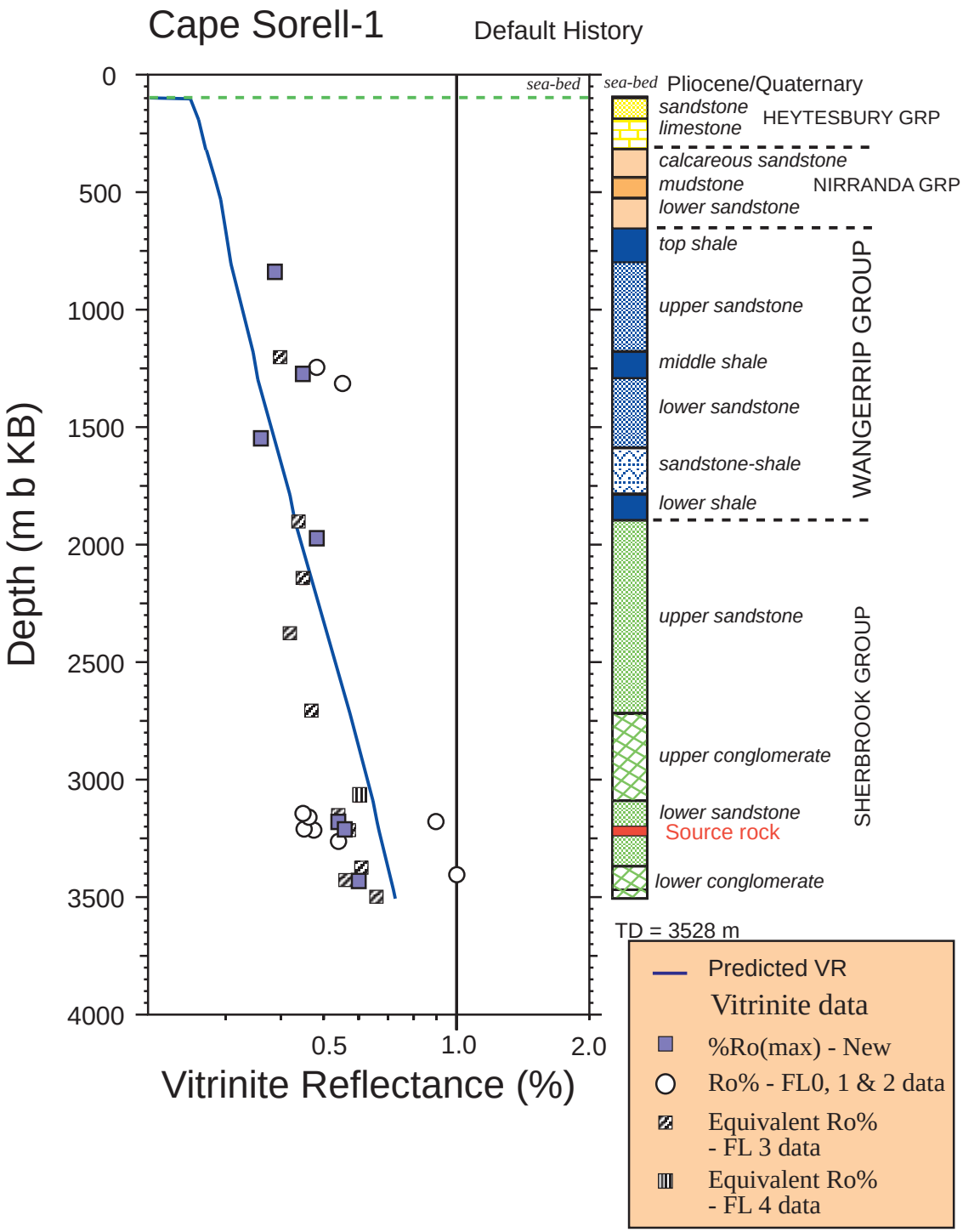

Figure 3.2: Measured VR data and predicted VR with respect to depth based on the Default Thermal History in **Cape Sorell-1.** The solid square symbols show new Ro(max) data (Table D.2), the cross-hatched square symbols denote open-file VRF™ data, the vertical hatched square shows VRE from sterane-hopane data and the circle symbols denote other open-file VR data (Table D.3). The solid line shows the VR profile calculated on the basis of the Default Thermal History (explained in Section 2.1), which is derived from the preserved stratigraphy in the well (Figure 3.3), an AFTA-revised present-day geothermal gradient of 26.7°C/km and a sea-bed temperature of 17.3°C. The majority of measured values plot well below the predicted profile, indicating either a transient recent increase in geothermal gradient, or that the majority of the measured organic maturity data underestimate the true maturity of the section. The latter explanation is preferred on the basis of the AFTA results presented in this report.

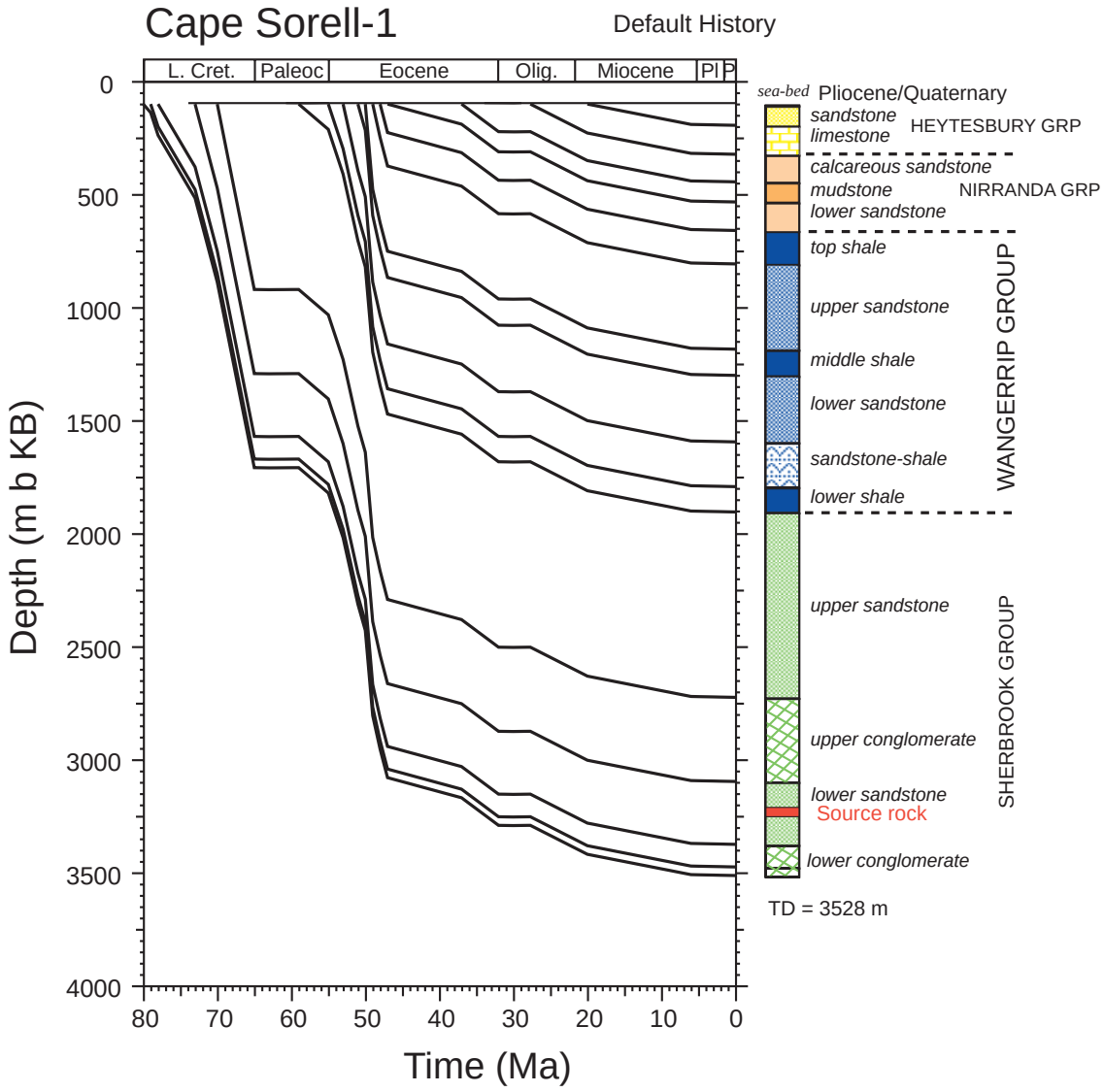

Figure 3.3: Default Burial History showing the history derived from the preserved stratigraphy in the **Cape Sorell-1 well.** This history, together with an AFTA-revised present-day geothermal gradient (26.7°C/km) and a sea-bed temperature of 17.3°C, has been used to calculate the Default Thermal Histories for each sample from which default parameters are calculated (see Table 3.1). Default parameters are compared with observed AFTA and VR data to evaluate the degree of heating which is attributable to the present thermal regime and hence to determine whether samples have been hotter in the past (see Table 3.2).

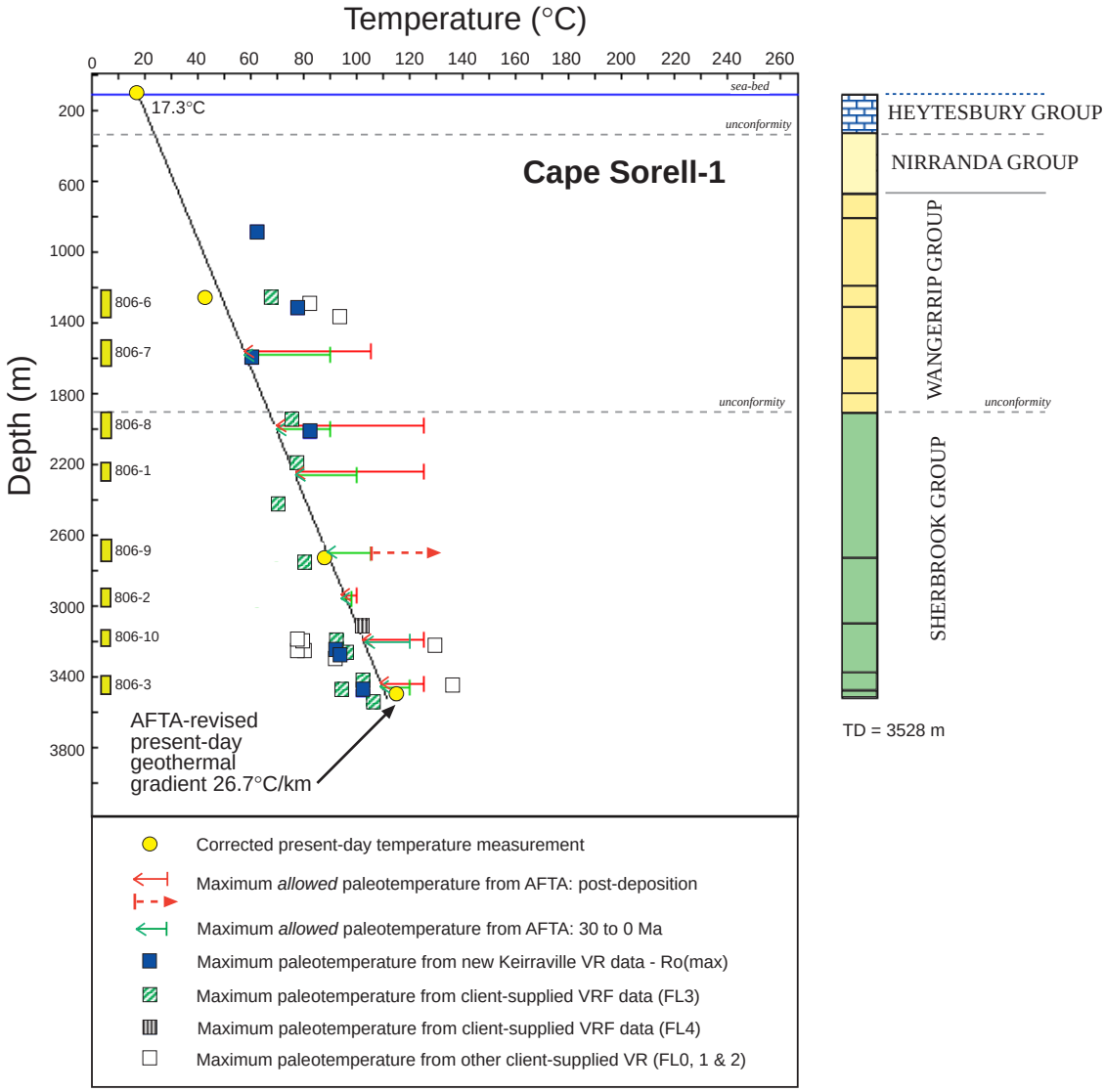

Figure 3.4: Plot of paleotemperatures derived from AFTA and organic reflectance data in the **Cape Sorell-1 well**, against depth and the estimated present temperature profile for this well based on a gradient of 26.7°C/km estimated from the corrected BHT data (Appendix A).

AFTA shows no requirement for post-depositional paleotemperatures any higher than the present-temperatures, but results from individual samples would allow additional heating within certain limits, as shown. The preferred interpretation of the AFTA results is that the whole drilled section is at maximum temperatures at the present-day.

Maximum paleotemperatures derived from the organic reflectance data, including the new Ro(max) values and the VRF measurements, are generally lower than the present temperatures (especially below ~2300 m), are interpreted to underestimate the true maximum temperatures experienced by the deeper Sherbrook Group section.

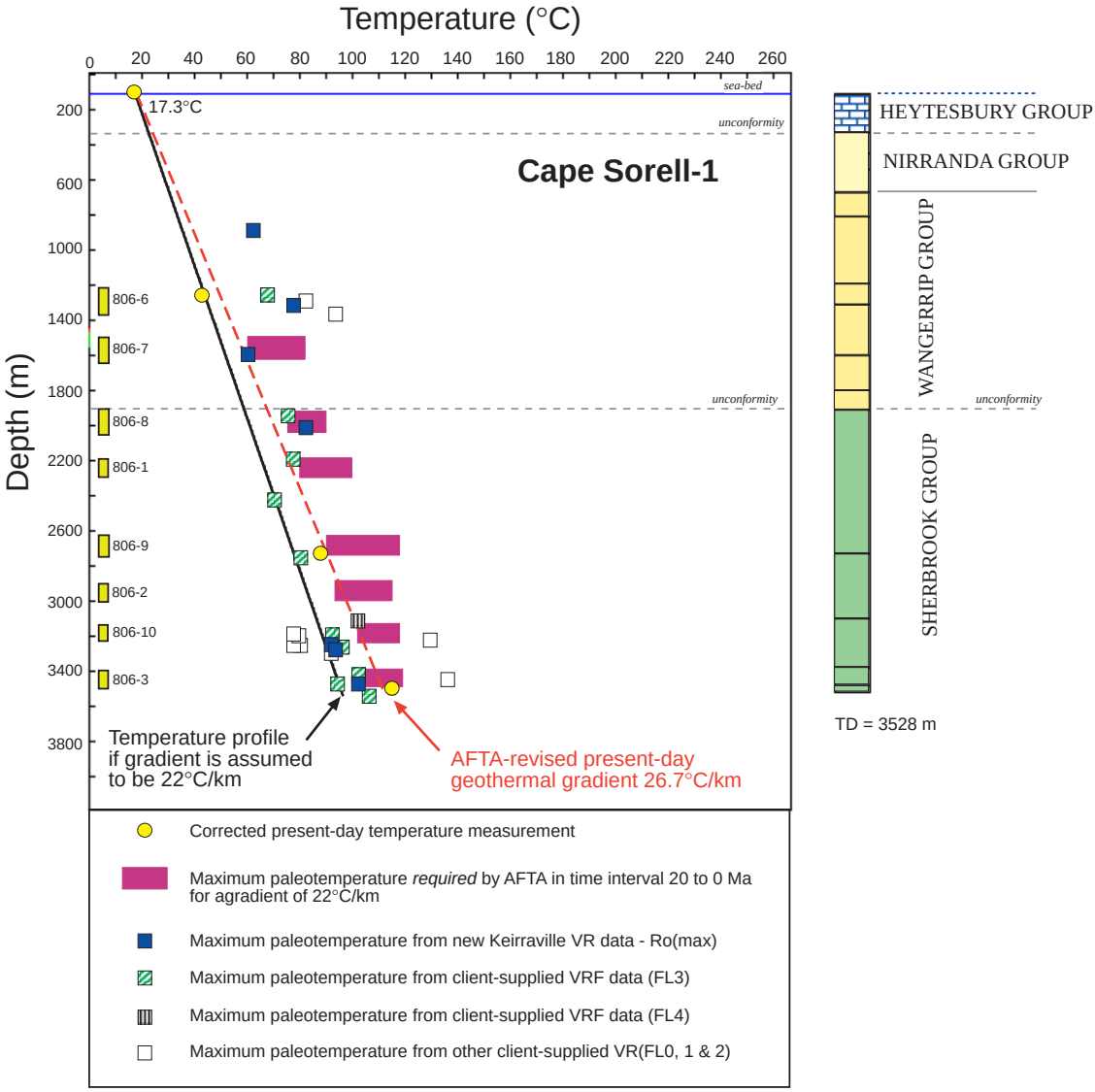

Figure 3.5: Plot of paleotemperatures derived from AFTA and organic reflectance data in the **Cape Sorell-1 well**, assuming a transient increase in present-day geothermal gradient from 22°C/km to 26.7°C/km over the last 10000 years.

AFTA shows a definite requirement for cooling from maximum paleotemperatures significantly higher than the "steady-state" temperatures estimate from a gradient from 22°C/km. Thus the AFTA results still indicate higher maximum paleotemperatures than the VR data in the deeper part of the Sherbrook Group, and it is not possible to reconcile the AFTA and VR results by manipulation of heating duration.

The preferred interpretation of the data is that the present-day gradient of 26.7°C/km based on the corrected BHT data has been acting over at least the last several tens of millions of year and that the Sherbrook Group Section is at maximum post-depositional temperatures at the present-day in response to this. Maximum paleotemperatures estimated from the organic reflectance data, including the new Ro(max) values and the VRF measurements, are generally lower than the present temperatures (especially below ~2300 m), thus underestimate the true maximum temperatures experienced by the deeper Sherbrook Group section.

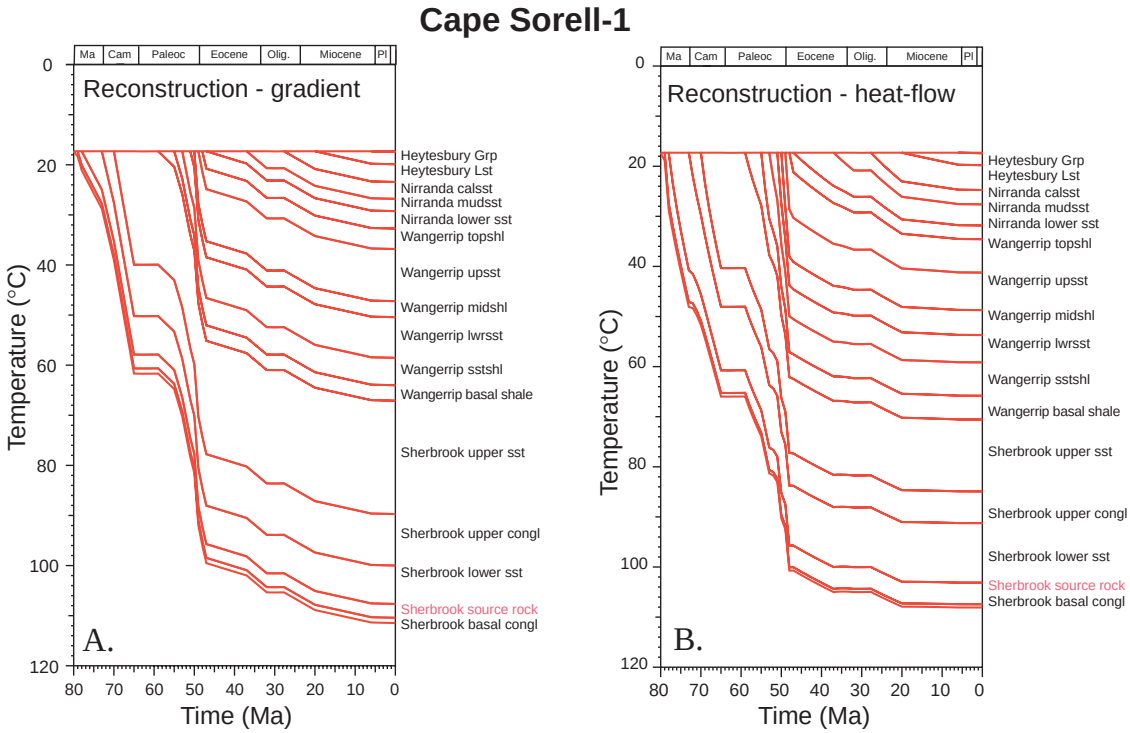

Figure 3.6: Reconstructed thermal history for the Cape Sorell-1 well derived from the interpretation of the AFTA and VR results. The history in the left hand figure is based on the preserved stratigraphy and a constant geothermal gradient with time equal to the present-day value of 27.6°C/km. The history in the right hand figure is based on the preserved stratigraphy and a constant heat flow (~48mWm^{-2}) with time equal to the present-day level for a set of default lithological and thermal conductivity parameters implemented in BasinMod™. Both thermal histories result in similar predictions of source rock maturation with time although it is clear that the heating rate over about the last 40 Ma is lower in the heat flow model due to the effects of decompaction.

4. Reconstructed source rock maturation and hydrocarbon generation histories

4.1 Predicted maturity-depth profile in Cape Sorell-1

Figure 4.1 shows the measured VR data (Tables D.2 & D.3, Appendix D) and AFTA-derived VRE values (Table iii) in Cape Sorell-1, together with two maturity-depth profiles predicted (using Burnham and Sweeney, 1989) for the **Cape Sorell-1 well**.

The dashed VR profile is based on a constant paleogeothermal gradient of 22°C/km designed to fit the VR and VRF data as described in Section 3.5. The AFTA-derived VRE values plot well above this profile, and clearly require higher post-depositional temperatures than the majority of the measured VR and VRF data in the Sherbrook Group section.

The preferred profile (solid line) is derived from the reconstructed thermal histories shown in Figure 3.6, for a constant paleogeothermal gradient of 26.7°C/km adopted from the AFTA-revised steady-state present-day gradient. This predicted profile shows an excellent fit to the AFTA-derived VRE values, strongly supporting the major conclusions of this study that the Late Cretaceous section is at maximum temperatures at the present-day and that the present-day AFTA-revised present-day gradient of 26.7°C/km has been in effect for at least the last few tens of millions of years.

We conclude from this analysis that the majority of measured VR & VRF values in the Late Cretaceous section plot well below the predicted profile, underestimating the true maturity of the section as a result of geochemical suppression.

4.2 Predicted variation of maturity with time

Figure ii (Executive Summary) shows the variation of vitrinite reflectance maturity with time in the **Cape Sorell-1 well** (using the maturation algorithm of Burnham and Sweeney, 1989) derived from the preferred reconstructed thermal histories shown in Figure 3.6.

Reconstruction 1 is based on a constant paleogeothermal gradient of 26.7°C/km estimated from the corrected BHT data (AFTA-revised) and constant sea-bed temperature of 17.3°C with time (see Figure 3.6A). Reconstruction 2 is based on a constant heat-flow of 49mWm^{-2} derived from the corrected BHT data combined with a set of assumed thermal conductivities and lithologies (default values from BasinMod™) for the drilled section and constant sea-bed temperature of 17.3°C with time (see Figure 3.6B).

Vitrinite reflectance in the entire drilled section is predicted to have increased progressively with time in both modelled histories, with the source rock interval (~3200-3240 m) reaching a level of ~0.66% R_o(max) at the present-day. The maximum rate of increase in VR occurs in the Late Paleocene-Eocene as a response to a relatively high burial rate producing a high heating rate during this time interval. Minor differences between the two modelled maturation histories in the Early Paleocene result from compaction effects not considered in the geothermal gradient model, but these have no significant influence on the assessment of the rates of maturation within the general oil window.

It is emphasised that since the AFTA results indicate that maximum paleotemperatures are at the present-day, these results provide no additional constraints on the paleo-heat flow history, and that considerable variation in the heat flow history would be allowed as long as the resulting paleotemperatures do not exceed present-day temperatures.

4.3 Predicted hydrocarbon generation with time

Predicted transformation ratio

Figure 4.2 shows the predicted variation in transformation ratio (TR) with time from the Sherbrook Group "source rock layer" (~3200–3240 m) in **Cape Sorell-1** based on the reconstructed thermal history based for the heat flow model illustrated in Figure 3.6B.

The model uses measured kinetics for a kerogen sample from the 3200 to 3240 m interval in Cape Sorell-1 well supplied by Chris Boreham. Variation of VR maturity with time is also shown for comparison. The history predicts the top of the source rock at ~3200 m reached a TR of ~0.07 at ~48 Ma for a VR of 0.5%, a TR of ~0.15 at ~38 Ma for a VR of 0.6% and a TR of ~0.3 for a VR of ~0.66% reached at the present-day.

Predicted oil generation

Predicted oil generation from the Sherbrook Group "source rock layer" (~3200–3240 m) based on the reconstructed thermal history for the heat flow model illustrated in Figure 3.6B, and measured kerogen kinetics is shown in Figure 4.3. A primary oil potential 400 mg/gTOC and a primary gas potential 100 mg/gTOC has been used for source rock horizon with an average TOC of 10%.

The left hand figure (Figure 4.3) shows cumulative in-situ generated oil and gas (at the top of the unit) through time, the middle figure shows in-situ generated oil through

time for the top and bottom of the unit and the right hand figure shows the variation of the rate of oil generation with time.

Progressively increasing hydrocarbon generation with time reflects progressive increase in temperature with time reaching maximum temperatures at the present-day. Maximum rate of oil generation occurs at ~48 Ma, in response to the maximum burial heating rate in the Early Eocene, during rapid deposition of the thick Wangeripp Group. The declining rate of oil generation since the Early Eocene reflects the declining heating rate resulting from relatively little burial from the Oligocene to the present-day.

Petrographic observations consistent with expulsion of oil

For a source rock with 30% transformation some expulsion is predicted, and observations made by Alan Cook during the course of the vitrinite reflectance determinations shows the widespread occurrence of oil in VR samples from the basal Late Cretaceous section (see maceral descriptions, Appendix D). Petrographic observations in the three deeper samples (GC806-10, -10.1 and –3) indicate a persistent oil haze, oil inclusions within both calcite cements and rare quartz overgrowths, oil seeping from shaley coal and bright yellow exsudatinite veins. Perhaps more interesting is Alan Cook's description of oil inclusions within quartz overgrowths in sample GC806-5.1 at ~885 m (2790 – 2820 feet) within the Wangeripp Group,

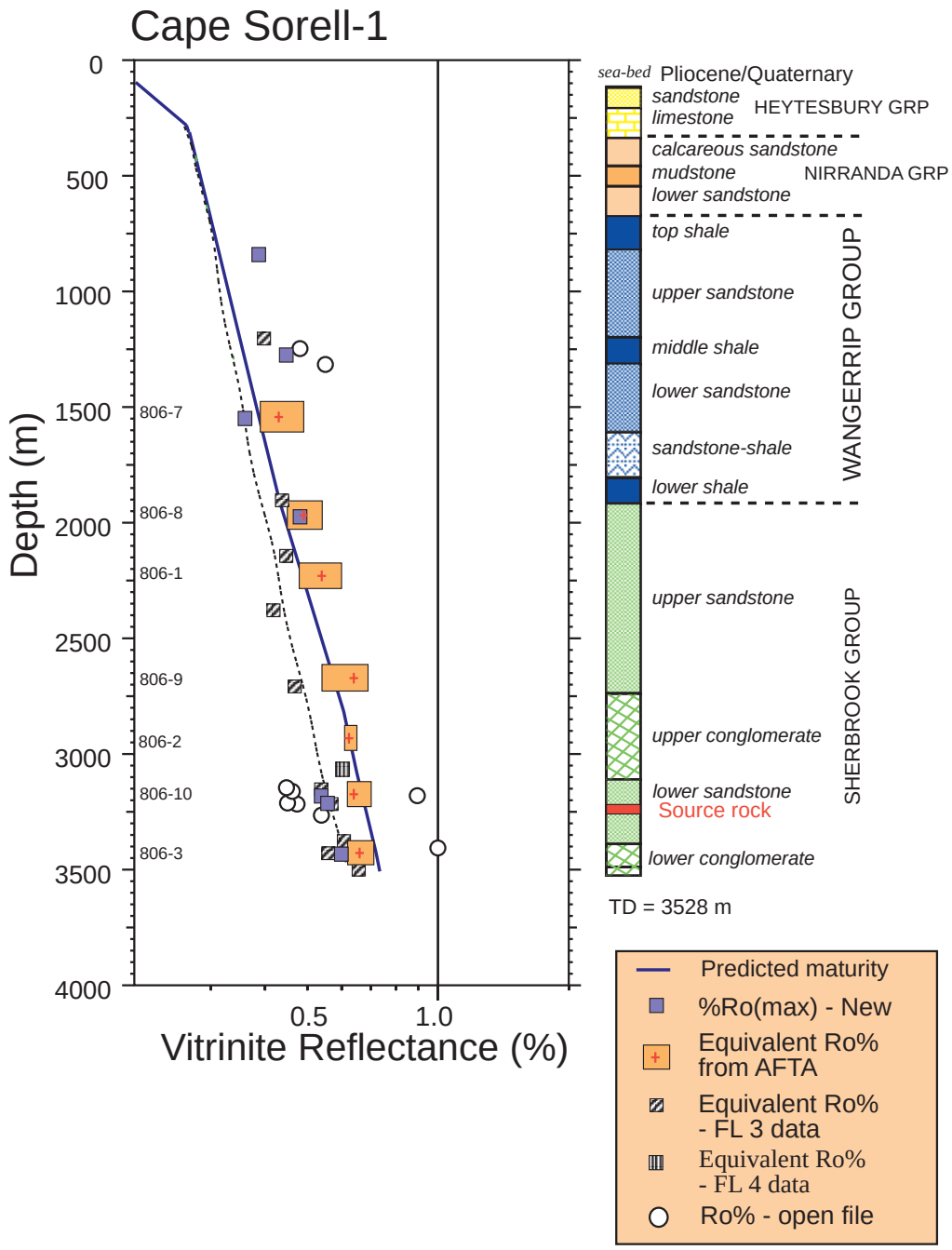

Figure 4.1: Measured VR and AFTA-derived VRE data together with the VR-profile from the AFTA-reconstructed Thermal History in **Cape Sorell-1**. Data symbols explained in the figure. The dashed VR profile is based on a constant paleogeothermal gradient of 22°C/km designed to fit the VR and VRF data as described in the text. The solid line is the predicted VR profile for a constant paleogeothermal gradient of 26.7°C/km adopted from the AFTA-revised steady-state present-day gradient, and this shows an excellent fit to the AFTA-derived VRE values. We conclude from this analysis that the majority of measured VR & VRF values in the Late Cretaceous section plot well below the predicted profile, underestimating the true maturity of the section as a result of geochemical suppression.

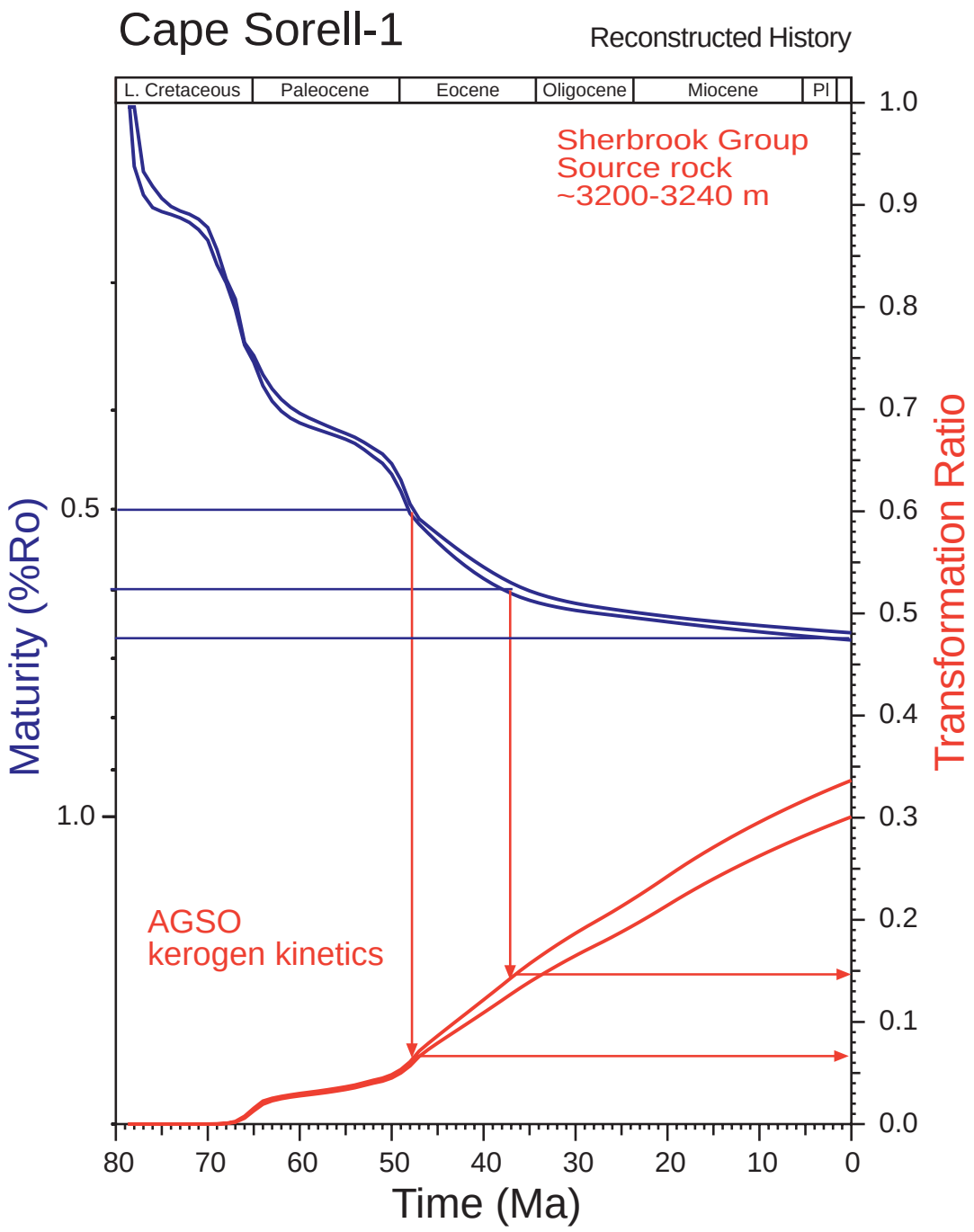

Figure 4.2: Predicted variation in transformation ratio (TR) with time from the Sherbrook Group "source rock layer" (~3200–3240 m) in **Cape Sorell-1** based on the reconstructed thermal history based on the heat flow model illustrated in Figure 3.6B, and kerogen kinetics determined on a sample from the Cape Sorell-1 well supplied by Chris Boreham. Variation of VR maturity with time is also shown for comparison.

The history predicts the top of source rock at ~3200 m reached a TR of ~0.07 at ~48 Ma for a VR of 0.5%, a TR of ~0.15 at ~38 Ma for a VR of 0.6% and a TR of ~0.3 for a VR of ~0.66% reached at the present-day.

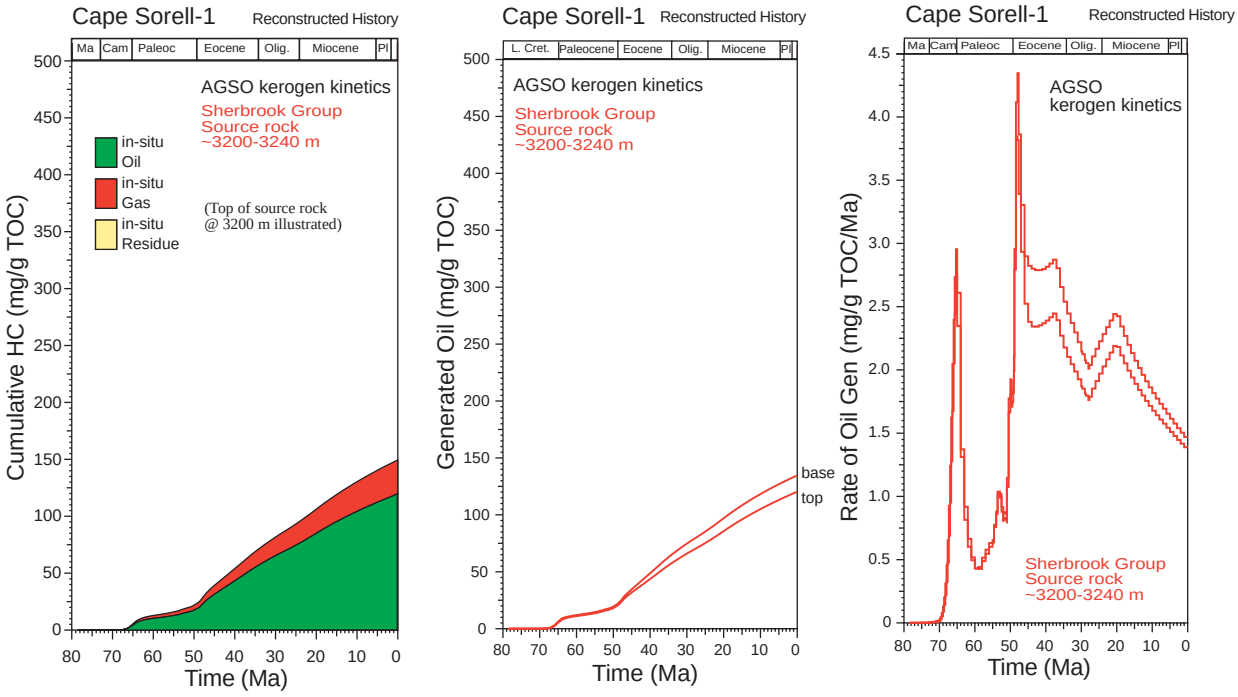

Figure 4.3: Predicted oil generation from the Sherbrook Group "source rock layer" (~3200–3240 m) based on the reconstructed thermal history for the heat flow model illustrated in Figure 3.6B, and kerogen kinetics determined on a sample from the Cape Sorell-1 well supplied by Chris Boreham. Primary oil potential 400 mg/gTOC and primary gas potential 100 mg/gTOC.

The left hand figure shows **cumulative in-situ generated oil and gas** (at the top of the unit) through time, the middle figure shows **in-situ generated oil** through time for top and bottom of the unit and the right hand figure shows the variation of the **rate of oil generation** with time.

Increasing hydrocarbon generation with time reflects progressive increase in temperature with time, reaching maximum temperatures at the present-day. Maximum rate of oil generation occurs at ~48 Ma is in response to maximum burial heating rate in the Early Eocene, during rapid deposition of the thick Wangerip Group. The declining rate of oil generation since the Early Eocene reflects the declining heating rate resulting from relatively little burial from the Oligocene to the present-day.

5. Provenance of the Wangeripp and Sherbrook Group sandstones

The AFTA results obtained in this study have provided tight constraints on key aspects of the post-depositional thermal history at Cape Sorell-1 and as a consequence has enabled the true maturity levels of the Sherbrook Group section to be assessed, despite significant geochemical suppression of the measured VR and VRF results.

The AFTA fission track age results also provide unique information on the provenance of apatites of the analysed Wangeripp and Sherbrook Group samples as described in detail in Table 3.3.

The normal expectation for these sediments is derivation from a Paleozoic and older terrain like that represented in outcrop on the Tasmanian mainland. Modelling of AFTA results in each sample assuming a Paleozoic source terrain which in the absence of any additional heating, would be expected to provide apatite with ages of 300 to 400 Ma to the basin. Instead most fission track ages are much younger than this (Appendix B) and reveal clear evidence for much more recent tectonic activity as discussed blow.

The resulting thermal histories obtained from samples of Late Cretaceous age indicate derivation of most apatite, and presumably other detrital components of the sediments, from a provenance terrain rapidly uplift and eroded in during the interval ~90 to 65 Ma, i.e. coeval with the deposition of the Late Cretaceous Sherbrook Group section. Thermal histories for a number of key samples are illustrated in Figure i (Executive Summary). Overlapping timing constraints from AFTA data in samples GC806-1, -8 &-9 from the Sherbrook Group record the thermal history of a sediment source terrain that cooled rapidly between ~90 Ma, and the youngest depositional age of these sediments at 65 Ma. Note that more recent cooling is allowed by the results from each sample (up to ~35 Ma – Late Eocene), but such high post-depositional temperatures are precluded by the thermal history analysis presented in the preceding sections.

AFTA results from sample GC806-2 show evidence for an additional, older provenance terrain which cooled from >100°C between ~300 and 200 Ma. This may possibly indicate contributions from a Mesozoic volcanogenic sediment as suggested by the broad range of chlorine in apatite grains from this sample (see Section A.6, Appendix A).

Most apatite fission track ages in Wangeripp Group sample GC806-7 are consistent with the Paleocene stratigraphic age (Appendix B), which is in turn consistent with a provenance terrain rapidly cooled from >~100°C immediately prior to deposition. Several older grains suggest a contribution from an older or cooler terrain, possibly including a Mesozoic volcanogenic source (see Section A.6, Appendix A).

AFTA results from sample Sherbrook Group sample GC806-10 and –3 are dominated by the high present-temperatures at which they reside and provide no effective provenance information.

Thus, the AFTA results from the Cape Sorell-1 well indicate kilometre-scale uplift and erosion of basement rocks adjacent to the Sorell Basin, during the Late Cretaceous to Paleocene, in order to rapidly provide sediment that had resided at over 100°C in the provenance terrain only 15 to 20 Ma earlier.

Unpublished AFTA results from the Paleozoic Merrideth granite from onshore west-coast Tasmania, at a similar latitude to Cape Sorell-1, indicate rapid cooling from >~100°C between ~95 and 65 Ma, remarkably similar to the timing obtained from Sherbrook Group samples in this study. Published raw fission track age data from other Paleozoic rocks in the area (Dumitru et al., 1991) are also consistent with significant cooling since the Early Cretaceous, but more detailed kinetic modelling are required to provide more precise conclusions from these data.

Such large-scale uplift and erosion was presumably a response to transpressional tectonics associated with a strike-slip margin developed between the west coast of Tasmania and Antarctica during the Late Cretaceous and Early Tertiary (e.g. Hinz et al., 1986). Hinz et al. (1986) attributed flower structures in the vicinity of Cape Sorrel-1 to Paleogene transpression. They indicate (p.405) – “A huge sediment pile of largely Paleocene age was deposited locally in the Cape Sorell sub-Basin, probably as a result of transtension and rapid block subsidence in this part of the strike slip zone.” The AFTA results presented here indicate that inversion along this margin probably commenced somewhat earlier and was much more widespread involving basement on the Tasmanian mainland. Finally, an Antarctic provenance for some of the sediment is also possible given the nature of this margin during the Late Cretaceous and Early Tertiary.

6. Recommendations for further work

6.1 Thermal history of the Wangeripp Group in Cape Sorell-1

The VR data has provided tentative evidence for a transient heating event localized within the Wangeripp Group section. Heating to paleotemperatures of at least 60 to 90°C compared to present temperatures of ~ 50°C may be due to hot fluid flow in a confined aquifer or minor igneous intrusion. Insufficient apatite was obtained from sample GC806-6, which encompassed this interval, to provide reliable information on the time of this transient heating. Collection of a second AFTA sample is recommended for both AFTA and the (U-Th)/He apatite dating technique. In general terms, integration of (U-Th)/He with AFTA results from the same sample can provide greater resolution of the younger Tertiary cooling episodes experienced by a sample, as the technique is very sensitive at paleotemperatures as low as 60 to 80°C. In principle, a very precise time of this possible heating within the Wangeripp Group could be directly determined.

6.2 Investigation of the regional tectonic history

The study has revealed evince for significant tectonic events along the west coast Tasmanian margin during the Late Cretaceous and Early Tertiary which is presumably related to the separation history of Australia and Antarctic. Recent AFTA studies on the Mussel platform indicate significant kilometre-scale “within basin” inversion during this same time interval, which has significant implications for hydrocarbon exploration (Duddy and Erout, 2001, in press).

This should be further investigated by application of AFTA-based thermal history studies in the Whelk-1, Clam-1 and Prawn-1 well and could also incorporate dredge samples of basement rock from Sonne Cruise S0-36C – dredge locations 28, 29 and 36 (Hinz et al., 1986).

References

AMOCO, 1982. Geochemical analyses, Cape Sorell No.1. Amoco Australia Petroleum Company, Well Completion Report, Appendix C.

ARMSTRONG J.P. ALIMI M.H., CLOE J.M. & NG K.H., 1983. A basic geochemical evaluation of eight sidewall cores from the Cape Sorell-1 well, drilled in Australia. Robertson Research (Singapore) Private Company, Report No. 1170.

BRAY R.J., GREEN P.F & DUDDY, I.R., 1992. Thermal History Reconstruction using apatite fission track analysis and vitrinite reflectance: a case study from the UK East Midlands and the Southern North Sea. In: Hardman, R.F.P. (ed.), Exploration Britain: Into the next decade. *Geological Society Special Publication*, 67, 3-25.

BOREHAM C.J. LOGAN G. & BRADSHAW M., 2000. Petroleum geochemistry of suspected oil stains from Cape Sorell-1. AGSO Professional Opinion 2000/36, unpublished.

BURNHAM A.K. & SWEENEY J.J., 1989. A chemical kinetic model of vitrinite reflectance maturation. *Geochimica et Cosmochimica Acta.*, 53, 2649-2657.

DUDDY I.R. & EROUT B., 2001. AFTA®-calibrated 2-D modelling of hydrocarbon generation and migration using Temispack®: Preliminary results from the Otway Basin. Submitted to: The Eastern Australian Basin Symposium, Melbourne, November 25-28th 2001.

DUMITRU T.A. HILL K.C., COYLE D.A, DUDDY I.R., FOSTER D.A, GLEADOW A.J.W., GREEN P.F., LASLETT G.M., KOHN B.P. & O'SULLIVAN P.B., 1991. Fission Track Thermochronology: application to Continental Rifting of Southeastern Australia. *APPEA Journal*, **31** (1), 131-142.

HINZ K. WILCOX J.B., WHITICAR M., KUDRAS H.-R., EXON N.F. & FEARY D.A. 1986. The West Tasmanian Margin: An underrated Petroleum Province? *In*: Glenie R.C. ed. *Second South-eastern Australia Oil Exploration Symposium*, 14-15 November, Melbourne. p. 395-410.

NEWMAN, J, AND MOORE, N., 2001. Vitrinite-inertinite reflectance and fluorescence: analysis of samples from Cape Sorell-1. Unpublished report for AGSO.

ROSS L.M., 1982. Source rock evaluation, Amoco No.1 Cape Sorell well, offshore Tasmania, Australia. Amoco Production Company research Center. Technical Services 825385CF.

SWEENEY J.J. & BURNHAM A.K., 1990. Evaluation of a simple model of vitrinite reflectance based on chemical kinetics. *AAPG Bulletin*, 74, 1559-1570.

APPENDIX A

Sample Details, Geological Data and Apatite Compositions

A.1 AFTA and VR sample details

Eight cuttings samples from the **Cape Sorell-1 well, offshore western Tasmania** were processed for AFTA and of these, seven contained sufficient high quality apatite suitable for analysis. Details of all AFTA samples, including sample depths, stratigraphic ages and estimates of present temperature for each sample, are summarised in Table A.1. Yields of apatite obtained from each AFTA sample are also summarised in Table A.1. Details of present temperature estimation are summarised in Section A.4 (below).

Eleven cuttings samples were also submitted to Alan Cook of Keiraville Konsultants for vitrinite reflectance determination. Eight of these samples were splits from the AFTA cuttings samples and three were samples collected specifically for VR over narrower sample intervals. Details of the new VR analyses are provided in Table D.2 (Appendix D), with complete organic maceral descriptions, including fluorescence observations and recognition of oil also provided in Appendix D. In addition, existing vitrinite reflectance data from 5 data sets were provided by AGSO, as listed in Table D.3 (Appendix D). Additional comments on the quality of the new VR data are provided in Section 1.3 of the main report. The quality of the supplied organic maturity data are unknown, but they are treated at face value in this report.

A.2 Apatite yields and data quality

Sufficient apatite suitable for analysis was provided by seven of the eight samples processed from **Cape Sorell-1.** Apatite yields suitable for fission track age determinations varied from excellent (>20 grains – the target for a determination) in two samples, good (15 to 19 grains) in one sample and fair (10 to 14 grains) in four samples, as summarised in Table A1. Track length data is of lesser quality with less than 20 confined track length measurements obtained for all samples compared with the target of 100 measurements. Despite the relatively low numbers of track length measurements, the good quality of the apatite and the more precise fission track age data are such that reliable constraints have been placed on the thermal history of the sampled well section.

A.3 Stratigraphic details

Details of the stratigraphic breakdown of the preserved section in the Cape Sorell-1 well, including chronostratic ages for the Formation tops, were supplied by AGSO. The resulting information is summarised in Table A.2, in the form of depths and ages of major units in each well. The stratigraphic age of each AFTA sample, derived from this information, is summarised in Table A.1, while similar information for organic maturity samples is summarised in Tables D.2 and D.3 (Appendix D).

Any *slight* errors in the estimated chronometric ages of each sample are not expected to affect the thermal history interpretation of either the AFTA or VR data to any significant degree, because of the profound effects of elevated paleotemperatures after deposition in all samples.

A.4 Present temperatures

In application of any technique involving estimation of paleotemperatures, it is critical to control the present temperature profile, since estimation of maximum paleotemperatures proceeds from trying to determine how much of the observed effect can be explained by the magnitude of present temperatures.

For **Cape Sorell-1**, corrected BHT values at three depths derived from measured temperatures recorded during logging were provided by AGSO. These data were combined with a present-day sea-bed temperature of 17.3°C also provided by AGSO, and a linear present-day geothermal of 27.6°C/km has been determined. The fit of the corrected temperature data to this linear gradient is quite good, as illustrated in Figure A.1, and this gradient has therefore been used to estimate the present-day temperature at which each AFTA and VR sample resides. Interpretation of the AFTA results (Section 3.2) suggests that a slight downward revision of the geothermal gradient to 26.7°C/km is warranted, but this is well within the typical uncertainty in an estimate of a present-day gradient. In the course of the study, the possibility of a lower present-day gradient of 22°C/km, more consistent with the VR data in the Late Cretaceous section of the well, was also investigated, but such a low gradient is both inconsistent with the corrected BHT values and the AFTA results, and has been rejected.

A.5 Grain morphologies

The majority of grains analysed from all samples from the Wangeripp and Sherbrook Group sediments are euhedral to sub-rounded euhedral in shape, with a lesser number of

to rounded and anhedral forms. There are obvious trends that can be related to the stratigraphy or possible provenance differences.

A.6 Apatite compositions

The annealing kinetics of fission tracks in apatite are affected by chemical composition, specifically the Cl content, as explained in more detail in Appendix C. In all samples collected for this study, Cl contents were measured in all apatite grains analysed (i.e. for both fission track age determination and track length measurement), and the measured compositions in individual grains have been employed in interpreting the AFTA data, using methods outlined in Appendix C.

Chlorine contents were measured using a fully automated Jeol JXA-5A electron microprobe equipped with a computer controlled X-Y-Z stage and three computer controlled wavelength dispersive crystal spectrometers, with an accelerating voltage of 15kV and beam current of 25nA. The beam was defocussed to 20 µm diameter to avoid problems associated with apatite decomposition, which occur under a fully focussed 1 µm - 2 µm beam. The X-Y co-ordinates of dated grains within the grain mount were transferred from the Autoscan Fission Track Stage to a file suitable for direct input into the electron microprobe. The identification of each grain was verified optically prior to analysis. Cl count rates from the analysed grains were converted to wt% Cl by reference to those from a Durango apatite standard (Melbourne University Standard APT151), analysed at regular intervals. This approach implicitly takes into account atomic number absorption and fluorescence matrix effects, which are normally calculated explicitly when analysing for all elements. A value of 0.43 wt% Cl was used for the Durango standard, based on repeated measurements on the same single fragment using pure rock salt (NaCl) as a standard for chlorine. This approach gives essentially identical results to Cl contents determined from full compositional measurements, but has the advantage of reducing analytical time by a factor of ten or more.

Cl contents in individual grains are listed in the fission track Age Data Sheets in Appendix B, together with histograms of Cl contents in individual samples and plots of fission track age against Cl content. Table B.3 (Appendix B) contains fission track age and length data grouped into 0.1 wt% Cl intervals on the basis of chlorine contents of the grains from which the data are derived.

The majority of **Cape Sorell-1** samples have apatites with Cl content between 0 and 0.5wt%, which are similar to the “normal sandstone” type (eg (quartzose and arkosic

sandstones) derived from mixed “granitic basement” terrains, as illustrated in Figure C.4b, Appendix C.

Sample 806-2 from the Sherbrook Group contains apatite with a relatively broad range of Cl up to 1.5%wt % Cl, a pattern which is typical of the presence of volcanogenic detritus in this sample (compare the histogram for this sample with that shown in Figure C.4c, Appendix C). As noted in the text, such volcanogenic detritus might be derived from reworking of volcanogenic sediments from Early Cretaceous Otway Group or from Triassic sediments of similar character known from the Tasmanian mainland.

Most apatite in Wangeripp Group sample GC806-7 contains less than 0.5 wt% Cl, typical of normal quartzose and arkosic sandstones (e.g. Figure C.4b, Appendix C), but one grain with ~1.4%wt % Cl suggests the presence of volcanogenic detritus in this sample (compare the histogram for this sample with that shown in Figure C.4c, Appendix C).

The histogram of Cl contents for apatites from Sherbrook Group sample GC806-1 show a more restricted range of Cl content, with less than 0.1 wt% Cl in all analysed grains. Such uniform composition suggests a more restricted provenance, perhaps a single granitic body, contributing sediment to this sample.

Lower limits of detection for chlorine content have been calculated for typical analytical conditions (beam current, counting time, etc.) and are listed in Table A.4. Errors in wt% composition are given as a percentage and quoted at 1σ for chlorine determinations. A generalised summary of errors for various wt% chlorine values is presented in Table A.5.

Table A.1: Details of fission track samples and apatite yields - samples from Cape Sorell-1 (Geotrack Report #806)

Sample number	Depth (m)	Sample type	Stratigraphic Subdivision	Stratigraphic age (Ma)	Present temperature *1 (°C)	Raw weight (g)	Washed weight (g)	Apatite yield *2
Cape Sorell-1								
GC806-6	1216-1372 *(3990-4500')*	cuttings	Wangerripp 4 - Wangerripp 3	53-50	50	195	150	none
GC806-7	1500-1631 *(4920-5350')*	cuttings	Wangerripp 5 - Wangerripp 4	55-51	57	196	150	fair
GC806-8	1929-2051 *(6330-6730')*	cuttings	Sherbrook 1	70-65	69	280	190	excellent
GC806-1	2198-2307 *(7210-7570')*	cuttings	Sherbrook 1	70-65	76	239	140	good
GC806-9	2637-2752 *(8650-9030')*	cuttings	Sherbrook 2 - Sherbrook 1	73-65	88	280	180	fair
GC806-2	2899-3008 *(9510-9870')*	cuttings	Sherbrook 2	73-70	96	220	140	excellent
GC806-10	3142-3249 *(10310-10660')*	cuttings	Sherbrook 3	78-73	102	293	170	fair
GC806-3	3399-3501 *(11150-11485')*	cuttings	Sherbrook 5 - Sherbrook 4	80-78	109	380	200	fair

*1 See Appendix A for discussion of present temperature data.

*2 Yield based on quantity of mineral suitable for age determination. Excellent: >20 grains; Good: 15-19 grains; Fair: 10-14 grains; Poor: 5-9 grains; Very Poor: <5 grains.

Table A.2: Summary of stratigraphy - Cape Sorell-1 (Geotrack Report #806)

	KB elevation (mAMSL)	Water Depth (m)	Stratigraphic Interval	Depth of Top TVD rKB (m)	Age of Top (Ma)
Cape Sorell-1					
	22	94	Miocene - Recent	116	0
			Heytesbury Gp	120	6
			Heytesbury lst	210	20
			Unconformity	338	27.7
			Nirranda Gp 1	338	32
			Nirranda Gp 2	460	37
			Nirranda Gp 3	549	47
			Wangerripp 1	675	48
			Wangerripp 2	823	49
			Wangerripp 3	1200	50
			Wangerripp 4	1316	51
			Wangerripp 5	1610	53
			Wangerripp 6	1808	55
			Unconformity	1920	59
			Sherbrook 1	1920	65
			Sherbrook 2	2740	70
			Sherbrook 3	3112	73
			Sherbrook 4	3390	78
			Sherbrook 5	3490	79
			TD	3523	80

All depths quoted are with respect to KB, except where otherwise stated.

Table A.3: Summary of temperature data - Cape Sorell-1 (Geotrack Report #806)

KB elevation (mAMSL)	Water Depth (m)	Depth (ft)	BHT (°F)	BHT (°C)	T.S.C (hrs)	Depth (m)	Client Corrected BHT (°C)	Corrected BHT (°C)	Geothermal gradient (°C/km)
Cape Sorell-1									
22	94								27.6
		4157	102.2	39.0	10	1267.0	43.0		
		9026	176.0	80.0	25	2751.0	88.0		
		11558	230.0	110.0	19	3523.0	115.0		

Client correction method unknown. A sea-bed temperature of 17.3°C has been assumed.

All depths quoted are with respect to KB, except where otherwise stated.

Table A.4: Lower Limits of Detection for Apatite Analyses (Geotrack Report #806)

Element	LLD (95% c.l.)		LLD (99% c.l.)	
	(wt%)	(ppm)	(wt%)	(ppm)
Cl	0.01	126	0.02	182

Table A.5: Per cent errors in chlorine content (Geotrack Report #806)

Chlorine content (wt%)	Error (%)
0.01	9.3
0.02	8.7
0.05	7.3
0.10	6.1
0.20	4.7
0.50	3.2
1.00	2.3
1.50	1.9
2.00	1.7
2.50	1.5
3.00	1.4

Errors quoted are at 1σ. See Appendix A for more details.

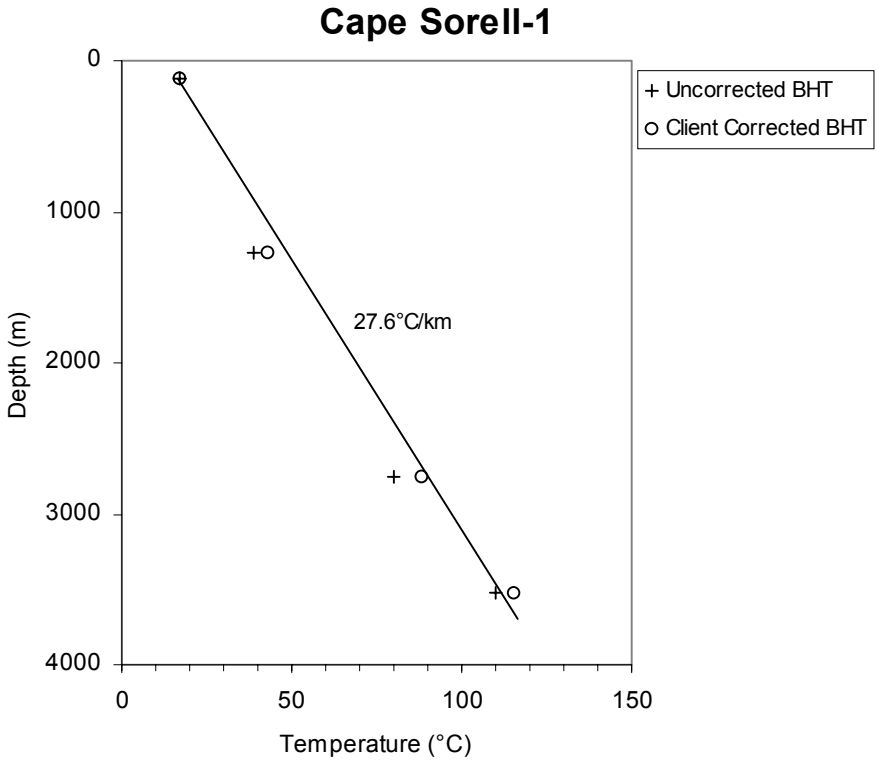

Figure A.1: Present temperature profile calculated for **well Cape Sorell-1.** See Table A.3 and Appendix A for more detail.

APPENDIX B

Sample Preparation, Analytical Details and Data Presentation

B.1 Sample Preparation

Core and outcrop samples are crushed in a jaw crusher and then ground to sand grade in a rotary disc mill. Cuttings samples are washed and dried before grinding to sand grade. The ground material is then washed to remove dust, dried and processed by conventional heavy liquid and magnetic separation techniques to recover heavy minerals. Apatite grains are mounted in epoxy resin on glass slides, polished and etched for 20 sec in 5M HNO_3 at 20°C to reveal the fossil fission tracks.

After etching, all mounts are cut down to 1.5 x 1 cm, and cleaned in detergent, alcohol and distilled water. The mounts are then sealed in intimate contact with low-uranium muscovite detectors within heat-shrink plastic film. Each batch of mounts is stacked between two pieces of uranium standard glass, which has been prepared in similar fashion. The stack is then inserted into an aluminium can for irradiation.

After irradiation, the mica detectors are removed from the grain mounts and standard glasses and etched in hydrofluoric acid to reveal the fission tracks produced by induced fission of ^{235}U in the apatite and standard glass.

B.2 Analytical Details

Fission track ages

Fission track ages are calculated using the standard fission track age equation using the zeta calibration method (equation five of Hurford and Green, 1983), viz:

$$\text{F.T. AGE} = \frac{1}{\lambda_D} \ln \left[1 + \left(\frac{\zeta \lambda_D \rho_s g \rho_D}{\rho_i} \right) \right] \qquad \text{B.1}$$

where:
- λ_D = Total decay constant of ^{238}U (= 1.55125 x 10^{-10})
- ζ = Zeta calibration factor
- ρ_s = Spontaneous track density
- ρ_i = Induced track density
- ρ_D = Track density from uranium standard glass
- g = A geometry factor (= 0.5)

Fission track ages are determined by the external detector method or EDM (Gleadow, 1981). The EDM has the advantage of allowing fission track ages to be determined on single grains. In apatite, tracks are counted in 20 grains from each mount wherever possible. In those samples where the desired number is not present, all available grains are counted, the actual number depending on the availability of suitably etched and oriented grains. Only grains oriented with surfaces parallel to the crystallographic c-axis are analysed. Such grains can be identified on the basis of the etching characteristics, as well as from morphological evidence in euhedral grains. The grain mount is scanned sequentially, and the first 20 suitably oriented grains identified are analysed.

Tracks are counted within an eyepiece graticule divided into 100 grid squares. In each grain, the number of spontaneous tracks (N_s) within a certain number of grid squares (N_a) is recorded. The number of induced tracks (N_i) in the corresponding location within the mica external detector is then counted. Spontaneous and induced track densities (ρ_s and ρ_i, respectively) are calculated by dividing the track counts by the total area counted, given by the product of Na and the area or each grid square (determined by calibration against a ruled stage graticule or diffraction grating). Fission track ages may be calculated by substituting track counts (N_s and N_i) for track densities (ρ_s and ρ_i) in equation B.1, since the areas cancel in the ratio.

Translation between apatite grains in the grain mount and external detector locations corresponding to each grain is carried out using Autoscan™ microcomputer-controlled automatic stages (Smith and Leigh Jones, 1985). This system allows repeated movement between grain and detector, and all grain locations are stored for later reference if required.

Neutron irradiations are carried out in a well-thermalised flux (X-7 facility; Cd ratio for Au ~98) in the Australian Atomic Energy Commission's HIFAR research reactor. Total neutron fluence is monitored by counting tracks in mica external detectors attached to two pieces of Corning Glass Works standard glass CN5 (containing ~11 ppm Uranium) included in the irradiation canister at each end of the sample stack. In determining track densities in external detectors irradiated adjacent to uranium standard glasses, 25 fields are normally counted in each detector. The total track count (N_D) is divided by the total area counted to obtain the track density (ρ_D). The positions of the counted fields are arranged in a 5 X 5 grid covering the whole area of the detector. For typical track densities of between ~5 X 10^5 and 5 X 10^6, this is a convenient arrangement to sample across the detector while gathering sufficient counts to achieve a precision of ~±2% in a reasonable time.

A small flux gradient is often present in the irradiation facility over the length of the sample package. If a detectable gradient is present, the track count in the external detector adjacent to each standard glass is converted to a track density (ρ_D) and a value for each mount in the stack is calculated by linear interpolation. When no detectable gradient is present, the track counts in the two external detectors are pooled to give a single value of ρ_D, which is used to calculate fission track ages for each sample.

A Zeta calibration factor (ζ) has been determined empirically for each observer by analysing a set of carefully chosen age standards with independently known K-Ar ages, following the methods outlined by Hurford and Green (1983) and Green (1985).

All track counting is carried out using Zeiss(R) Axioplan microscopes, with an overall linear magnification of 1068 x using dry objectives.

For further details and background information on practical aspects of fission track age determination, see e.g. Fleischer, Price and Walker (1975), Naeser (1979) and Hurford (1986).

Track length measurements

For track length studies in apatite, the full lengths of "confined" fission tracks are measured. Confined tracks are those which do not intersect the polished surface but have been etched from other tracks or fractures, so that the whole length of the track is etched. Confined track lengths are measured using a digitising tablet connected to a microcomputer, superimposed on the microscope field of view via a projection tube. With this system, calibrated against a stage graticule ruled in 2 μm divisions, individual tracks can be measured to a precision of ± 0.2 μm. Tracks are measured only in prismatic grains, characterised by sharp polishing scratches with well-etched tracks of narrow cone angle in all orientations, because of the anisotropy of annealing of fission tracks in apatite (as discussed by Green et al. 1986). Tracks are also measured following the recommendations of Laslett et al. (1982), the most important of which is that only horizontal tracks should be measured. One hundred tracks are measured whenever possible. In apatite samples with low track density, or in those samples in which only a small number of apatite grains are obtained, fewer confined tracks may be available. In such cases, the whole mount is scanned to measure as many confined tracks as possible.

Integrated fission track age and length measurement

Fission track age determination and length measurement are now made in a single pass of the grain mount, in an integrated approach. The location of each grain in which

tracks are either counted or measured is recorded for future reference. Thus, track length measurements can be tied to age determination in individual grains. As a routine procedure we do not measure the age of every grain in which lengths are determined, as this would be much too time-consuming. Likewise we do not only measure ages in grain in which lengths are measured, as this would bias the age data against low track density grains. Nevertheless, the ability to determine the fission track age of certain grains from which length data originate can be a particularly useful aid to interpretation in some cases. Grain location data are not provided in this report, but are available on request.

B.3 Data Presentation

Fission track age data

Data sheets summarising the apatite fission track age data, including full details of fission track age data for individual apatite grains in each sample, together with the primary counting results and statistical data, are given in the following pages. Individual grain fission track ages are calculated from the ratio of spontaneous to induced fission track counts for each grain using equation B.1, and errors in the single grain ages are calculated using Poissonian statistics, as explained in more detail by Galbraith (1981) and Green (1981). All errors are quoted as $\pm 1\sigma$ throughout this report, unless otherwise stated.

The variability of fission track ages between individual apatite grains within each sample can be assessed using a chi-squared (χ^2) statistic (Galbraith, 1981), the results of which are summarised for each sample in the data sheets. If all the grains counted belong to a single age population, the probability of obtaining the observed χ^2 value, for ν degrees of freedom (where ν = number of crystals -1), is listed in the data sheets as $P(\chi^2)$ or P(chi squared).

A $P(\chi^2)$ value greater than 5% can be taken as evidence that all grains are consistent with a single population of fission track age. In this case, the best estimate of the fission track age of the sample is given by the "pooled age", calculated from the ratio of the total spontaneous and induced track counts in all grains analysed. Errors for the pooled age are calculated using the "conventional" technique outlined by Green (1981), based on the total number of tracks counted for each track density measurement (see also Galbraith, 1981).

A $P(\chi^2)$ value of less than 5% denotes a significant spread of single grain ages, suggesting real differences exist between the fission track ages of individual apatite

grains. A significant spread in grain ages can result either from inheritance of detrital grains from mixed source areas (in sedimentary rocks), or from differential annealing in apatite grains of different composition, within a narrow range of temperature.

Calculation of the pooled age inherently assumes that only a single population of ages is present, and is thus not appropriate to samples containing a significant spread of fission track ages. In such cases Galbraith, has recently devised a means of estimating the modal age of a distribution of single grain fission track ages which is referred to as the "central age". Calculation of the central age assumes that all single grain ages belong to a Normal distribution of ages, with a standard deviation (σ) known as the "age dispersion". An iterative algorithm (Galbraith and Laslett, 1993) is used to provide estimates of the central age with its associated error, and the age dispersion, which are all quoted in the data sheets. Note that this treatment replaces use of the "mean age", which has used been in the past for those samples in which $P(\chi^2)<5\%$. For samples in which $P(\chi^2)>5\%$, the central age and the pooled age should be equal, and the age dispersion should be less than ~10%.

Table B.1 summarises the fission track age data in apatite from each sample analysed.

Construction of radial plots of single grain age data

Single grain age data are best represented in the form of radial plot diagrams (Galbraith, 1988, 1990). As illustrated in Figure B.1, these plots display the variation of individual grain ages in a plot of y against x, where:

$$y = (z_j - z_o) / \sigma_i \qquad x = 1/\sigma_j \qquad \text{B.2}$$

and; z_j = Fission track age of grain j
z_o = A reference age
σ_j = Error in age for grain j

In this plot, all points on a straight line from the origin define a single value of fission track age, and, at any point, the value of x is a measure of the precision of each individual grain age. Therefore, precise individual grain ages fall to the right of the plot (small error, high x), which is useful, for example, in enabling precise, young grains to be identified. The age scale is shown radially around the perimeter of the plot (in Ma). If all grains belong to a single age population, all data should scatter between y = +2 and y = -2, equivalent to scatter within $\pm 2\sigma$. Scatter outside these boundaries shows a significant spread of individual grain ages, as also reflected in the values of $P(\chi^2)$ and age dispersion.

In detail, rather than using the fission track age for each grain as in equation B.2, we use:

$$z_j = \frac{N_{sj}}{N_{ij}} \qquad \sigma_j = \{1/N_{sj} + 1/N_{ij}\} \qquad \text{B.3}$$

as we are interested in displaying the scatter within the data from each sample in comparison with that allowed by the Poissonian uncertainty in track counts, without the additional terms which are involved in determination of the fission track age (ρ_D, ζ, etc).

Zero ages cannot be displayed in such a plot. This can be achieved using a modified plot, (Galbraith, 1990) with:

$$z_j = \text{arc sin}\sqrt{\left\{\frac{N_{sj}+3/8}{N_{sj}+N_{ij}+3/4}\right\}} \qquad \sigma_j = \frac{1}{2}\sqrt{\left\{\frac{1}{N_{sj}+N_{ij}}\right\}} \qquad \text{B.4}$$

Note that the numerical terms in the equation for z_j are standard terms, introduced for statistical reasons. Using this arc-sin transformation, zero ages plot on a diagonal line which slopes from upper left to lower right. Note that this line does not go through the origin. Figure B.2 illustrates this difference between conventional and arc-sin radial plots, and also provides a simple guide to the structure of radial plots.

Use of arc-sin radial plots is particularly useful in assessing the relative importance of zero ages. For instance, grains with $N_s = 0$, $N_i = 1$ are compatible with ages up to ~900 Ma (at the 95% confidence level), whereas grains with $N_s = 0$, $N_i = 50$ are only compatible with ages up to ~14 Ma. The two data would readily be distinguishable on the radial plot as the 0,50 datum would plot well to the right (high x) compared to the 0,1 datum.

In this report the value of z corresponding to the stratigraphic age of each sample (or the midpoint of the range where appropriate) is adopted as the reference value, z_o. This allows rapid assessment of the fission track age of individual grains in relation to the stratigraphic age, which is a key component in the interpretation of AFTA data, as explained in more detail in Appendix C.

Note that the x axis of the radial plot is normally not labelled, as this would obscure the age scale around the plot. In general labelling is not considered necessary, as we are concerned only with relative variation within the data, rather than absolute values of precision.

Radial plots of the single grain age data in apatite from each sample analysed in this report are shown on the fission track age data summary sheets at the end of this Appendix. Use of radial plots to provide thermal history information is explained in Appendix C and Figure C.7.

Track length data

Distributions of confined track lengths in apatite from each sample are shown as simple histograms on the fission track age data summary sheets at the end of this Appendix. For every track length measurement, the length is recorded to the nearest 0.1 μm, but the measurements have been grouped into 1 μm intervals for construction of these histograms. Each distribution has been normalised to 100 tracks for each sample to facilitate comparison. A summary of the length distribution in each sample is presented in Table B.2, which also shows the mean track length in each sample and its associated error, the standard deviation of each distribution and the number of tracks (N) measured in each sample. The angle which each confined track makes with the crystallographic c-axis is also routinely recorded, as is the width of each fracture within which tracks are revealed. These data are not provided in this report, but can be supplied on request.

Breakdown of data into compositional groups

In Table B.3, AFTA data are grouped into compositional intervals of 0.1 wt% Cl width. Parameters for each interval represent the data from all grains with Cl contents within each interval. Also shown are the parameters for each compositional interval predicted from the Default Thermal History (see Section 2.1). These data form the basis of interpretation of the AFTA data, which takes full account of the influence of Cl content on annealing kinetics, as described in Appendix C. Distributions of Cl contents in all apatites analysed from each sample (i.e. for both age and length determinations) are shown on the fission track age data summary sheets at the end of this Appendix.

Plots of fission track age against Cl content for individual apatite grains

Fission track ages of single apatite grains within individual samples are plotted against the Cl content of each grain on the fission track age data summary sheets at the end of this Appendix. These plots are useful in assessing the degree of annealing, as expressed by the fission track age data. For example, if grains with a range of Cl contents from zero to some upper limit all give similar fission track ages which are significantly less than the stratigraphic age, then grains with these compositions must have been totally annealed. Alternatively, if fission track age falls rapidly with decreasing Cl content, the sample displays a high degree of partial annealing.

B.4 A note on terminology

Note that throughout this report, the term "fission track age" is understood to denote the parameter calculated from the fission track age equation, using the observed spontaneous and induced track counts (either pooled for all grains or for individual grains). The resulting number (with units of Ma) should not be taken as possessing any significance in terms of events taking place at the time indicated by the measured fission track age, but should rather be regarded as a measure of the integrated thermal history of the sample, and should be interpreted in that light using the principles outlined in Appendix C. Use of the term "apparent age" is not considered to be useful in this regard, as almost every fission track age should be regarded as an apparent age, in the classic sense, and repeated use becomes cumbersome.

References

Fleischer, R. L., Price, P. B., and Walker, R. M. (1975) Nuclear tracks in solids, University of California Press, Berkeley.

Galbraith, R. F. (1981) On statistical models for fission-track counts. *Mathematical Geology*, 13, 471-488.

Galbraith, R. F. (1988) Graphical display of estimates having differing standard errors. *Technometrics*, 30, 271-281.

Galbraith, R. F. (1990) The radial plot: graphical assessment of spread in ages. *Nuclear Tracks*, 17, 207-214.

Galbraith R.F. & Laslett G.M. (1993) Statistical methods for mixed fission track ages. *Nuclear Tracks* 21, 459-470.

Gleadow, A. J. W. (1981) Fission track dating methods; what are the real alternatives? *Nuclear Tracks*, 5, 3-14.

Green, P. F. (1981) A new look at statistics in fission track dating. *Nuclear Tracks 5*, 77-86.

Green, P. F. (1985) A comparison of zeta calibration baselines in zircon, sphene and apatite. *Chem. Geol. (Isot. Geol. Sect.)*, 58, 1-22.

Green, P. F., Duddy, I. R., Gleadow, A. J. W., Tingate, P. R. and Laslett, G. M. (1986) Thermal annealing of fission tracks in apatite 1. A qualitative description. *Chem. Geol. (Isot. Geosci. Sect.)*, 59, 237-253.

Hurford, A. J. (1986) Application of the fission track dating method to young sediments: Principles, methodology and Examples. *In:* Hurford, A. J., Jäger, E. and Ten Cate, J. A. M. (*eds*), Dating young sediments, CCOP Technical Publication 16, CCOP Technical Secretariat, Bangkok, Thailand.

Hurford, A. J. and Green, P. F. (1982) A user's guide to fission track dating calibration. *Earth. Planet. Sci Lett.* 59, 343-354.

Hurford, A. J. and Green, P. F. (1983) The zeta age calibration of fission track dating. *Isotope Geoscience* 1, 285-317.

Laslett, G. M., Kendall, W. S., Gleadow, A. J. W. and Duddy, I. R. (1982) Bias in measurement of fission track length distributions. *Nuclear Tracks*, 6, 79-85.

Naeser, C. W. (1979) Fission track dating and geologic annealing of fission tracks. *In:* Jäger, E. and Hunziker, J. C. (*eds*), Lectures in Isotope Geology, Springer Verlag, Berlin.

Smith, M. J. and Leigh-Jones, P. (1985) An automated microscope scanning stage for fission-track dating. *Nuclear Tracks*, 10, 395-400.

Table B.1: Apatite fission track analytical results - samples from Cape Sorell-1 (Geotrack Report #806)

Sample number	Number of grains	ρ_D (N_D) x10^6/cm²	ρ_s (N_s) x10^6/cm²	ρ_i (N_i) x10^6/cm²	Uranium content (ppm)	$P(\chi^2)$ (%)	Age dispersion (%)	Fission track age (Ma)
Cape Sorell-1								
GC806-1	19	1.109 (1847)	0.209 (59)	0.919 (259)	9	36	10	47.9 ± 7.0
GC806-2	20	1.127 (1847)	0.759 (247)	2.096 (682)	21	<1	43	77.2 ± 6.1 *74.2 ± 9.9**
GC806-3	13	1.146 (1847)	0.212 (50)	1.241 (292)	12	<1	141	37.2 ± 5.8 *24.7 ± 11.4**
GC806-6			No apatite					
GC806-7	12	1.165 (1847)	0.942 (182)	2.122 (410)	21	<1	66	97.6 ± 9.1 *92.2 ± 20.8**
GC806-8	20	1.183 (1847)	0.575 (204)	2.412 (856)	23	1	35	53.4 ± 4.4 *51.1 ± 6.3**
GC806-9	14	1.202 (1847)	0.317 (67)	2.445 (517)	23	1	54	29.6 ± 3.9 *27.9 ± 5.9**
GC806-10	10	1.221 (1847)	0.163 (38)	1.516 (354)	14	<1	198	24.9 ± 4.3 *11.5 ± 8.2**

ρ_s = spontaneous track density; ρ_i = induced track density; ρ_D = track density in glass standard external detector. Brackets show number of tracks counted. ρ_D and ρ_i measured in mica external detectors; ρ_s measured in internal surfaces.
*Central age, used where sample contains a significant spread of single grain ages ($P(\chi^2)$<5%). Errors quoted at 1σ.
Ages calculated using dosimeter glass CN5, with a zeta of 380.4 ± 5.7 (Analyst: C. O'Brien) for samples; 1 - 10

Table B.2: Length distribution summary data - samples from Cape Sorell-1 (Geotrack Report #806)

Sample number	Mean track length (µm)	Standard deviation (µm)	Number of tracks (N)	Number of tracks in Length Intervals (µm)																			
				1	2	3	4	5	6	7	8	9	10	11	12	13	14	15	16	17	18	19	20
Cape Sorell-1																							
GC806-1	10.97 ± 0.50	1.51	9	-	-	-	-	-	-	-	-	1	1	4	-	2	1	-	-	-	-	-	-
GC806-2	9.76 ± 0.79	1.94	6	-	-	-	-	-	-	1	-	1	-	2	2	-	-	-	-	-	-	-	-
GC806-3	10.70 ± 0.43	0.85	4	-	-	-	-	-	-	-	-	-	1	2	1	-	-	-	-	-	-	-	-
GC806-6	No apatite	-	-	-	-	-	-	-	-	-	-	-	-	-	-	-	-	-	-	-	-	-	-
GC806-7	12.36 ± 0.28	1.01	13	-	-	-	-	-	-	-	-	-	-	1	4	5	2	1	-	-	-	-	-
GC806-8	11.76 ± 0.31	1.27	17	-	-	-	-	-	-	-	-	-	1	3	7	5	-	-	1	-	-	-	-
GC806-9	12.05 ± 0.65	1.13	3	-	-	-	-	-	-	-	-	-	-	-	2	-	1	-	-	-	-	-	-
GC806-10	10.34 ± 1.48	2.09	2	-	-	-	-	-	-	-	-	1	-	-	1	-	-	-	-	-	-	-	-

Track length measurements by: C. O'Brien for samples; 1 - 10

Table B.3: AFTA Data in Compositional Groups - (Geotrack Report #806)

Cl	Default fission track age*	Measured fission track age	Error in age	P (χ2)	Number of grains	Default fission track length*	Mean track length	Error in length	Std deviation	Number of lengths	Number of grains	Number of tracks in length interval																				
												1	2	3	4	5	6	7	8	9	10	11	12	13	14	15	16	17	18	19	20
Wt %	(Ma)	(Ma)	(Ma)			(µm)	(µm)	(µm)	(µm)			(µm)																				
Cape Sorell-1																																
806-1†	**51.5**	**47.9**	**7.0**	**36.0**	**19**	**11.4**	**11.0**	**0.5**	**1.5**	**9**	**5**	**0**	**0**	**0**	**0**	**0**	**0**	**0**	**0**	**1**	**1**	**4**	**0**	**2**	**1**	**0**	**0**	**0**	**0**	**0**	**0**
0.0-0.1	51.5	47.9	7.0	36.0	19	11.4	11.0	0.5	1.5	9	5	0	0	0	0	0	0	0	0	1	1	4	0	2	1	0	0	0	0	0	0
806-2†	**23.2**	**74.2**	**9.7**	**0.0**	**20**	**11.1**	**9.8**	**0.8**	**1.9**	**6**	**4**	**0**	**0**	**0**	**0**	**0**	**0**	**1**	**0**	**1**	**0**	**2**	**2**	**0**	**0**	**0**	**0**	**0**	**0**	**0**	**0**
0.0-0.1	10.1	61.6	11.1	2.0	10	9.1	0.0	0.0	0.0	0	0	0	0	0	0	0	0	0	0	0	0	0	0	0	0	0	0	0	0	0	0
0.1-0.2	22.4	62.9	14.5	4.0	5	9.2	9.7	1.4	2.0	2	1	0	0	0	0	0	0	0	0	1	0	0	1	0	0	0	0	0	0	0	0
0.2-0.3	32.6	98.2	34.3	100.0	1	9.5	0.0	0.0	0.0	0	0	0	0	0	0	0	0	0	0	0	0	0	0	0	0	0	0	0	0	0	0
0.3-0.4	-	-	-	-	-	-	-	-	-	-	-	-	-	-	-	-	-	-	-	-	-	-	-	-	-	-	-	-	-	-	-
0.4-0.5	-	-	-	-	-	-	-	-	-	-	-	-	-	-	-	-	-	-	-	-	-	-	-	-	-	-	-	-	-	-	-
0.5-0.6	51.5	66.7	24.2	100.0	1	10.6	11.3	0.0	0.0	1	1	0	0	0	0	0	0	0	0	0	0	0	1	0	0	0	0	0	0	0	0
0.6-0.7	-	-	-	-	-	-	-	-	-	-	-	-	-	-	-	-	-	-	-	-	-	-	-	-	-	-	-	-	-	-	-
0.7-0.8	54.0	88.7	47.3	100.0	1	11.1	0.0	0.0	0.0	0	0	0	0	0	0	0	0	0	0	0	0	0	0	0	0	0	0	0	0	0	0
0.8-0.9	-	-	-	-	-	-	-	-	-	-	-	-	-	-	-	-	-	-	-	-	-	-	-	-	-	-	-	-	-	-	-
0.9-1.0	-	-	-	-	-	-	-	-	-	-	-	-	-	-	-	-	-	-	-	-	-	-	-	-	-	-	-	-	-	-	-
1.0-1.1	-	-	-	-	-	-	-	-	-	-	-	-	-	-	-	-	-	-	-	-	-	-	-	-	-	-	-	-	-	-	-
1.1-1.2	55.9	178.9	73.4	100.0	1	11.5	10.7	0.1	0.1	2	1	0	0	0	0	0	0	0	0	0	0	2	0	0	0	0	0	0	0	0	0
1.2-1.3	-	-	-	-	-	-	-	-	-	-	-	-	-	-	-	-	-	-	-	-	-	-	-	-	-	-	-	-	-	-	-
1.3-1.4	56.2	0.0	0.0	0.0	0	11.6	6.5	0.0	0.0	1	1	0	0	0	0	0	0	1	0	0	0	0	0	0	0	0	0	0	0	0	0
1.4-1.5	56.4	181.2	45.3	100.0	1	11.6	0.0	0.0	0.0	0	0	0	0	0	0	0	0	0	0	0	0	0	0	0	0	0	0	0	0	0	0
806-3†	**2.3**	**24.7**	**11.4**	**0.0**	**13**	**9.1**	**10.7**	**0.4**	**0.9**	**4**	**3**	**0**	**0**	**0**	**0**	**0**	**0**	**0**	**0**	**0**	**1**	**2**	**1**	**0**	**0**	**0**	**0**	**0**	**0**	**0**	**0**
0.0-0.1	0.6	17.7	9.5	0.0	12	8.9	10.8	0.6	1.0	3	2	0	0	0	0	0	0	0	0	0	1	1	1	0	0	0	0	0	0	0	0
0.1-0.2	-	-	-	-	-	-	-	-	-	-	-	-	-	-	-	-	-	-	-	-	-	-	-	-	-	-	-	-	-	-	-
0.2-0.3	-	-	-	-	-	-	-	-	-	-	-	-	-	-	-	-	-	-	-	-	-	-	-	-	-	-	-	-	-	-	-
0.3-0.4	-	-	-	-	-	-	-	-	-	-	-	-	-	-	-	-	-	-	-	-	-	-	-	-	-	-	-	-	-	-	-
0.4-0.5	-	-	-	-	-	-	-	-	-	-	-	-	-	-	-	-	-	-	-	-	-	-	-	-	-	-	-	-	-	-	-
0.5-0.6	22.5	127.0	50.7	100.0	1	9.1	10.3	0.0	0.0	1	1	0	0	0	0	0	0	0	0	0	0	1	0	0	0	0	0	0	0	0	0

* Fission Track Age and Mean Track Length predicted from the Default Thermal History (i.e. if the sample has not been hotter in the past)

† Combined data for all compositional groups

Table B.3: Continued - (Geotrack Report #806)

Cl Wt %	Default fission track age* (Ma)	Measured fission track age (Ma)	Error in age (Ma)	P (χ2)	Number of grains	Default fission track length* (µm)	Mean track length (µm)	Error in length (µm)	Std deviation (µm)	Number of lengths	Number of grains	Number of tracks in length interval (µm): 1	2	3	4	5	6	7	8	9	10	11	12	13	14	15	16	17	18	19	20
806-7†	**46.9**	**92.2**	**20.6**	**0.0**	**12**	**13.1**	**12.4**	**0.3**	**1.0**	**13**	**6**	**0**	**0**	**0**	**0**	**0**	**0**	**0**	**0**	**0**	**0**	**1**	**4**	**5**	**2**	**1**	**0**	**0**	**0**	**0**	**0**
0.0-0.1	46.4	63.5	20.9	0.0	7	13.0	12.2	0.4	1.0	8	3	0	0	0	0	0	0	0	0	0	0	1	3	2	2	0	0	0	0	0	0
0.1-0.2	46.8	117.4	26.0	4.0	3	13.1	12.2	0.3	0.6	4	2	0	0	0	0	0	0	0	0	0	0	0	1	3	0	0	0	0	0	0	0
0.2-0.3	-	-	-	-	-	-	-	-	-	-	-	-	-	-	-	-	-	-	-	-	-	-	-	-	-	-	-	-	-	-	-
0.3-0.4	-	-	-	-	-	-	-	-	-	-	-	-	-	-	-	-	-	-	-	-	-	-	-	-	-	-	-	-	-	-	-
0.4-0.5	48.0	237.2	99.2	100.0	1	13.4	14.2	0.0	0.0	1	1	0	0	0	0	0	0	0	0	0	0	0	0	0	0	1	0	0	0	0	0
0.5-0.6	-	-	-	-	-	-	-	-	-	-	-	-	-	-	-	-	-	-	-	-	-	-	-	-	-	-	-	-	-	-	-
0.6-0.7	-	-	-	-	-	-	-	-	-	-	-	-	-	-	-	-	-	-	-	-	-	-	-	-	-	-	-	-	-	-	-
0.7-0.8	-	-	-	-	-	-	-	-	-	-	-	-	-	-	-	-	-	-	-	-	-	-	-	-	-	-	-	-	-	-	-
0.8-0.9	-	-	-	-	-	-	-	-	-	-	-	-	-	-	-	-	-	-	-	-	-	-	-	-	-	-	-	-	-	-	-
0.9-1.0	-	-	-	-	-	-	-	-	-	-	-	-	-	-	-	-	-	-	-	-	-	-	-	-	-	-	-	-	-	-	-
1.0-1.1	-	-	-	-	-	-	-	-	-	-	-	-	-	-	-	-	-	-	-	-	-	-	-	-	-	-	-	-	-	-	-
1.1-1.2	-	-	-	-	-	-	-	-	-	-	-	-	-	-	-	-	-	-	-	-	-	-	-	-	-	-	-	-	-	-	-
1.2-1.3	-	-	-	-	-	-	-	-	-	-	-	-	-	-	-	-	-	-	-	-	-	-	-	-	-	-	-	-	-	-	-
1.3-1.4	-	-	-	-	-	-	-	-	-	-	-	-	-	-	-	-	-	-	-	-	-	-	-	-	-	-	-	-	-	-	-
1.4-1.5	49.3	217.8	97.5	100.0	1	13.8	0.0	0.0	0.0	0	0	0	0	0	0	0	0	0	0	0	0	0	0	0	0	0	0	0	0	0	0
806-8†	**53.5**	**51.1**	**6.2**	**1.0**	**20**	**12.2**	**11.8**	**0.3**	**1.3**	**17**	**10**	**0**	**0**	**0**	**0**	**0**	**0**	**0**	**0**	**0**	**1**	**3**	**7**	**5**	**0**	**0**	**1**	**0**	**0**	**0**	**0**
0.0-0.1	53.5	49.8	6.4	1.0	19	12.1	11.5	0.3	1.0	12	7	0	0	0	0	0	0	0	0	0	1	2	5	4	0	0	0	0	0	0	0
0.1-0.2	54.2	74.6	26.0	100.0	1	12.2	10.9	0.0	0.0	1	1	0	0	0	0	0	0	0	0	0	0	1	0	0	0	0	0	0	0	0	0
0.2-0.3	55.0	0.0	0.0	0.0	0	12.4	12.1	0.5	0.8	3	1	0	0	0	0	0	0	0	0	0	0	0	2	1	0	0	0	0	0	0	0
0.3-0.4	-	-	-	-	-	-	-	-	-	-	-	-	-	-	-	-	-	-	-	-	-	-	-	-	-	-	-	-	-	-	-
0.4-0.5	-	-	-	-	-	-	-	-	-	-	-	-	-	-	-	-	-	-	-	-	-	-	-	-	-	-	-	-	-	-	-
0.5-0.6	-	-	-	-	-	-	-	-	-	-	-	-	-	-	-	-	-	-	-	-	-	-	-	-	-	-	-	-	-	-	-
0.6-0.7	-	-	-	-	-	-	-	-	-	-	-	-	-	-	-	-	-	-	-	-	-	-	-	-	-	-	-	-	-	-	-
0.7-0.8	57.9	0.0	0.0	0.0	0	13.1	15.2	0.0	0.0	1	1	0	0	0	0	0	0	0	0	0	0	0	0	0	0	0	1	0	0	0	0
806-9†	**39.2**	**27.9**	**5.8**	**1.0**	**14**	**10.2**	**12.1**	**0.7**	**1.1**	**3**	**2**	**0**	**0**	**0**	**0**	**0**	**0**	**0**	**0**	**0**	**0**	**0**	**2**	**0**	**1**	**0**	**0**	**0**	**0**	**0**	**0**
0.0-0.1	36.7	23.4	6.1	1.0	11	9.8	11.1	0.0	0.0	1	1	0	0	0	0	0	0	0	0	0	0	0	1	0	0	0	0	0	0	0	0
0.1-0.2	43.1	21.7	16.1	100.0	1	10.2	0.0	0.0	0.0	0	0	0	0	0	0	0	0	0	0	0	0	0	0	0	0	0	0	0	0	0	0
0.2-0.3	48.6	56.9	17.7	100.0	1	10.5	12.5	0.8	1.2	2	1	0	0	0	0	0	0	0	0	0	0	0	1	0	1	0	0	0	0	0	0
0.3-0.4	-	-	-	-	-	-	-	-	-	-	-	-	-	-	-	-	-	-	-	-	-	-	-	-	-	-	-	-	-	-	-
0.4-0.5	53.0	53.6	29.8	100.0	1	11.2	0.0	0.0	0.0	0	0	0	0	0	0	0	0	0	0	0	0	0	0	0	0	0	0	0	0	0	0

* Fission Track Age and Mean Track Length predicted from the Default Thermal History (i.e. if the sample has not been hotter in the past)
† Combined data for all compositional groups

Table B.3: Continued - (Geotrack Report #806)

Cl Wt %	Default fission track age* (Ma)	Measured fission track age (Ma)	Error in age (Ma)	P (χ2)	Number of grains	Default fission track length* (µm)	Mean track length (µm)	Error in length (µm)	Std deviation (µm)	Number of lengths	Number of grains	Number of tracks in length interval (µm) 1	2	3	4	5	6	7	8	9	10	11	12	13	14	15	16	17	18	19	20
806-10†	**6.5**	**11.5**	**8.2**	**0.0**	**10**	**9.9**	**10.3**	**1.5**	**2.1**	**2**	**1**	**0**	**0**	**0**	**0**	**0**	**0**	**0**	**0**	**1**	**0**	**0**	**1**	**0**	**0**	**0**	**0**	**0**	**0**	**0**	**0**
0.0-0.1	2.6	7.5	2.5	88.0	9	9.4	0.0	0.0	0.0	0	0	0	0	0	0	0	0	0	0	0	0	0	0	0	0	0	0	0	0	0	0
0.1-0.2	-	-	-	-	-	-	-	-	-	-	-	-	-	-	-	-	-	-	-	-	-	-	-	-	-	-	-	-	-	-	-
0.2-0.3	-	-	-	-	-	-	-	-	-	-	-	-	-	-	-	-	-	-	-	-	-	-	-	-	-	-	-	-	-	-	-
0.3-0.4	-	-	-	-	-	-	-	-	-	-	-	-	-	-	-	-	-	-	-	-	-	-	-	-	-	-	-	-	-	-	-
0.4-0.5	-	-	-	-	-	-	-	-	-	-	-	-	-	-	-	-	-	-	-	-	-	-	-	-	-	-	-	-	-	-	-
0.5-0.6	41.4	90.4	19.9	100.0	1	9.9	10.3	1.5	2.1	2	1	0	0	0	0	0	0	0	0	1	0	0	1	0	0	0	0	0	0	0	0

* Fission Track Age and Mean Track Length predicted from the Default Thermal History (i.e. if the sample has not been hotter in the past)
† Combined data for all compositional groups

Estimates	z_i
Standard errors	σ_i
Reference value	z_o
Standardised estimates	$y_i = (z_i - z_o) / \sigma_i$
Precision	$x_i = 1 / \sigma_i$

PLOT y_i against x_i

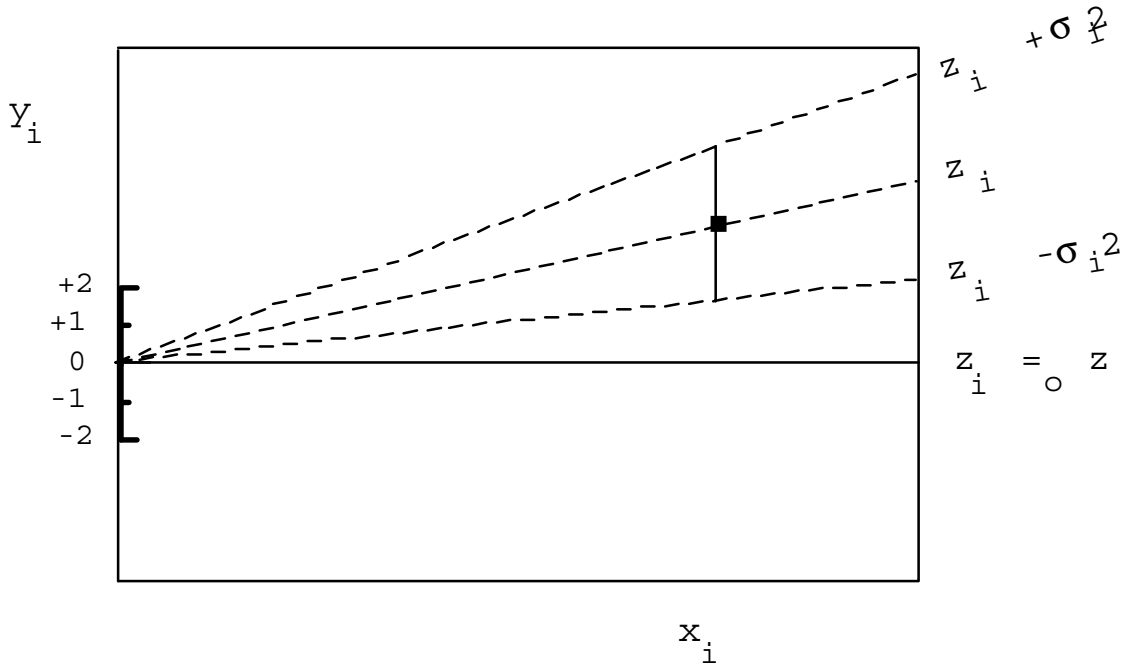

Slope of line from origin through data point $= y_i / x_i$

$= \{(z_i - z_o)/\sigma_i\} / \{1/\sigma_i\}$

$= z_i - z_o$

Key Points:

Radial lines emanating from the origin correspond to fixed values of z

Data points with higher values of x_i have greater precision.

Error bars on all points are the same size in this plot.

Figure B.1 Basic construction of a radial plot. In AFTA, the estimates z_i correspond to the fission track age values for individual apatite grains. Any convenient value of age can be chosen as the reference value corresponding to the horizontal in the radial plot. Radial lines emanating from the origin with positive slopes correspond to fission track ages greater than the reference value. Lines with negative slopes correspond to fission track ages less than the reference value.

Normal radial plot (equations B.2 and B.3)

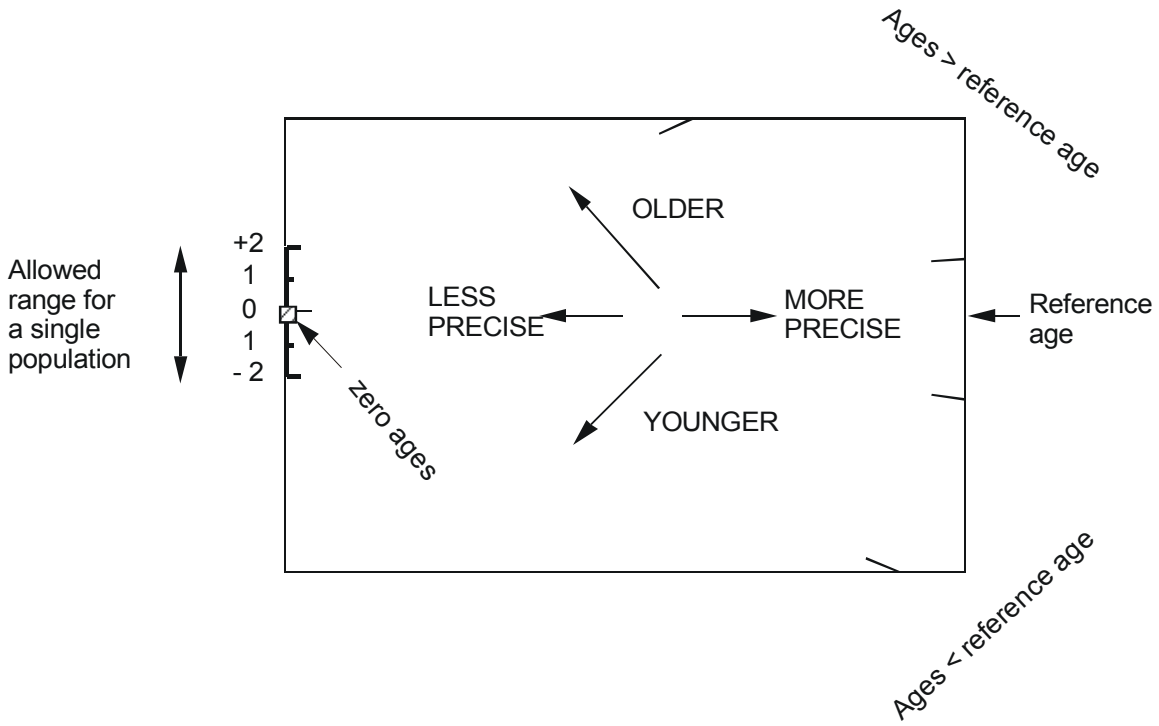

Arc-sin radial plot (equations B.2 and B.4)

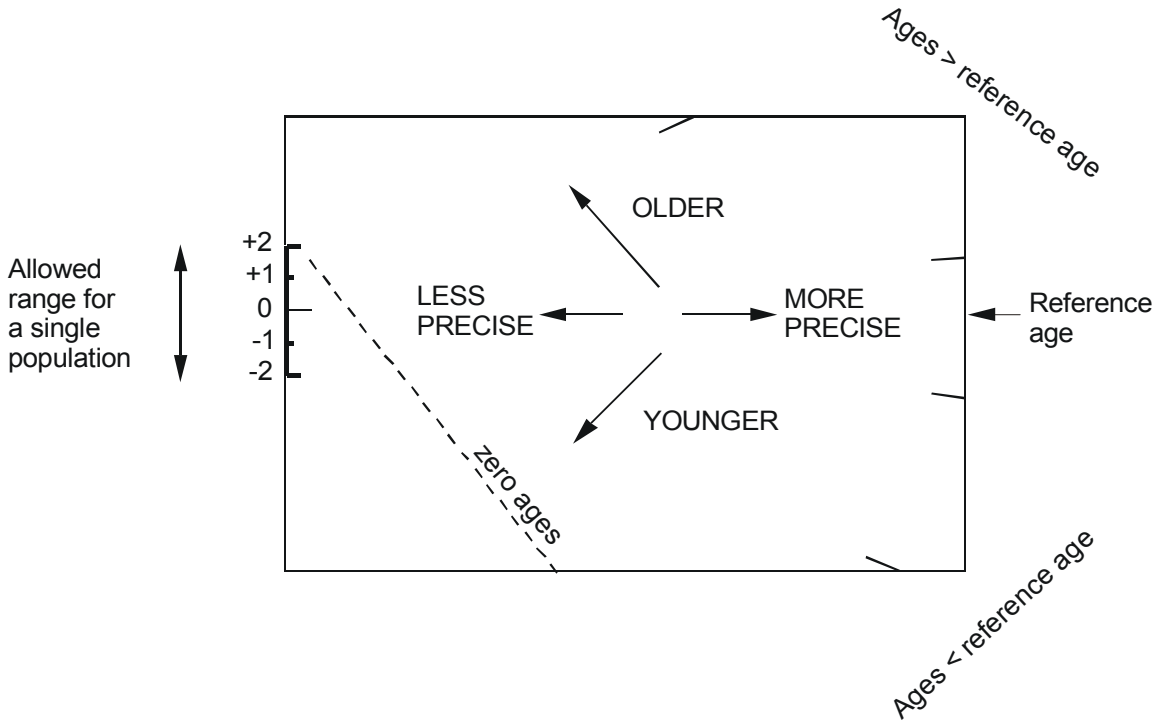

Figure B.2 Simplified structure of Normal and Arc-sin radial plots.

Fission Track Age Data Sheets - Glossary

N_s	=	Number of spontaneous tracks in N_a grid squares
N_i	=	Number of induced tracks in N_a grid squares
N_a	=	Number of grid squares counted in each grain
RATIO	=	N_S/N_i
U (ppm)	=	Uranium content of each grain (= U content of standard glass * ρ_i/ρ_D)
Cl (wt%)	=	Weight percent chlorine content of each grain
ρ_s	=	Spontaneous track density (ρ_s) = N_s/ (N_a*area of basic unit)
ρ_i	=	Induced track density (ρ_i) = N_i/(N_a*area of basic unit)
F.T. AGE	=	Fission track age, calculated using equation B.1
Area of basic unit	=	Area of one grid square
Chi squared	=	χ^2 parameter, used to assess variation of single grain ages within the sample
P(chi squared)	=	Probability of obtaining observed χ^2 value for the relevant number of degrees of freedom, if all grains belong to a single population
Age Dispersion	=	% variation in single grain ages - see discussion in text re "Central age"
N_s/N_i	=	Pooled ratio, total spontaneous tracks divided by total induced tracks for all grains
Mean ratio	=	Mean of (N_s/N_i) for individual grains
Zeta	=	Calibration constant, determined empirically for each observer
ρ_D	=	Track density (ρ_D) from uranium standard glass (interpolated from values at each end of stack)
ND	=	Total number of tracks counted for determining ρ_D
POOLED AGE	=	Fission track age calculated from pooled ratio N_s/N_i. Valid only when P(χ2) > 5%
CENTRAL AGE	=	Alternative to pooled age when P(χ2)< 5%

Key to Figures:

A: Radial plot of single grain ages *(See Figures B.1 and B.2 for details of radial plot construction)*	B: Distribution of Cl contents in apatite grains
C: Single grain age vs weight % Cl for individual apatite grains.	D: Distribution of confined track lengths

GC806-1 Apatite
Counted by: COB

Cape Sorell-1 7210-7570'

Slide ref	Current grain no	N_s	N_i	N_a	ρ_s	ρ_i	RATIO	U (ppm)	Cl (wt%)	F.T. AGE (Ma)
G885-1	3	9	20	24	5.959E+05	1.324E+06	0.450	13.6	0.02	94.2 ± 37.9
G885-1	4	0	2	32	0.000E+00	9.932E+04	0.000	1.0	0.00	0.0 ± 346.7
G885-1	5	8	23	32	3.973E+05	1.142E+06	0.348	11.7	0.06	72.9 ± 30.0
G885-1	6	0	2	21	0.000E+00	1.513E+05	0.000	1.6	0.00	0.0 ± 346.7
G885-1	7	6	39	14	6.810E+05	4.427E+06	0.154	45.5	0.07	32.4 ± 14.2
G885-1	8	9	47	32	4.469E+05	2.334E+06	0.191	24.0	0.08	40.2 ± 14.7
G885-1	9	4	21	18	3.531E+05	1.854E+06	0.190	19.1	0.00	40.0 ± 21.9
G885-1	11	4	4	10	6.356E+05	6.356E+05	1.000	6.5	0.00	207.5 ± 146.8
G885-1	12	0	1	30	0.000E+00	5.297E+04	0.000	0.5	0.00	0.0 ± 1557.8
G885-1	13	1	3	10	1.589E+05	4.767E+05	0.333	4.9	0.00	69.9 ± 80.7
G885-1	14	4	6	24	2.648E+05	3.973E+05	0.667	4.1	0.04	139.1 ± 89.8
G885-1	15	0	1	9	0.000E+00	1.766E+05	0.000	1.8	0.00	0.0 ± 1557.8
G885-1	16	0	8	24	0.000E+00	5.297E+05	0.000	5.4	0.03	0.0 ± 47.5
G885-1	17	2	9	12	2.648E+05	1.192E+06	0.222	12.3	0.02	46.7 ± 36.5
G885-1	18	0	3	25	0.000E+00	1.907E+05	0.000	2.0	0.01	0.0 ± 175.9
G885-1	19	3	14	42	1.135E+05	5.297E+05	0.214	5.4	0.03	45.0 ± 28.7
G885-1	22	7	34	40	2.781E+05	1.351E+06	0.206	13.9	0.03	43.3 ± 18.0
G885-1	23	2	17	24	1.324E+05	1.126E+06	0.118	11.6	0.01	24.8 ± 18.5
G885-1	24	0	5	25	0.000E+00	3.178E+05	0.000	3.3	0.00	0.0 ± 85.4
		59	259		2.093E+05	9.187E+05		9.4		

Area of basic unit = 6.293E-07 cm^{-2}
χ^2 = 19.497 with 18 degrees of freedom
P(χ^2) = 36.2%
Age Dispersion = 9.924% (did not converge)

Ns / Ni = 0.228 ± 0.033
Mean Ratio = 0.215 ± 0.060

Ages calculated using a zeta of 380.4 ± 5.7 for CN5 glass
ρ_D = 1.109E+06cm^{-2} ND = 1847
ρ_D interpolated between top of can; ρ_D = 1.109E+06cm^{-2} ND = 872
bottom of can; ρ_D = 1.239E+06cm^{-2} ND = 975

POOLED AGE = 47.9 ± 7.0 Ma
CENTRAL AGE = 47.9 ± 7.2 Ma

A:

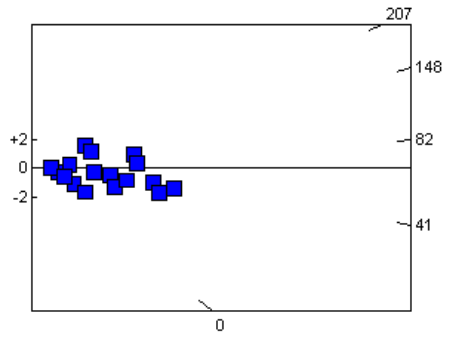

B:

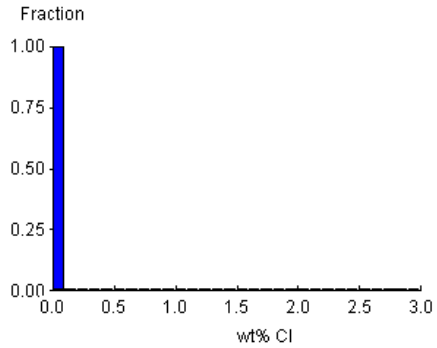

C:

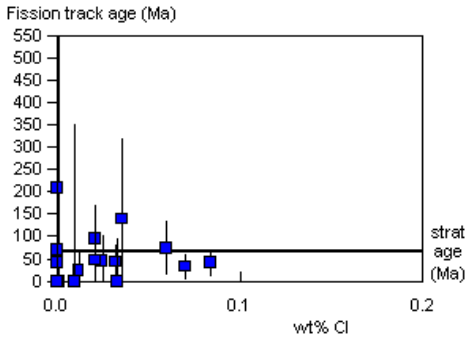

D:

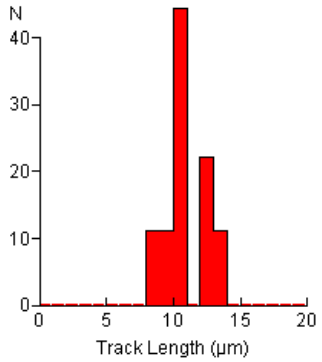

Mean track length 10.97 ± 0.50 µm Std. Dev. 1.51 µm 9 tracks

GC806-2 Apatite
Counted by: COB

Cape Sorell-1 9510-9870'

Slide ref	Current grain no	N_s	N_i	N_a	ρ_s	ρ_i	RATIO	U (ppm)	Cl (wt%)	F.T. AGE (Ma)
G885-2	3	8	51	36	3.531E+05	2.251E+06	0.157	22.8	0.01	33.5 ± 12.8
G885-2	4	1	11	21	7.567E+04	8.324E+05	0.091	8.4	0.19	19.5 ± 20.3
G885-2	5	3	5	9	5.297E+05	8.828E+05	0.600	8.9	0.00	127.4 ± 93.1
G885-2	6	8	42	20	6.356E+05	3.337E+06	0.190	33.7	0.14	40.7 ± 15.7
G885-2	8	12	93	18	1.059E+06	8.210E+06	0.129	83.0	0.01	27.6 ± 8.5
G885-2	9	8	20	42	3.027E+05	7.567E+05	0.400	7.7	0.03	85.2 ± 35.7
G885-2	10	1	15	24	6.621E+04	9.932E+05	0.067	10.0	0.01	14.3 ± 14.8
G885-2	11	6	20	40	2.384E+05	7.945E+05	0.300	8.0	0.00	64.0 ± 29.8
G885-2	12	18	41	42	6.810E+05	1.551E+06	0.439	15.7	0.00	93.4 ± 26.5
G885-2	17	3	9	9	5.297E+05	1.589E+06	0.333	16.1	0.00	71.1 ± 47.4
G885-2	18	6	14	27	3.531E+05	8.240E+05	0.429	8.3	0.00	91.2 ± 44.6
G885-2	19	2	12	30	1.059E+05	6.356E+05	0.167	6.4	0.13	35.6 ± 27.2
G885-2	21	30	35	36	1.324E+06	1.545E+06	0.857	15.6	1.48	181.2 ± 45.4
G885-2	22	11	13	21	8.324E+05	9.837E+05	0.846	9.9	1.19	178.9 ± 73.5
G885-2	23	14	45	21	1.059E+06	3.405E+06	0.311	34.4	0.14	66.4 ± 20.4
G885-2	24	14	31	10	2.225E+06	4.926E+06	0.452	49.8	0.08	96.1 ± 31.1
G885-2	25	12	26	36	5.297E+05	1.148E+06	0.462	11.6	0.27	98.2 ± 34.4
G885-2	26	10	32	30	5.297E+05	1.695E+06	0.313	17.1	0.52	66.7 ± 24.2
G885-2	27	75	155	20	5.959E+06	1.232E+07	0.484	124.5	0.11	102.9 ± 14.8
G885-2	28	5	12	25	3.178E+05	7.628E+05	0.417	7.7	0.77	88.7 ± 47.3
		247	682		7.592E+05	2.096E+06		21.2		

Area of basic unit = 6.293E-07 cm^{-2}
χ^2 = 51.212 with 19 degrees of freedom
P(χ^2) = 0.0%
Age Dispersion = 42.670%

Ns / Ni = 0.362 ± 0.027
Mean Ratio = 0.372 ± 0.049

Ages calculated using a zeta of 380.4 ± 5.7 for CN5 glass
ρ_D = 1.127E+06cm^{-2} ND = 1847
ρ_D interpolated between top of can; ρ_D = 1.109E+06cm^{-2} ND = 872
bottom of can; ρ_D = 1.239E+06cm^{-2} ND = 975

POOLED AGE = 77.2 ± 6.1 Ma
CENTRAL AGE = 74.2 ± 9.9 Ma

A:

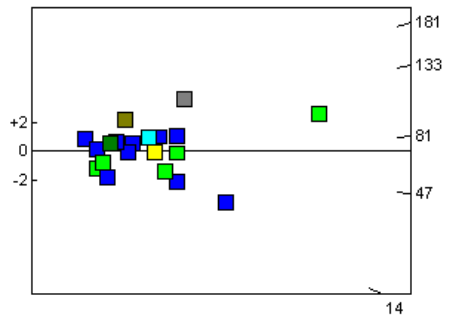

B:

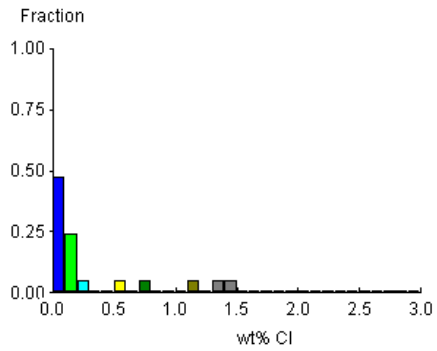

C:

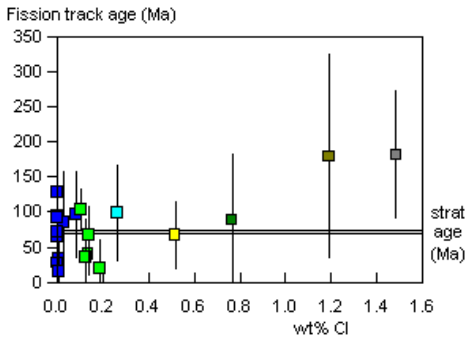

D:

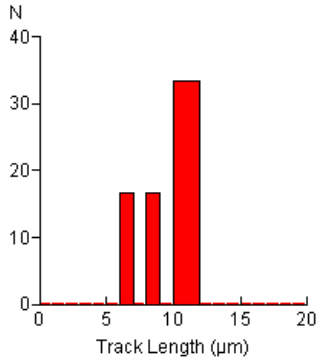

Mean track length 9.76 ± 0.79 µm Std. Dev. 1.94 µm 6 tracks

GC806-3 Apatite
Counted by: COB

Cape Sorell-1 11150-11485'

Slide ref	Current grain no	N_s	N_i	N_a	ρ_s	ρ_i	RATIO	U (ppm)	Cl (wt%)	F.T. AGE (Ma)
G885-3	3	1	3	20	7.945E+04	2.384E+05	0.333	2.4	0.00	72.2 ± 83.4
G885-3	4	0	11	30	0.000E+00	5.827E+05	0.000	5.8	0.03	0.0 ± 33.9
G885-3	5	0	1	25	0.000E+00	6.356E+04	0.000	0.6	0.00	0.0 ± 1599.2
G885-3	6	1	4	21	7.567E+04	3.027E+05	0.250	3.0	0.01	54.3 ± 60.7
G885-3	7	0	33	28	0.000E+00	1.873E+06	0.000	18.6	0.00	0.0 ± 10.3
G885-3	8	33	65	40	1.311E+06	2.582E+06	0.508	25.7	0.00	109.7 ± 23.6
G885-3	9	0	39	21	0.000E+00	2.951E+06	0.000	29.4	0.00	0.0 ± 8.7
G885-3	11	0	20	12	0.000E+00	2.648E+06	0.000	26.3	0.00	0.0 ± 17.6
G885-3	13	0	17	42	0.000E+00	6.432E+05	0.000	6.4	0.00	0.0 ± 20.9
G885-3	14	10	17	30	5.297E+05	9.005E+05	0.588	9.0	0.58	127.0 ± 50.7
G885-3	15	5	42	40	1.986E+05	1.669E+06	0.119	16.6	0.00	25.9 ± 12.3
G885-3	16	0	35	50	0.000E+00	1.112E+06	0.000	11.1	0.00	0.0 ± 9.7
G885-3	17	0	5	15	0.000E+00	5.297E+05	0.000	5.3	0.00	0.0 ± 88.2
		50	292		2.124E+05	1.241E+06		12.3		

Area of basic unit = 6.293E-07 cm^{-2}
χ^2 = 67.999 with 12 degrees of freedom
P(χ^2) = 0.0%
Age Dispersion = 141.262%

Ns / Ni = 0.171 ± 0.026
Mean Ratio = 0.138 ± 0.059

Ages calculated using a zeta of 380.4 ± 5.7 for CN5 glass
ρ_D = 1.146E+06cm^{-2} ND = 1847
ρ_D interpolated between top of can; ρ_D = 1.109E+06cm^{-2} ND = 872
bottom of can; ρ_D = 1.239E+06cm^{-2} ND = 975

POOLED AGE = 37.2 ± 5.8 Ma
CENTRAL AGE = 24.7 ± 11.4 Ma

A:

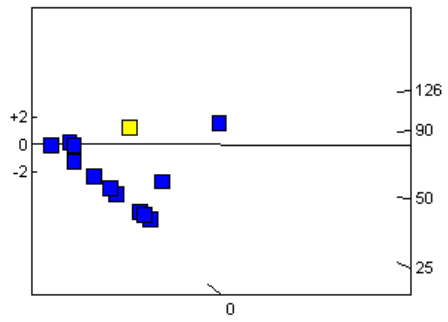

B:

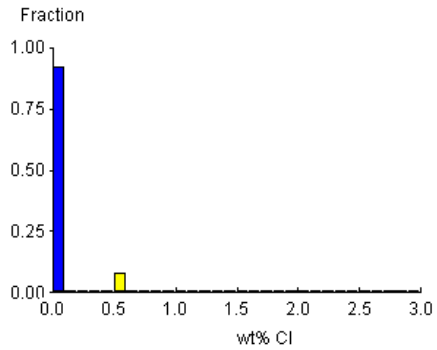

C:

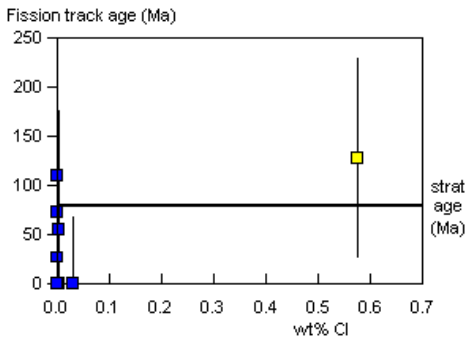

D:

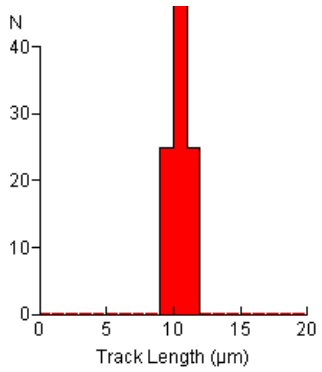

Mean track length 10.70 ± 0.43 µm Std. Dev. 0.85 µm 4 tracks

GC806-7 Apatite
Counted by: COB

Cape Sorell-1 4920-5350'

Slide ref	Current grain no	N_s	N_i	N_a	ρ_s	ρ_i	RATIO	U (ppm)	Cl (wt%)	F.T. AGE (Ma)
G885-4	3	30	107	36	1.324E+06	4.723E+06	0.280	46.2	0.03	61.8 ± 12.9
G885-4	4	9	42	27	5.297E+05	2.472E+06	0.214	24.2	0.00	47.3 ± 17.4
G885-4	5	4	12	24	2.648E+05	7.945E+05	0.333	7.8	0.00	73.4 ± 42.4
G885-4	6	32	29	16	3.178E+06	2.880E+06	1.103	28.2	0.07	239.9 ± 61.9
G885-4	7	41	52	42	1.551E+06	1.967E+06	0.788	19.3	0.12	172.3 ± 36.3
G885-4	8	1	8	14	1.135E+05	9.080E+05	0.125	8.9	0.00	27.6 ± 29.3
G885-4	9	3	28	12	3.973E+05	3.708E+06	0.107	36.3	0.03	23.7 ± 14.4
G885-4	10	37	88	70	8.399E+05	1.998E+06	0.420	19.6	0.11	92.5 ± 18.3
G885-4	11	10	10	20	7.945E+05	7.945E+05	1.000	7.8	1.42	217.8 ± 97.6
G885-4	13	2	17	12	2.648E+05	2.251E+06	0.118	22.0	0.00	26.0 ± 19.5
G885-4	14	12	11	24	7.945E+05	7.283E+05	1.091	7.1	0.41	237.2 ± 99.2
G885-4	15	1	6	10	1.589E+05	9.534E+05	0.167	9.3	0.19	36.8 ± 39.8
		182	410		9.421E+05	2.122E+06		20.8		

Area of basic unit = 6.293E-07 cm^{-2}
χ^2 = 51.826 with 11 degrees of freedom
P(χ^2) = 0.0%
Age Dispersion = 66.014%

Ns / Ni = 0.444 ± 0.040
Mean Ratio = 0.479 ± 0.115

Ages calculated using a zeta of 380.4 ± 5.7 for CN5 glass
ρ_D = 1.165E+06cm^{-2} ND = 1847
ρ_D interpolated between top of can; ρ_D = 1.109E+06cm^{-2} ND = 872
bottom of can; ρ_D = 1.239E+06cm^{-2} ND = 975

POOLED AGE = 97.6 ± 9.1 Ma
CENTRAL AGE = 92.2 ± 20.8 Ma

A:

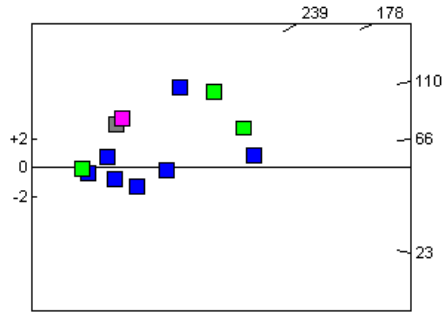

B:

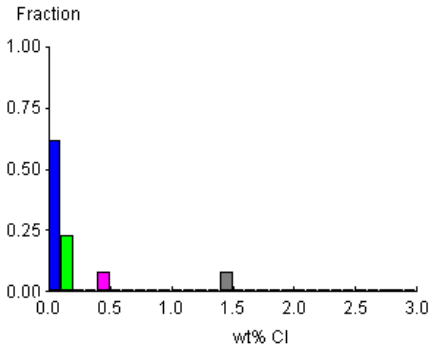

C:

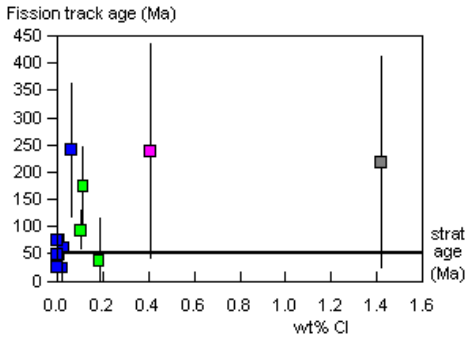

D:

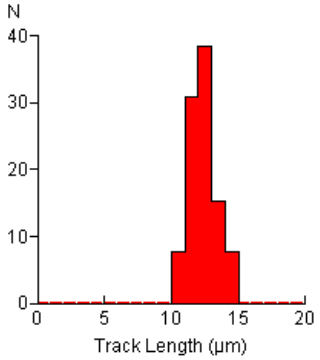

Mean track length 12.36 ± 0.28 µm Std. Dev. 1.01 µm 13 tracks

GC806-8 Apatite
Counted by: COB

Cape Sorell-1 6330-6730'

Slide ref	Current grain no	N_s	N_i	N_a	ρ_s	ρ_i	RATIO	U (ppm)	Cl (wt%)	F.T. AGE (Ma)
G885-5	3	4	15	9	7.063E+05	2.648E+06	0.267	25.5	0.00	59.7 ± 33.7
G885-5	4	36	123	16	3.575E+06	1.222E+07	0.293	117.7	0.03	65.5 ± 12.6
G885-5	6	29	74	15	3.072E+06	7.839E+06	0.392	75.5	0.01	87.6 ± 19.3
G885-5	7	16	76	56	4.540E+05	2.157E+06	0.211	20.8	0.03	47.2 ± 13.1
G885-5	8	0	9	30	0.000E+00	4.767E+05	0.000	4.6	0.01	0.0 ± 44.1
G885-5	9	29	135	64	7.200E+05	3.352E+06	0.215	32.3	0.08	48.2 ± 9.9
G885-5	10	1	2	30	5.297E+04	1.059E+05	0.500	1.0	0.02	111.6 ± 136.7
G885-5	12	1	19	16	9.932E+04	1.887E+06	0.053	18.2	0.04	11.8 ± 12.1
G885-5	13	2	48	30	1.059E+05	2.543E+06	0.042	24.5	0.01	9.4 ± 6.8
G885-5	14	6	25	18	5.297E+05	2.207E+06	0.240	21.3	0.01	53.8 ± 24.5
G885-5	15	10	39	20	7.945E+05	3.099E+06	0.256	29.9	0.01	57.5 ± 20.4
G885-5	16	14	73	63	3.531E+05	1.841E+06	0.192	17.7	0.02	43.0 ± 12.6
G885-5	19	2	13	35	9.080E+04	5.902E+05	0.154	5.7	0.00	34.5 ± 26.2
G885-5	20	5	17	30	2.648E+05	9.005E+05	0.294	8.7	0.00	65.9 ± 33.6
G885-5	21	6	57	30	3.178E+05	3.019E+06	0.105	29.1	0.00	23.6 ± 10.2
G885-5	22	3	8	12	3.973E+05	1.059E+06	0.375	10.2	0.00	83.9 ± 56.8
G885-5	23	0	9	24	0.000E+00	5.959E+05	0.000	5.7	0.02	0.0 ± 44.1
G885-5	25	20	40	24	1.324E+06	2.648E+06	0.500	25.5	0.01	111.6 ± 30.7
G885-5	26	11	33	12	1.457E+06	4.370E+06	0.333	42.1	0.20	74.6 ± 26.1
G885-5	27	9	41	30	4.767E+05	2.172E+06	0.220	20.9	0.07	49.2 ± 18.2
		204	856		5.748E+05	2.412E+06		23.2		

Area of basic unit = 6.293E-07 cm^{-2}
χ^2 = 35.749 with 19 degrees of freedom
P(χ^2) = 1.1%
Age Dispersion = 34.821%

Ns / Ni = 0.238 ± 0.019
Mean Ratio = 0.232 ± 0.033

Ages calculated using a zeta of 380.4 ± 5.7 for CN5 glass
ρ_D = 1.183E+06cm^{-2} ND = 1847
ρ_D interpolated between top of can; ρ_D = 1.109E+06cm^{-2} ND = 872
bottom of can; ρ_D = 1.239E+06cm^{-2} ND = 975

POOLED AGE = 53.4 ± 4.4 Ma
CENTRAL AGE = 51.1 ± 6.3 Ma

A:

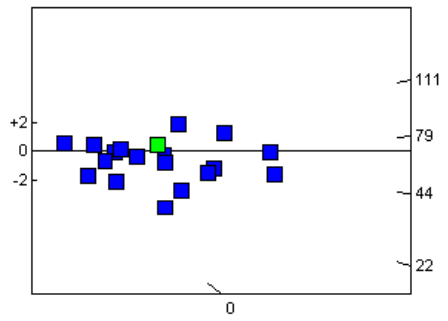

B:

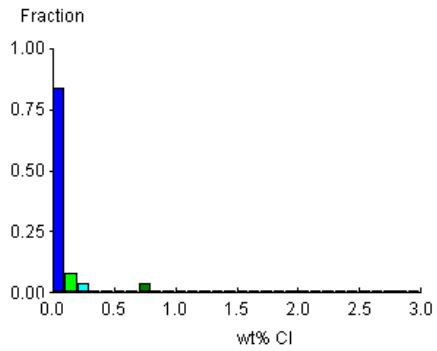

C:

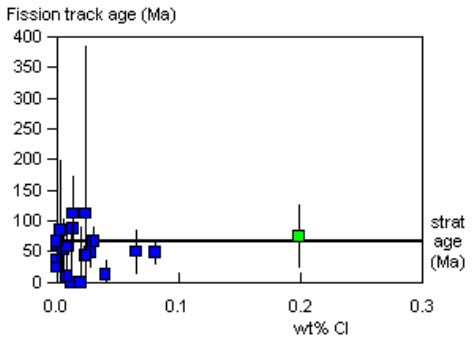

D:

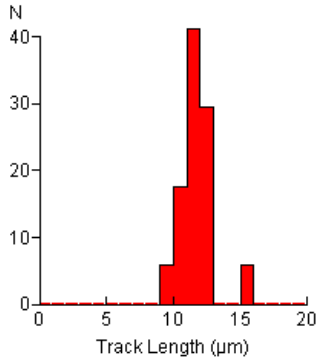

Mean track length 11.76 ± 0.31 µm Std. Dev. 1.27 µm 17 tracks

GC806-9 Apatite
Counted by: COB

Cape Sorell-1 8650-9030'

Slide ref	Current grain no	N_s	N_i	N_a	ρ_s	ρ_i	RATIO	U (ppm)	Cl (wt%)	F.T. AGE (Ma)
G885-6	3	13	52	24	8.607E+05	3.443E+06	0.250	32.7	0.24	56.9 ± 17.7
G885-6	4	2	16	18	1.766E+05	1.413E+06	0.125	13.4	0.06	28.5 ± 21.4
G885-6	5	1	6	30	5.297E+04	3.178E+05	0.167	3.0	0.00	38.0 ± 41.1
G885-6	6	2	21	30	1.059E+05	1.112E+06	0.095	10.5	0.20	21.7 ± 16.1
G885-6	7	1	51	25	6.356E+04	3.242E+06	0.020	30.7	0.00	4.5 ± 4.5
G885-6	8	0	33	45	0.000E+00	1.165E+06	0.000	11.1	0.06	0.0 ± 10.8
G885-6	10	0	6	15	0.000E+00	6.356E+05	0.000	6.0	0.00	0.0 ± 73.2
G885-6	11	15	78	21	1.135E+06	5.902E+06	0.192	56.0	0.00	43.8 ± 12.4
G885-6	12	5	66	20	3.973E+05	5.244E+06	0.076	49.7	0.01	17.3 ± 8.0
G885-6	14	4	54	32	1.986E+05	2.682E+06	0.074	25.4	0.00	16.9 ± 8.8
G885-6	15	0	6	18	0.000E+00	5.297E+05	0.000	5.0	0.04	0.0 ± 73.2
G885-6	16	4	17	18	3.531E+05	1.501E+06	0.235	14.2	0.41	53.6 ± 29.8
G885-6	17	8	68	20	6.356E+05	5.403E+06	0.118	51.2	0.00	26.8 ± 10.1
G885-6	18	12	43	20	9.534E+05	3.416E+06	0.279	32.4	0.01	63.5 ± 20.8
		67	517		3.169E+05	2.445E+06		23.2		

Area of basic unit = 6.293E-07 cm^{-2}
χ^2 = 26.989 with 13 degrees of freedom
P(χ^2) = 1.2%
Age Dispersion = 53.644%

Ns / Ni = 0.130 ± 0.017
Mean Ratio = 0.116 ± 0.026

Ages calculated using a zeta of 380.4 ± 5.7 for CN5 glass
ρ_D = 1.202E+06cm^{-2} ND = 1847
ρ_D interpolated between top of can; ρ_D = 1.109E+06cm^{-2} ND = 872
bottom of can; ρ_D = 1.239E+06cm^{-2} ND = 975

POOLED AGE = 29.6 ± 3.9 Ma
CENTRAL AGE = 27.9 ± 5.9 Ma

A:

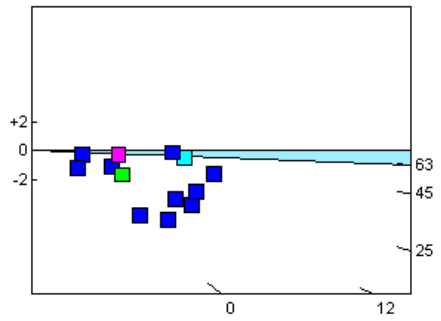

B:

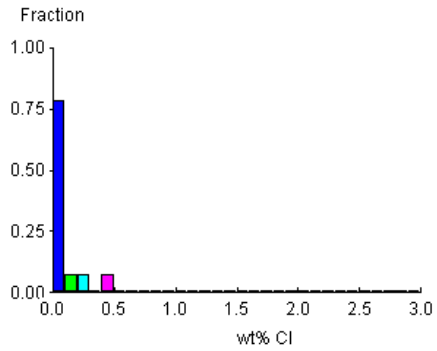

C:

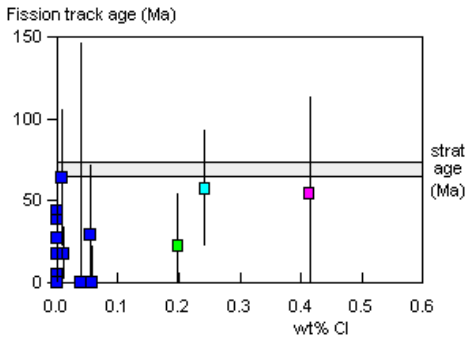

D:

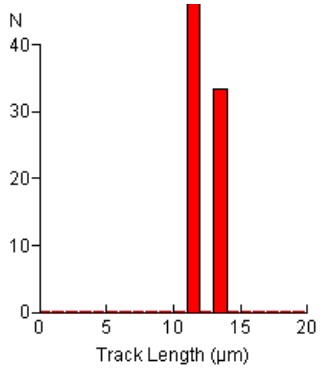

Mean track length 12.05 ± 0.65 µm Std. Dev. 1.13 µm 3 tracks

GC806-10 Apatite
Counted by: COB

Cape Sorell-1 10310-10660'

Slide ref	Current grain no	N_s	N_i	N_a	ρ_s	ρ_i	RATIO	U (ppm)	Cl (wt%)	F.T. AGE (Ma)
G885-7	3	0	8	32	0.000E+00	3.973E+05	0.000	3.7	0.05	0.0 ± 52.3
G885-7	4	0	10	20	0.000E+00	7.945E+05	0.000	7.4	0.01	0.0 ± 40.3
G885-7	5	3	98	54	8.828E+04	2.884E+06	0.031	26.9	0.00	7.1 ± 4.2
G885-7	6	6	112	18	5.297E+05	9.888E+06	0.054	92.3	0.00	12.4 ± 5.2
G885-7	9	29	74	64	7.200E+05	1.837E+06	0.392	17.2	0.60	90.4 ± 20.0
G885-7	10	0	18	28	0.000E+00	1.022E+06	0.000	9.5	0.08	0.0 ± 21.0
G885-7	11	0	13	35	0.000E+00	5.902E+05	0.000	5.5	0.00	0.0 ± 29.9
G885-7	12	0	7	20	0.000E+00	5.562E+05	0.000	5.2	0.05	0.0 ± 61.4
G885-7	14	0	11	40	0.000E+00	4.370E+05	0.000	4.1	0.05	0.0 ± 36.1
G885-7	15	0	3	60	0.000E+00	7.945E+04	0.000	0.7	0.00	0.0 ± 193.1
		38	354		1.628E+05	1.516E+06		14.2		

Area of basic unit = 6.293E-07 cm-²
χ^2 = 55.694 with 9 degrees of freedom
P(χ^2) =0.0%
Age Dispersion =197.621% (did not converge)

Ns / Ni = 0.107 ± 0.018
Mean Ratio = 0.048 ± 0.039

Ages calculated using a zeta of 380.4 ± 5.7 for CN5 glass
ρ_D = 1.221E+06cm-² ND =1847
ρ_D interpolated between top of can; ρ_D = 1.109E+06cm-² ND =872
bottom of can; ρ_D = 1.239E+06cm-² ND =975

POOLED AGE = 24.9 ± 4.3 Ma
CENTRAL AGE = 11.5 ± 8.2 Ma

A:

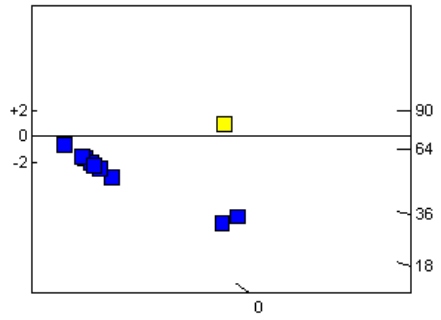

B:

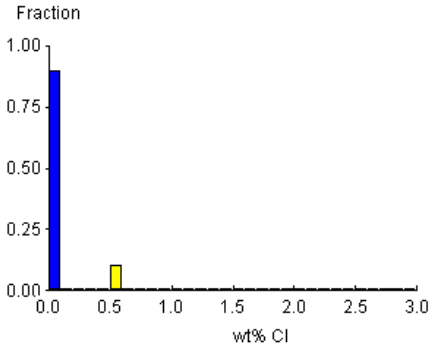

C:

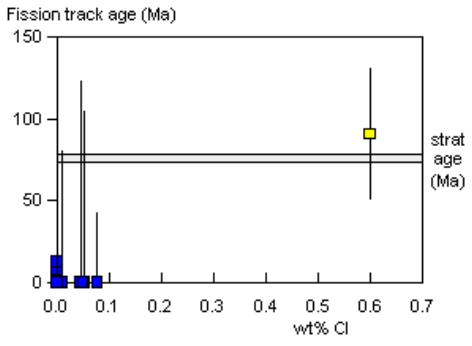

D:

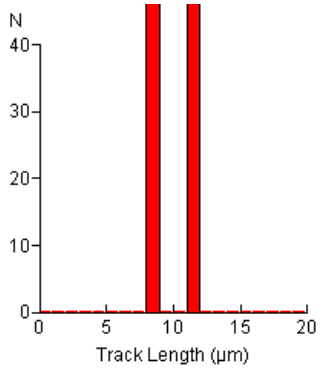

Mean track length 10.34 ± 1.48 µm Std. Dev. 2.09 µm 2 tracks

APPENDIX C

Principles of Interpretation of AFTA Data in Sedimentary Basins

C.1 Introduction

Detrital apatite grains are incorporated into sedimentary rocks from three dominant sources - crystalline basement rocks, older sediments and contemporaneous volcanism. Apatites derived from the first two sources will, in general, contain fission tracks when they are deposited, with AFTA parameters characteristic of the source regions. However, apatites derived from contemporaneous volcanism, or from rapidly uplifted basement, will contain no tracks when they are deposited. For now, we will restrict discussion to this situation, and generalise at a later point to cover the case of apatites which contain tracks that have been inherited from source regions.

C.2 Basic principles of Apatite Fission Track Analysis

Fission tracks are trails of radiation damage, which are produced within apatite grains at a more or less constant rate through geological time, as a result of the spontaneous fission of ^{238}U impurity atoms. Therefore, the number of fission events which occur within an apatite grain during a fixed time interval depends on the magnitude of the time interval and the uranium content of the grain. Each fission event leads to the formation of a single fission track, and the proportion of tracks which can intersect a polished surface of an apatite grain depends on the length of the tracks. Therefore, the number of tracks which are etched in unit area of the surface of an apatite grain (the "spontaneous track density") depends on three factors - (i) The time over which tracks have been accumulating; (ii) The uranium content of the apatite grain; and, (iii) The distribution of track lengths in the grain. In sedimentary rocks which have not been subjected to temperatures greater than ~50°C since deposition, spontaneous fission tracks have a characteristic distribution of confined track lengths, with a mean length in the range 14-15 µm and a standard deviation of ~1 µm. In such samples, by measuring the spontaneous track density and the uranium content of a collection of apatite grains, a "fission track age" can be calculated which will be equal to the time over which tracks have been accumulating. The technique is calibrated against other isotopic systems using age standards which also have this type of length distribution (see Appendix B).

In samples which have been subjected to temperatures greater than ~50°C after deposition, fission tracks are shortened because of the gradual repair of the radiation damage which constitutes the unetched tracks. In effect, the tracks shrink from each end, in a process which is known as fission track "annealing". The final length of each individual track is essentially determined by the maximum temperature which that track has experienced. A time difference of an order of magnitude produces a change in fission track parameters which is equivalent to a temperature change of only ~10°C, so temperature is by far the dominant factor in determining the final fission track parameters. As temperature increases, all existing tracks shorten to a length determined by the prevailing temperature, regardless of when they were formed. After the temperature has subsequently decreased, all tracks formed prior to the thermal maximum are "frozen" at the degree of length reduction they attained at that time. Thus, the length of each track can be thought of as a maximum-reading thermometer, recording the maximum temperature to which it has been subjected.

Therefore, in samples for which the present temperature is maximum, all tracks have much the same length, resulting in a narrow, symmetric distribution. The degree of shortening will depend on the temperature, with the mean track length falling progressively from ~14 µm at 50°C, to zero at around 110°-120°C - the precise temperature depending on the timescale of heating and the composition of the apatites present in the sample (see below). Values quoted here relate to times of the order of 10^7 years (heating rates around 1 to 10°C/Ma) and average apatite composition. If the effective timescale of heating is shorter than 10^7 years, the temperature responsible for a given degree of track shortening will be higher, depending in detail on the kinetics of the annealing process (Green et al., 1986; Laslett et al., 1987; Duddy et al., 1988; Green et al., 1989b). Shortening of tracks produces an accompanying reduction in the fission track age, because of the reduced proportion of tracks which can intersect the polished surface. Therefore, the fission track age is also highly temperature dependent, falling to zero at around 120°C due to total erasure of all tracks.

Samples which have been heated to a maximum paleotemperature less than ~120°C at some time in the past and subsequently cooled will contain two populations of tracks, and will show a more complex distribution of lengths and ages. If the maximum paleotemperature was less than ~50°C then the two components will not be resolvable, but for maximum paleotemperatures between ~50° and 120°C the presence of two components can readily be identified. Tracks formed prior to the thermal maximum will all be shortened to approximately the same degree (the precise value depending on the maximum paleotemperature), while those formed during and after cooling will be longer, due to the lower prevailing temperatures. The length distribution in such

samples will be broader than in the simple case, consisting of a shorter and a longer component, and the fission track age will reflect the amount of length reduction shown by the shorter component (determined by the maximum paleotemperature).

If the maximum paleotemperature was sufficient to shorten tracks to between 9 and 11 μm, and cooling to temperatures of ~50°C or less was sufficiently rapid, tracks formed after cooling will have lengths of 14-15 μm and the resulting track length distribution will show a characteristic bimodal form. If the maximum paleotemperature was greater than ~110 to 120°C, all pre-existing tracks will be erased, and all tracks now present will have formed after the onset of cooling. The fission track age in such samples relates directly to the time of cooling.

In thermal history scenarios in which a heating episode is followed by cooling and then temperature increases again, the tracks formed during the second heating phase will undergo progressive shortening. The tracks formed prior to the initial cooling, which were shortened in the first heating episode, will not undergo further shortening until the temperature exceeds the maximum temperature reached in the earlier heating episode. (In practice, differences in timescale of heating can complicate this simple description. In detail, it is the integrated time-temperature effect of the two heating episodes which should be considered.) If the maximum and peak paleotemperatures in the two episodes are sufficiently different (>~10°C), and the later peak paleotemperature is less than the earlier maximum value, then the AFTA parameters allow determination of both episodes. As the peak paleotemperature in the later episode approaches the earlier maximum, the two generations of tracks become increasingly more difficult to resolve, and when the two paleotemperatures are the same, both components are shortened to an identical degree and all information on the earlier heating phase will be lost.

No information is preserved on the approach to maximum paleotemperature because the great majority of tracks formed up to that time have the same mean track length. Only those tracks formed in the last few per cent of the history prior to the onset of cooling are not shortened to the same degree (because temperature dominates over time in the annealing kinetics). These form a very small proportion of the total number of tracks and therefore cannot be resolved within the length distribution because of the inherent spread of several μm in the length distribution.

To summarise, AFTA allows determination of the magnitude of the maximum temperature and the time at which cooling from that maximum began. In some circumstances, determination of a subsequent peak paleotemperature and the time of cooling is also possible.

C.3 Quantitative understanding of fission track annealing in apatite

Annealing kinetics and modelling the development of AFTA parameters

Our understanding of the behaviour of fission tracks in apatite during geological thermal histories is based on study of the response of fission tracks to elevated temperatures in the laboratory (Green et al., 1986; Laslett et al., 1987; Duddy et al., 1988; Green et al., 1989b), in geological situations (Green et al., 1989a), observations of the lengths of spontaneous tracks in apatites from a wide variety of geological environments (Gleadow et al., 1986), and the relationship between track length reduction and reduction in fission track age observed in controlled laboratory experiments (Green, 1988).

These studies resulted in the capability to simulate the development of AFTA parameters resulting from geological thermal histories for an apatite of average composition (Durango apatite, ~0.43 wt% Cl). Full details of this modelling procedure have been explained in Green et al. (1989b). The following discussion presents a brief explanation of the approach.

Geological thermal histories involving temperatures varying through time are broken down into a series of isothermal steps. The progressive shortening of track length through sequential intervals is calculated using the extrapolated predictions of an empirical kinetic model fitted to laboratory annealing data. Contributions from tracks generated throughout the history (remembering that new tracks are continuously generated through time as new fissions occur) are summed to produce the final distribution of track lengths expected to result from the input history. In summing these components, care is taken to allow for various biases which affect revelation of confined tracks (Laslett et al., 1982). The final length reduction of each component of tracks is converted to a contribution of fission track age, using the relationship between track length and density reduction determined by Green (1988). These age contributions are summed to generate the final predicted fission track age.

This approach depends critically on the assumption that extrapolation of the laboratory-based kinetic model to geological timescales, over many orders of magnitude in time, is valid. This was assessed critically by Green et al. (1989b), who showed that predictions from this approach agree well with observed AFTA parameters in apatites of the appropriate composition in samples from a series of reference wells in the Otway Basin of south-east Australia (Gleadow and Duddy, 1981; Gleadow et al., 1983; Green et al., 1989a). This point is illustrated in Figure C.1. Green et al. (1989b) also quantitatively assessed the errors associated with extrapolation of the Laslett et al. (1987) model from

laboratory to geological timescales (i.e. precision, as opposed to accuracy). Typical levels of precision are ~0.5 µm for mean lengths <~10 µm, and ~0.3 µm for lengths >~10 µm. These figures are equivalent to an uncertainty in estimates of maximum paleotemperature derived using this approach of ~10°C. Precision is largely independent of thermal history for any reasonable geological history. Accuracy of prediction from this model is limited principally by the effect of apatite composition on annealing kinetics, as explained in the next section.

Compositional effects

Natural apatites essentially have the composition $Ca_5(PO_4)_3(F,OH,Cl)$. Most common detrital and accessory apatites are predominantly Fluor-apatites, but may contain appreciable amounts of chlorine. The amount of chlorine in the apatite lattice exerts a subtle compositional control on the degree of annealing, with apatites richer in fluorine being more easily annealed than those richer in chlorine. The result of this effect is that in a single sample, individual apatite grains may show a spread in the degree of annealing (i.e. length reduction and fission track age reduction). This effect becomes most pronounced in the temperature range 90 - 120°C (assuming a heating timescale of ~10 Ma), and can be useful in identifying samples exposed to paleotemperatures in this range. At temperatures below ~80°C, the difference in annealing sensitivity is less marked, and compositional effects can largely be ignored.

Our original quantitative understanding of the kinetics of fission track annealing, as described above, relates to a single apatite (Durango apatite) with ~0.43 wt% Cl, on which most of our original experimental studies were carried out. Recently, we have extended this quantitative understanding to apatites with Cl contents up to ~3 wt%. This new, multi-compositional kinetic model is based both on new laboratory annealing studies on a range of apatites with different F-Cl compositions (Figure C.2), and on observations of geological annealing in apatites from a series of samples from exploration wells in which the section is currently at maximum temperature since deposition. A composite model for Durango apatite composition was first created by fitting a common model to the old laboratory data (from Green et al., 1986) and the new geological data for a similar composition. This was then extended to other compositions on the basis of the multi-compositional laboratory and geological data sets. Details of the multi-compositional model are contained in a Technical Note, available from Geotrack in Melbourne.

The multi-compositional model allows prediction of AFTA parameters for any Cl content between 0 and 3 wt%, using a similar approach to that used in our original single composition modelling, as outlined above. Then, for an assumed or measured distribution of Cl contents within a sample, the composite parameters for the sample can be predicted. The range of Cl contents from 0 to 3 wt% spans the range of compositions commonly encountered, as discussed in the next section.

Predictions of the new multi-compositional model are in good agreement with the geological constraints on annealing rates provided by the Otway Basin reference wells, as shown in Figure C.3. However, note that the AFTA data from these Otway Basin wells were among those used in construction of the new model, so this should not be viewed as independent verification, but rather as a demonstration of the overall consistency of the model.

Distributions of Cl content in common AFTA samples

Figure C.4a shows a histogram of Cl contents, measured by electron microprobe, in apatite grains from more than 100 samples of various types. Most grains have Cl contents less than ~0.5 wt%. The majority of grains with Cl contents greater than this come from volcanic sources and basic intrusives, and contain up to ~2 wt% Cl. Figure C.4b shows the distribution of Cl contents measured in randomly selected apatite grains from 61 samples of "typical" quartzo-feldspathic sandstone. This distribution is similar to that in Figure C.4a, except for a more rapid fall-off as Cl content increases. Apatites from most common sandstones give distributions of Cl content which are very similar to that in Figure C.4b. Volcanogenic sandstones typically contain apatites with higher Cl contents, with a much flatter distribution for Cl contents up to ~1.5%, falling to zero at ~2.5 to 3 wt%, as shown in Figure C.4c. Cl contents in granitic basement samples and high-level intrusives are typically much more dominated by compositions close to end-member Fluorapatite, although many exceptions occur to this general rule.

Information about the spread of Cl contents in samples analysed in this report can be found in Appendix A.

Alternative kinetic models

Recently, both Carlson (1990) and Crowley et al. (1991) have published alternative kinetic models for fission track annealing in apatite. Carlson's model is based on our laboratory annealing data for Durango apatite (Green et al., 1986) and other (unpublished) data. In his abstract, Carlson claims that because his model is "based on explicit physical mechanisms, extrapolations of annealing rates to the lower temperatures and longer timescales required for the interpretation of natural fission track

length distributions can be made with greater confidence than is the case for purely empirical relationships fitted to the experimental annealing data". As explained in detail by Green et al. (1993), all aspects of Carlson's model are in fact purely empirical, and his model is inherently no "better" for the interpretation of data than any other. In fact, detailed inspection shows that Carlson's model does not fit the laboratory data set at all well. Therefore, we recommend against use of this model to interpret AFTA data.

The approach taken by Crowley et al. (1991) is very similar to that taken by Laslett et al., (1987). They have fitted models to new annealing data in two apatites of different composition - one close to end-member Fluorapatite (B-5) and one having a relatively high Sr content (113855). The model developed by Crowley et al. (1991) from their own annealing data for the B-5 apatite gives predictions in geological conditions which are consistently higher than measured values, as shown in Figure C.5. Corrigan (1992) reported a similar observation in volcanogenic apatites in samples from a series of West Texas wells. Since the B-5 apatite is close to end-member Fluor-apatite, while the Otway Group apatites contain apatites with Cl contents from zero up to ~3 wt% (and the West Texas apatites have up to 1 wt%), the fluorapatites should have mean lengths rather less than the measured values, which should represent a mean over the range of Cl contents present. Therefore, the predictions of the Crowley et al. (1991) B-5 model appear to be consistently high.

We attribute this to the rather restricted temperature-time conditions covered by the experiments of Crowley et al. (1991), with annealing times between one and 1000 hours, in contrast to times between 20 minutes and 500 days in the experiments of Green et al. (1986). In addition, few of the measured length values in Crowley et al.'s study fall below 11 μm (in only five out of 60 runs in which lengths were measured in apatite B-5) and their model is particularly poorly defined in this region.

Crowley et al. (1991) also fitted a new model to the annealing data for Durango apatite published by Green et al. (1986). Predictions of their fit to our data are not very much different to those from the Laslett et al. (1987) model (Figure C.6). We have not pursued the differences between their model and ours in detail because the advent of our multi-compositional model has rendered the single compositional approach obsolete.

C.4 Evidence for elevated paleotemperatures from AFTA

The basic principle involved in the interpretation of AFTA data in sedimentary basins is to determine whether the degree of annealing shown by tracks in apatite from a particular sample could have been produced if the sample has never been hotter than its present temperature at any time since deposition. To do this, the burial history derived

from the stratigraphy of the preserved sedimentary section is used to calculate a thermal history for each sample using the present geothermal gradient and surface temperature (i.e. assuming these have not changed through time). This is termed the "Default Thermal History". For each sample, the AFTA parameters predicted as a result of the Default Thermal History are then compared to the measured data. If the data show a greater degree of annealing than calculated on the basis of this history, the sample must have been hotter at some time in the past. In this case, the AFTA data are analysed to provide estimates of the magnitude of the maximum paleotemperature in that sample, and the time at which cooling commenced from the thermal maximum.

The degree of annealing is assessed in two ways - from fission track age and track length data. The stratigraphic age provides a basic reference point for the interpretation of fission track age, because reduction of the fission track age below the stratigraphic age unequivocally reveals that appreciable annealing has taken place after deposition of the host sediment. Large degrees of fission track age reduction, with the pooled or central fission track age very much less than the stratigraphic age, indicate severe annealing, which requires paleotemperatures of at least ~100°C for any reasonable geological time-scale of heating (>~1 Ma). Note that this applies even when apatites contain tracks inherited from source areas. More moderate degrees of annealing can be detected by inspection of the single grain age data, as the most sensitive (fluorine-rich) grains will begin to give fission track ages significantly less than the stratigraphic age before the central or pooled age has been reduced sufficiently to give a noticeable signal. Note that this aspect of the single grain age data can also be used for apatites which have tracks inherited from source areas. If signs of moderate annealing (from single grain age reduction) or severe annealing (from the reduction in pooled or central age) are seen in samples in which the Default Thermal History predicts little or no effect, the sample must have been subjected to elevated paleotemperatures at some time in the past. Figure C.7 shows how increasing degrees of annealing are observable in radial plots of the single grain fission track age data.

Similarly, the present temperature from which a sample is taken, and the way in which this has been approached (as inferred from the preserved sedimentary section), forms a basic point of reference for track length data. The observed mean track length is compared with the mean length predicted from the Default Thermal History. If the observed degree of track shortening in a sample is greater than that expected from the Default Thermal History (i.e. the mean length is significantly less than the predicted value), either the sample must have been subjected to higher paleotemperatures at some time after deposition, or the sample contains shorter tracks which were inherited from sediment source areas at the time the sediment was deposited. If shorter tracks were

inherited from source areas, the sample should still contain a component of longer tracks corresponding to the tracks formed after deposition. In general, the fission track age should be greater than the stratigraphic age. This can be assessed quantitatively using the computer models for the development of AFTA parameters described in an earlier section. If the presence of shorter tracks cannot be explained by their inheritance from source areas, the sample must have been hotter in the past.

C.5 Quantitative determination of the magnitude of maximum paleotemperature and the timing of cooling using AFTA

Values of maximum paleotemperature and timing of cooling in each sample are determined using a forward modelling approach based on the quantitative description of fission track annealing described in earlier sections. The Default Thermal History described above is used as the basis for this forward modelling, but with the addition of episodes of elevated paleotemperatures as required to explain the data. AFTA parameters are modelled iteratively through successive thermal history scenarios in order to identify thermal histories that can account for observed parameters. The range of values of maximum paleotemperature and timing of cooling which can account for the measured AFTA parameters (fission track age and track length distribution) are defined using a maximum likelihood-based approach. In this way, best estimates ("maximum likelihood values") can be defined together with ±95% confidence limits.

In samples in which all tracks have been totally annealed at some time in the past, only a minimum estimate of maximum paleotemperature is possible. In such cases, AFTA data provide most control on the time at which the sample cooled to temperatures at which tracks could be retained. The time at which cooling began could be earlier than this time, and therefore the timing also constitutes a minimum estimate.

Comparison of the AFTA parameters predicted by the multi-compositional model with measured values in samples which are currently at their maximum temperatures since deposition shows a good degree of consistency, suggesting the uncertainty in application of the model should be less than ±10°C. This constitutes a significant improvement over earlier approaches, since the kinetic models used are constrained in both laboratory and geological conditions. It should be appreciated that relative differences in maximum paleotemperature can be identified with greater precision than absolute paleotemperatures, and it is only the estimation of absolute paleotemperature values to which the ±10°C uncertainty relates.

Cooling history

If the data are of high quality and provided that cooling from maximum paleotemperatures began sufficiently long ago (so that the history after this time is represented by a significant proportion of the total tracks in the sample), determination of the magnitude of a subsequent peak paleotemperature and the timing of cooling from that peak may also be possible (as explained in Section C.2). A similar approach to that outlined above provides best estimates and corresponding ±95% confidence limits for this episode. Such estimates may simply represent part of a protracted cooling history, and evidence for a later discrete cooling episode can only be accepted if this scenario provides a significantly improved fit to the data. Geological evidence and consistency of estimates between a series of samples can also be used to verify evidence for a second episode.

In practise, most typical AFTA datasets are only sufficient to resolve two discrete episodes of heating and cooling. One notable exception to this is when a sample has been totally annealed in an early episode, and has then undergone two (or more) subsequent episodes with progressively lower peak paleotemperatures in each. But in general, complex cooling histories involving a series of episodes of heating and cooling will allow resolution of only two episodes, and the results will depend on which episodes dominate the data. Typically this will be the earliest and latest episodes, but if multiple cooling episodes occur within a narrow time interval the result will represent an approximation to the actual history.

C.6 Qualitative assessment of AFTA parameters

Various aspects of thermal history can often be assessed by qualitative assessment of AFTA parameters. For example, samples which have reached maximum paleotemperatures sufficient to produce total annealing, and which only contain tracks formed after the onset of cooling, can be identified from a number of lines of evidence. In a vertical sequence of samples showing increasing degrees of annealing, the transition from rapidly decreasing fission track age with increasing depth to more or less the same age over a range of depth denotes the transition from partial to total annealing of all tracks formed prior to the thermal maximum. In samples in which all tracks have been totally annealed, the single grain age data should show that none of the individual grain fission track ages are significantly older than the time of cooling, and grains in all compositional groups should give the same fission track age unless the sample has been further disturbed by a later episode. If the sample cooled rapidly to sufficiently low temperatures, little annealing will have taken place since cooling, and all grains will

give ages which are compatible with a single population around the time of cooling, as shown in Figure C.7.

Inspection of the distribution of single grain ages in partially annealed samples can often yield useful information on the time of cooling, as the most easily annealed grains (those richest in fluorine) may have been totally annealed prior to cooling, while more retentive (Cl-rich) compositions were only partially annealed (as in Figure C.7, centre). The form of the track length distribution can also provide information, from the relative proportions of tracks with different lengths. All of these aspects of the data can be used to reach a preliminary thermal history interpretation.

C.7 Allowing for tracks inherited from source areas

The effect of tracks inherited from source areas, and present at the time the apatite is deposited in the host sediment, is often posed as a potential problem for AFTA. However, this can readily be allowed for in analysing both the fission track age and length data.

In assessing fission track age data to determine the degree of annealing, the only criterion used is the comparison of fission track age with the value expected on the basis of the Default Thermal History. From this point of view, inherited tracks do not affect the conclusion: if a grain or a sample gives a fission track age which is significantly less than expected, the grain or sample has clearly undergone a higher degree of annealing than can be accounted for by the Default Thermal History, and therefore must have been hotter in the past, whether the sample contained tracks when it was deposited or not.

The presence of inherited tracks does impose a limit on our ability to detect post-depositional annealing from age data alone, as in samples which contain a fair proportion of inherited tracks, moderate degrees of annealing may reduce the fission track age from the original value, but not to a value which is significantly less than the stratigraphic age. This is particularly noticeable in the case of Tertiary samples containing apatites derived from Paleozoic basement. In such cases, although fission track age data may show no evidence of post-depositional annealing, track length data may well show such evidence quite clearly.

The influence of track lengths inherited from source areas can be allowed for by comparison of the fission track age with the value predicted by the Default Thermal History combined with inspection of the track length distribution. If the mean length is much less than the length predicted by the Default Thermal History, either the sample has been subjected to elevated paleotemperatures, sufficient to produce the observed degree of length reduction, or else the sample contains a large proportion of shorter

tracks inherited from source areas. However, in the latter case, the sample should give a pooled or central fission track age correspondingly older than the stratigraphic age, while the length distribution should contain a component of longer track lengths corresponding to the value predicted by the Default Thermal History. It is important in this regard that the length of a track depends primarily on the maximum temperature to which it has been subjected, whether in the source regions or after deposition in the sedimentary basin. Thus, any tracks retaining a provenance signature will have lengths towards the shorter end of the distribution where track lengths will not have "equilibrated" with the temperatures attained since deposition.

In general, it is only in extreme cases that inherited tracks render track length data insensitive to post-depositional annealing. For example, if practically all the tracks in a particular sample were formed prior to deposition, perhaps in a Pliocene sediment in which apatites were derived from a stable Paleozoic shield with fission track ages of ~300 Ma or more, the track length distribution will, in general, be dominated by inheritance, as only ~2% of tracks would have formed after deposition. Post-depositional heating will not be detectable as long as the maximum paleotemperature is insufficient to cause greater shortening than that which occurred in the source terrain. Even in such extreme cases, once a sample is exposed to temperatures sufficient to produce greater shortening than that inherited from source areas, the inherited tracks and those formed after deposition will all undergo the same degree of shortening, and the effects of post-depositional annealing can be recognised. In such cases, the presence of tracks inherited from source areas is actually very useful, because the number of tracks formed after deposition is so small that little or no information would be available without the inherited tracks.

C.8 Plots of fission track age and mean track length vs depth and temperature

AFTA data from well sequences are usually plotted as shown in Figure C.8. This figure shows AFTA data for two scenarios: one in which deposition has been essentially continuous from the Carboniferous to the present and all samples are presently at their maximum paleotemperature since deposition (Figure C.8a); and, one in which the section was exposed to elevated paleotemperatures prior to cooling in the Early Tertiary (Figure C.8b).

In both figures, fission track age and mean track length are plotted against depth and present temperature. Presentation of AFTA data in this way often provides insight into the thermal history interpretation, following principles outlined earlier in this Appendix.

In Figure C.8a**,** for samples at temperatures below ~70°C, the fission track age is either greater than or close to the stratigraphic age, and little fission track age reduction has affected these samples. Track lengths in these samples are all greater than ~13 µm. In progressively deeper samples, both the fission track age and mean track length are progressively reduced to zero at a present temperature of around 110°C, with the precise value depending on the spread of apatite compositions present in the sample. Track length distributions in the shallowest samples would be a mixture of tracks retaining information on the thermal history of source regions, while in deeper samples, all tracks would be shortened to a length determined by the prevailing temperature. This pattern of AFTA parameters is characteristic of a sequence which is currently at maximum temperatures.

The data in Figure C.8b show a very different pattern. The fission track age data show a rapid decrease in age, with values significantly less than the stratigraphic age at temperatures of ~40 to 50°C, at which such a degree of age reduction could not be produced in any geological timescale. Below this rapid fall, the fission track ages do not change much over ~1 km (30°C). This transition from rapid fall to consistent ages is diagnostic of the transition from partial to total annealing. Samples above the "break-in slope" contain two generations of tracks: those formed prior to the thermal maximum, which have been partially annealed (shortened) to a degree which depends on the maximum paleotemperature; and, those formed after cooling, which will be longer. Samples below the break-in slope contain only one generation of tracks, formed after cooling to lower temperatures at which tracks can be retained. At greater depths, where temperatures increase to ~90°C and above, the effect of present temperatures begins to reduce the fission track ages towards zero, as in the "maximum temperatures now" case.

The track length data also reflect the changes seen in the fission track age data. At shallow depths, the presence of the partially annealed tracks shortened prior to cooling causes the mean track length to decrease progressively as the fission track age decreases. However, at depths below the break in slope in the age profile, the track length increases again as the shorter component is totally annealed and so does not contribute to the measured distribution of track lengths. At greater depths, the mean track lengths decrease progressively to zero once more due to the effects of the present temperature regime.

Examples of such data have been presented, e.g. by Green (1989) and Kamp and Green (1990).

C.9 Determining paleogeothermal gradients and amount of section removed on unconformities

Estimates of maximum paleotemperatures in samples over a range of depths in a vertical sequence provides the capability of determining the paleogeothermal gradient immediately prior to the onset of cooling from those maximum paleotemperatures. The degree to which the paleogeothermal gradient can be constrained depends on a number of factors, particularly the depth range over which samples are analysed. If samples are only analysed over ~1 km, then the paleotemperature difference over that range may be only ~20 to 30°C. Since maximum paleotemperatures can often only be determined within a ~10°C range, this introduces considerable uncertainty into the final estimate of paleogeothermal gradient (see Figure C.9).

Another important factor is the difference between maximum paleotemperatures and present temperatures ("net cooling"). If this is only ~10°C, which is similar to the uncertainty in absolute paleotemperature determination, only broad limits can be established on the paleogeothermal gradient. In general, the control on the paleogeothermal gradient improves as the amount of net cooling increases. However, if the net cooling becomes so great that many samples were totally annealed prior to the onset of cooling - so that only minimum estimates of maximum paleotemperatures are possible - constraints on the paleogeothermal gradient from AFTA come only from that part of the section in which samples were not totally annealed. In this case, integration of AFTA data with VR measurements can be particularly useful in constraining the paleo-gradient.

Having constrained the paleogeothermal gradient at the time cooling from maximum paleotemperatures began, if we assume a value for surface temperature at that time, the amount of section subsequently removed by uplift and erosion can be calculated as shown in Figure C.10. The *net* amount of section removed is obtained by dividing the difference between the paleo-surface temperature (T_S) and the intercept of the paleotemperature profile at the present ground surface (T_i) by the estimated paleogeothermal gradient. The *total* amount of section removed is obtained by adding the thickness of section subsequently redeposited above the unconformity to the *net* amount estimated as in Figure C.10. If the analysis is performed using depths from the appropriate unconformity, then the analysis will directly yield the *total* amount of section removed.

Geotrack have developed a method of deriving estimates of both the paleogeothermal gradient and the net amount of section removed using estimated paleotemperatures

derived from AFTA and VR. Perhaps more importantly, this method also provides rigorous values for upper and lower 95% confidence limits on each parameter. The method is based on maximum likelihood estimation of the paleogeothermal gradient and the surface intercept, from a table of paleotemperature and depth values. The method is able to accept ranges for paleotemperature estimates (e.g. where the maximum paleotemperature can only be constrained to between, for example, 60 and 90°C), as well as upper and lower limits (e.g. <60°C for samples which show no detectable annealing; >110°C in samples which were totally annealed). Estimates of paleotemperature from AFTA and VR may be combined or analysed separately. Some results from this method have been reported by Bray et al. (1992). Full details of the methods employed are presented in a confidential, in-house, Geotrack research report, copies of which are available on request from the Melbourne office.

Results are presented in two forms. Likelihood profiles, plotting the log-likelihood as a function of either gradient or section removed, portray the probability of a given value of gradient or section removed. The best estimate is given by the value of gradient or section removed for which the log-likelihood is maximised. Ideally, the likelihood profiles should show a quadratic form, and values of gradient or section removed at which the log-likelihood has fallen by two from the maximum value define the upper and lower 95% confidence limits on the estimates. An alternative method of portraying this information is a crossplot of gradient against section removed, in which values which fall within 95% confidence limits (in two dimensions) are contoured. Note that the confidence limits defined by this method are rather tighter than those from the likelihood profiles, as the latter only reflect variation in one parameter, whereas the contoured crossplot takes variation of both parameters into account.

It must be emphasised that this method relies on the assumption that the paleotemperature profile was linear both throughout the section analysed and through the overlying section which has been removed. While the second part of this assumption can never be confirmed independently, visual inspection of the paleotemperature estimates as a function of depth should be sufficient to verify or deny the linearity of the paleotemperature profile through the preserved section.

Results of this procedure are shown in this report if the data allow sufficiently well-defined paleotemperature estimates to justify use of the method. Where the AFTA data suggest that the section is currently at maximum temperature since deposition, or that the paleotemperature profile was non-linear, or where data are of insufficient quality to allow rigorous paleotemperature estimation, the method is not used.

References

Carlson, W.D. (1990) Mechanisms and kinetics of apatite fission-track annealing. *American Mineralogist*, 75, 1120 - 1139.

Corrigan, J. (1992) Annealing models under the microscope, *On Track*, 2, 9-11.

Crowley, K.D., Cameron, M. and Schaefer, R.L. (1991) Experimental studies of annealing of etched fission tracks in apatite. *Geochimica et Cosmochimica Acta*, 55, 1449-1465.

Duddy, I.R., Green, P.F. and Laslett G.M. (1988) Thermal annealing of fission tracks in apatite 3. Variable temperature behaviour. *Chem. Geol. (Isot. Geosci. Sect.)* , 73, 25-38.

Gleadow, A.J.W. and Duddy, I.R. (1981) A natural long-term track annealing experiment for apatite. *Nuclear Tracks*, 5, 169-174.

Gleadow, A.J.W., Duddy, I.R. and Lovering, J.F. (1983) Fission track analysis; a new tool for the evaluation of thermal histories and hydrocarbon potential. *APEA J,* 23, 93-102.

Gleadow, A.J.W., Duddy, I.R., Green, P.F. and Lovering, J.F. (1986) Confined fission track lengths in apatite - a diagnostic tool for thermal history analysis. *Contr. Min. Petr.*, 94, 405-415.

Green, P.F. (1988) The relationship between track shortening and fission track age reduction in apatite: Combined influences of inherent instability, annealing anisotropy, length bias and system calibration. *Earth Planet. Sci. Lett.*, 89, 335-352.

Green, P.F., Duddy, I.R., Gleadow, A.J.W., Tingate, P.R. and Laslett, G.M. (1986) Thermal annealing of fission tracks in apatite 1. A qualitative description. *Chem. Geol. (Isot. Geosci. Sect.)* , 59, 237-253.

Green, P.F., Duddy, I.R., Gleadow, A.J.W. and Lovering, J.F. (1989a) Apatite Fission Track Analysis as a paleotemperature indicator for hydrocarbon exploration. *In:* Naeser, N.D. and McCulloh, T. (eds.) *Thermal history of sedimentary basins - methods and case histories*, Springer-Verlag, New York, 181-195.

Green, P.F., Duddy, I.R., Laslett, G.M., Hegarty, K.A., Gleadow, A.J.W. and Lovering, J.F. (1989b) Thermal annealing of fission tracks in apatite 4. Quantitative modelling techniques and extension to geological timescales. *Chem. Geol. (Isot. Geosci. Sect.)*, 79, 155-182

Green, P.F., Laslett, G.M. and Duddy, I.R. (1993) Mechanisms and kinetics of apatite fission track annealing: Discussion. *American Mineralogist*, 78, 441-445.

Laslett, G.M., Kendall, W.S., Gleadow, A.J.W. and Duddy, I.R. (1982) Bias in measurement of fission track length distributions. *Nuclear Tracks*, 6, 79-85.

Laslett, G.M., Green, P.F., Duddy, I.R. and Gleadow, A.J.W. (1987) Thermal annealing of fission tracks in apatite 2. A quantitative analysis. *Chem. Geol. (Isot. Geosci. Sect.)*, 65, 1-13.

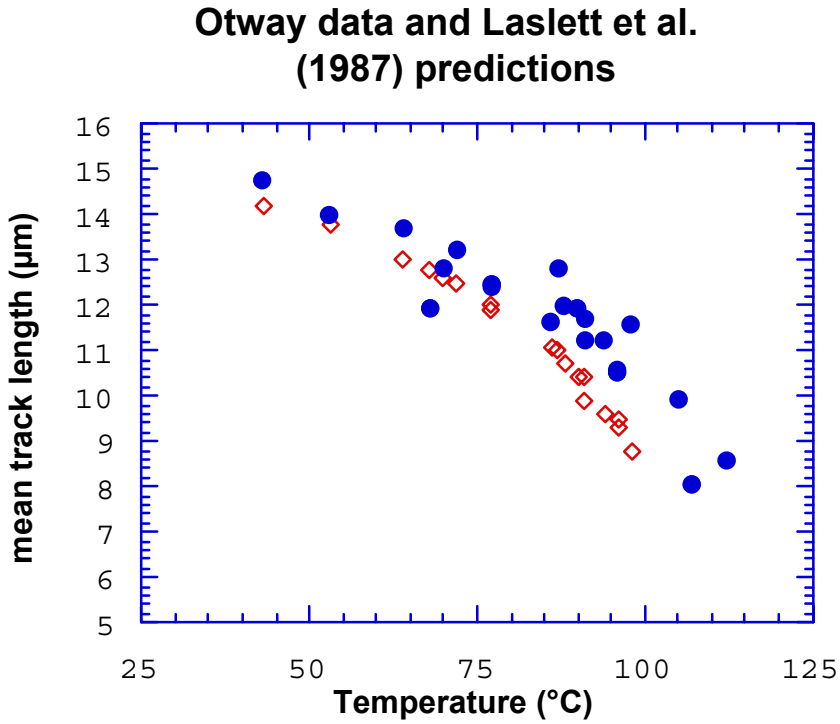

Figure C.1a Comparison of mean track length (solid circles) measured in samples from four Otway Basin reference wells (from Green et al, 1989a) and predicted mean track lengths (open diamonds) from the kinetic model of fission track annealing from Laslett et al. (1987). The predictions underestimate the measured values, but they refer to an apatite composition that is more easily annealed than the majority of apatites in these samples, so this is expected.

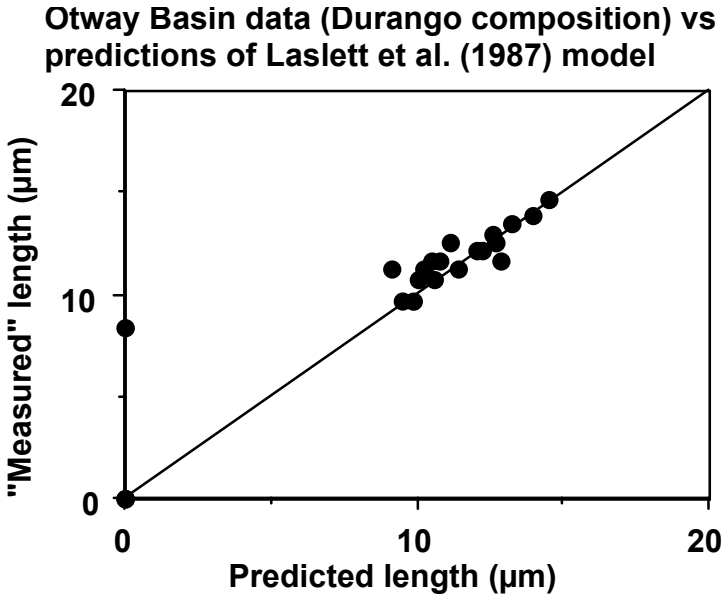

Figure C.1b Comparison of the mean track length in apatites of the same Cl content as Durango apatite from the Otway Group samples illustrated in figure C.1a, with values predicted for apatite of the same composition by the model of Laslett et al. (1987). The agreement is clearly very good except possibly at lengths below ~10 µm.

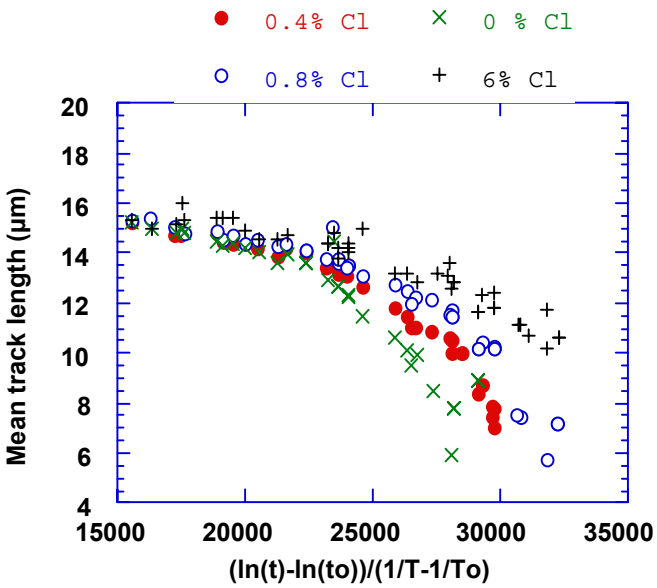

Figure C.2 Mean track length in apatites with four different chlorine contents, as a combined function of temperature and time, to reduce the data to a single scale. Fluorapatites are more easily annealed than chlorapatites, and the annealing kinetics show a progressive change with increasing Cl content.

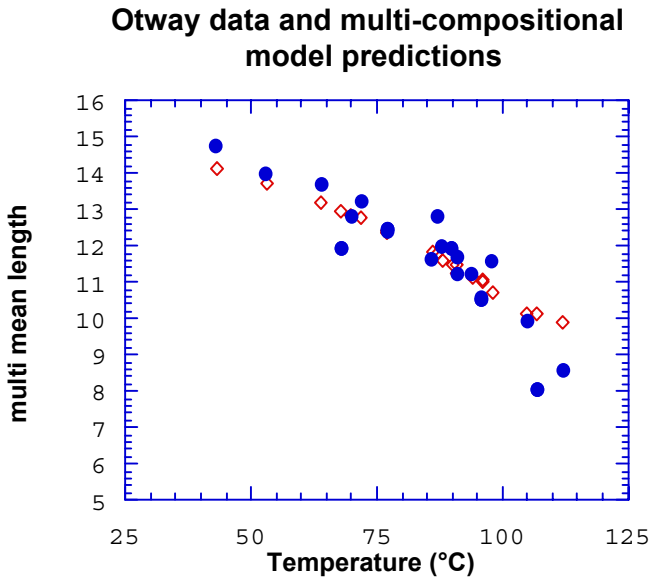

Figure C.3 Comparison of measured mean track length (solid circles) in samples from four Otway Basin reference wells (from Green et al, 1989a) and predicted mean track lengths (open diamonds) from the new multi-compositional kinetic model of fission track annealing described in Section C.3. This model takes into account the spread of Cl contents in apatites from the Otway Group samples and the influence of Cl content on annealing rate. The agreement is clearly very good over the range of the data.

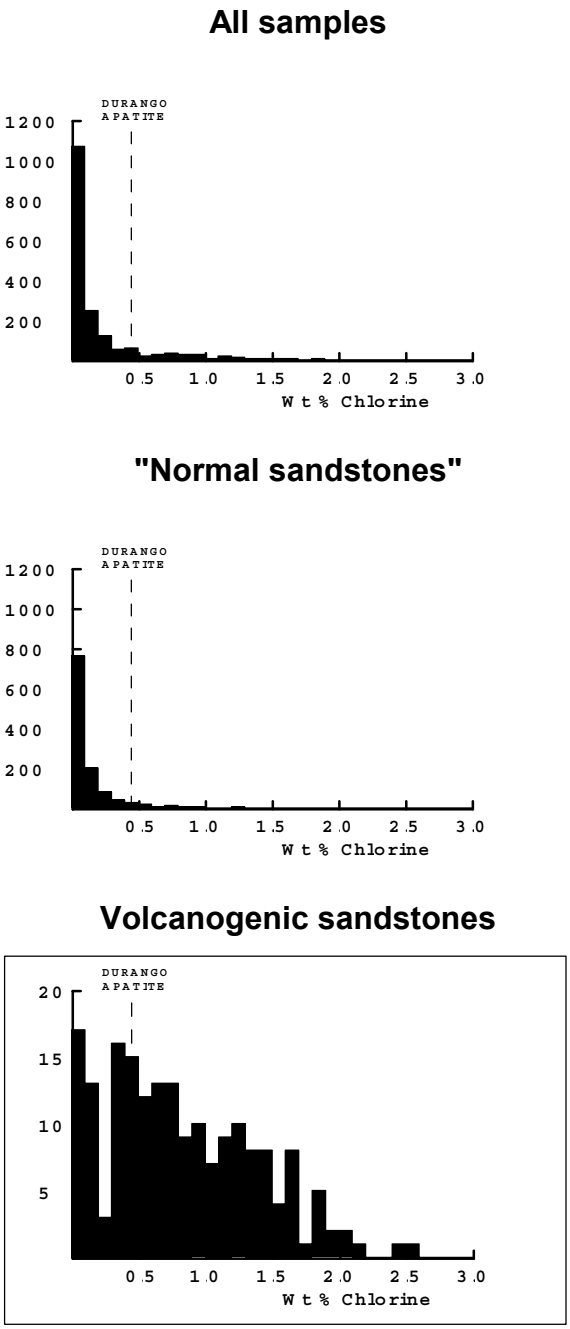

Figure C.4 **a:** Histogram of Cl contents (wt%) in over 1750 apatite grains from over 100 samples of various sedimentary and igneous rocks. Most samples give Cl contents below ~0.5 wt %, while those apatites giving higher Cl contents are characteristic of volcanogenic sandstones and basic igneous sources.

b: Histogram of Cl contents (wt%) in 1168 apatite grains from 61 samples which can loosely be characterised as "normal sandstone". The distribution is similar to that in the upper figure, except for a lower number of grains with Cl contents greater than ~1%.

c: Histogram of Cl contents (wt%) in 188 apatite grains from 15 samples of volcanogenic sandstone. The distribution is much flatter than the other two, with much higher proportion of Cl-rich grains.

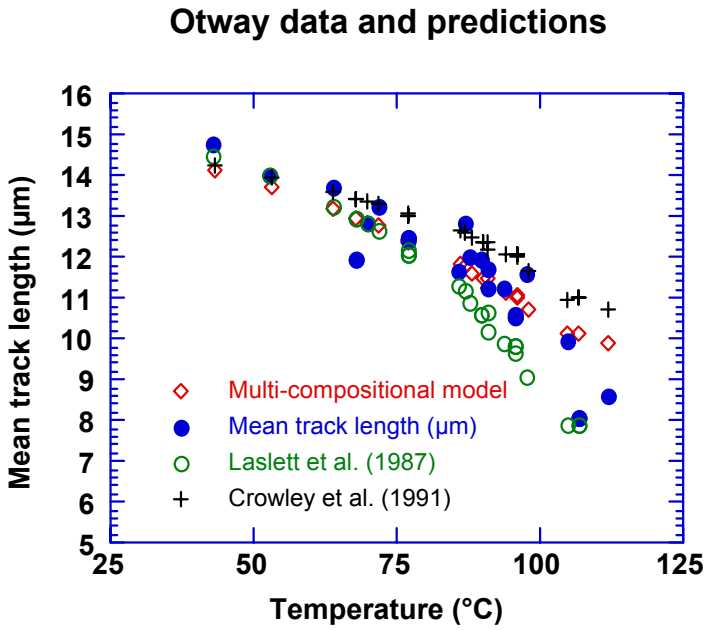

Figure C.5 Comparison of mean track length in samples from four Otway Basin reference wells (from Green et al, 1989a) and predicted mean track lengths from three kinetic models for fission track annealing. The Crowley et al. (1991) model relates to almost pure Fluorapatite (B-5), yet overpredicts mean lengths in the Otway Group samples which are dominated by Cl-rich apatites. The predictions of that model are therefore not reliable.

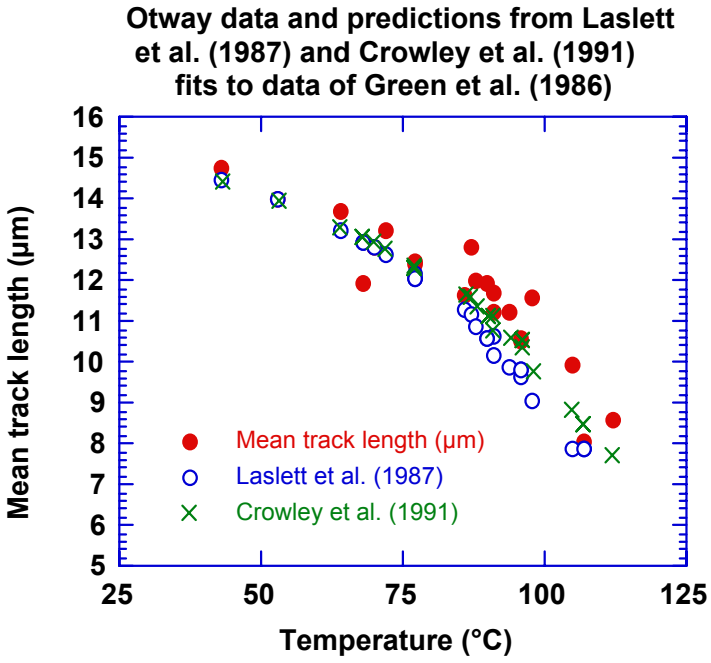

Figure C.6 Comparison of mean track length in samples from four Otway Basin reference wells with values predicted from Laslett et al. (1987) and the model fitted to the annealing data of Green et al. (1986) by Crowley et al. (1991). The predictions of the two models are not very different.

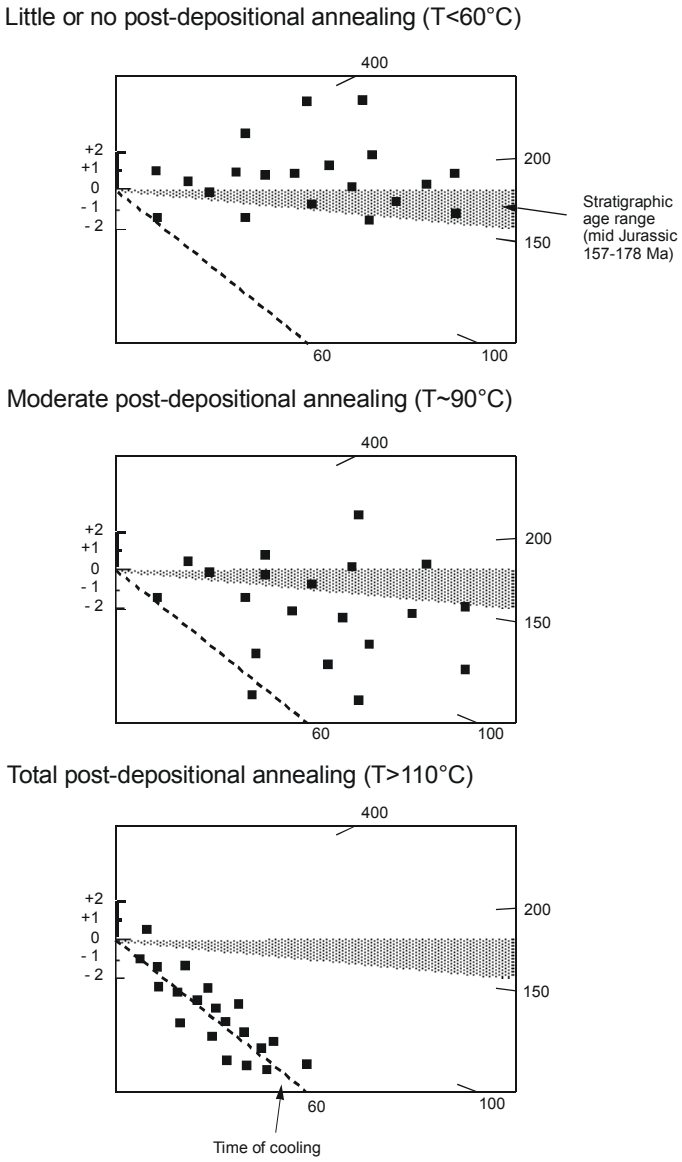

Figure C.7 Radial plots of single grain age data in three samples of mid-Jurassic sandstone that have been subjected to varying degrees of post-depositional annealing prior to cooling at ~60 Ma. The mid-point of the stratigraphic age range has been taken as the reference value (corresponding to the horizontal).

The upper diagram represents a sample which has remained at paleotemperatures less than ~60°C, and has therefore undergone little or no post-depositional annealing. All single grain ages are either compatible with the stratigraphic age (within y = ±2 in the radial plot) or older than the stratigraphic age ($y_i > 2$).

The centre diagram represents a sample which has undergone a moderate degree of post-depositional annealing, having reached a maximum paleotemperature of around ~90°C prior to cooling. While some of the individual grain ages are compatible with the stratigraphic age ($-2 < y_i < +2$) and some may be significantly greater than the stratigraphic age ($y_i > 2$), a number of grains give ages which are significantly less than the stratigraphic age ($y < 2$).

The lower diagram represents a sample in which all apatite grains were totally annealed, at paleotemperatures greater than ~110°C, prior to rapid cooling at ~60 Ma. All grains give fission track ages compatible with a fission track age of ~60 Ma (i.e., all data plot within ±2 of the radial line corresponding to an age of ~60 Ma), and most are significantly younger than the stratigraphic age.

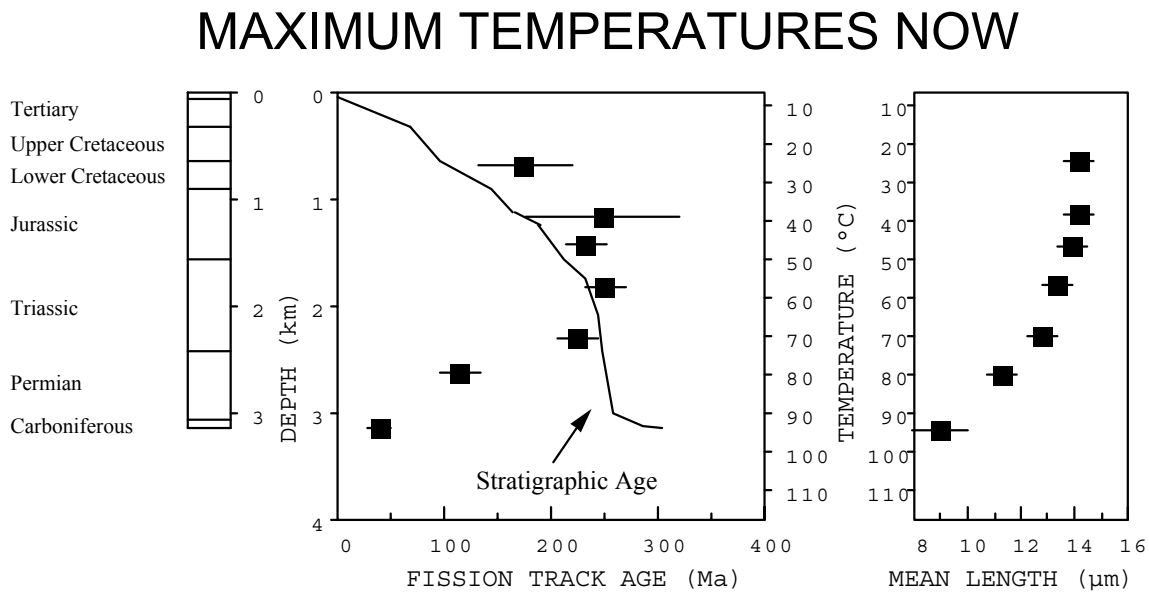

Figure C.8a Typical pattern of AFTA parameters in a well in which samples throughout the entire section are currently at their maximum temperatures since deposition. Both the fission track age and mean track length undergo progressive reduction to zero at temperatures of ~100 - 110°C, the actual value depending on the range of apatite compositions present.

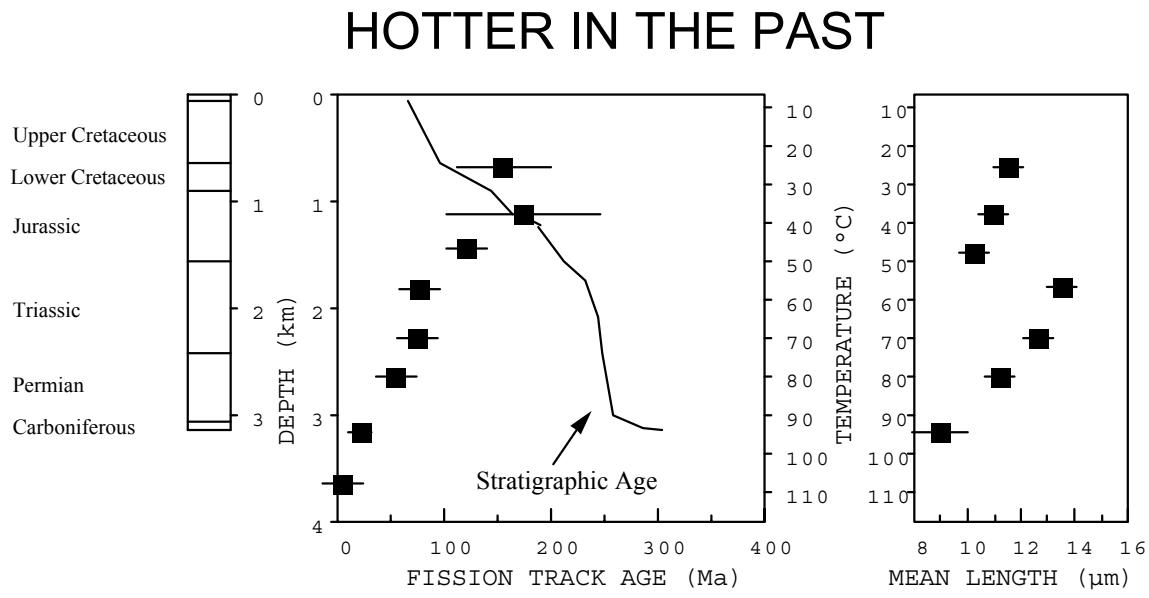

Figure C.8b Typical pattern of AFTA parameters in a well in which samples throughout the section were exposed to elevated paleotemperatures after deposition (prior to cooling in the Early Tertiary, in this case). Both the fission track age and mean track length show more reduction at temperatures of ~40 to 50°C than would be expected at such temperatures. At greater depths (higher temperatures), the constancy of fission track age and the increase in track length are both diagnostic of exposure to elevated paleotemperatures. See Appendix C for further discussion

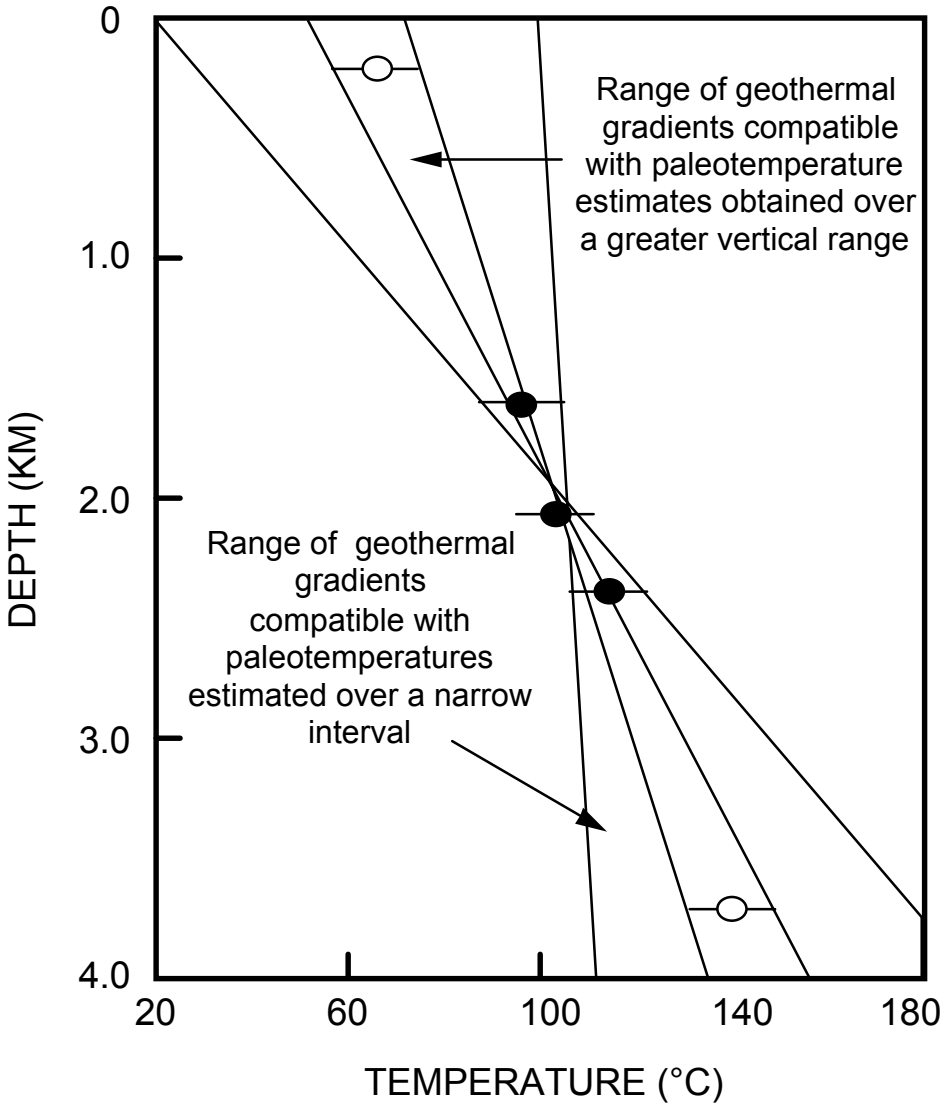

Figure C.9 It is important to obtain paleotemperature constraints over as great a range of depths as possible in order to provide a reliable estimate of paleogeothermal gradient. If paleotemperatures are only available over a narrow depth range, then the paleogeothermal gradient can only be very loosely constrained.

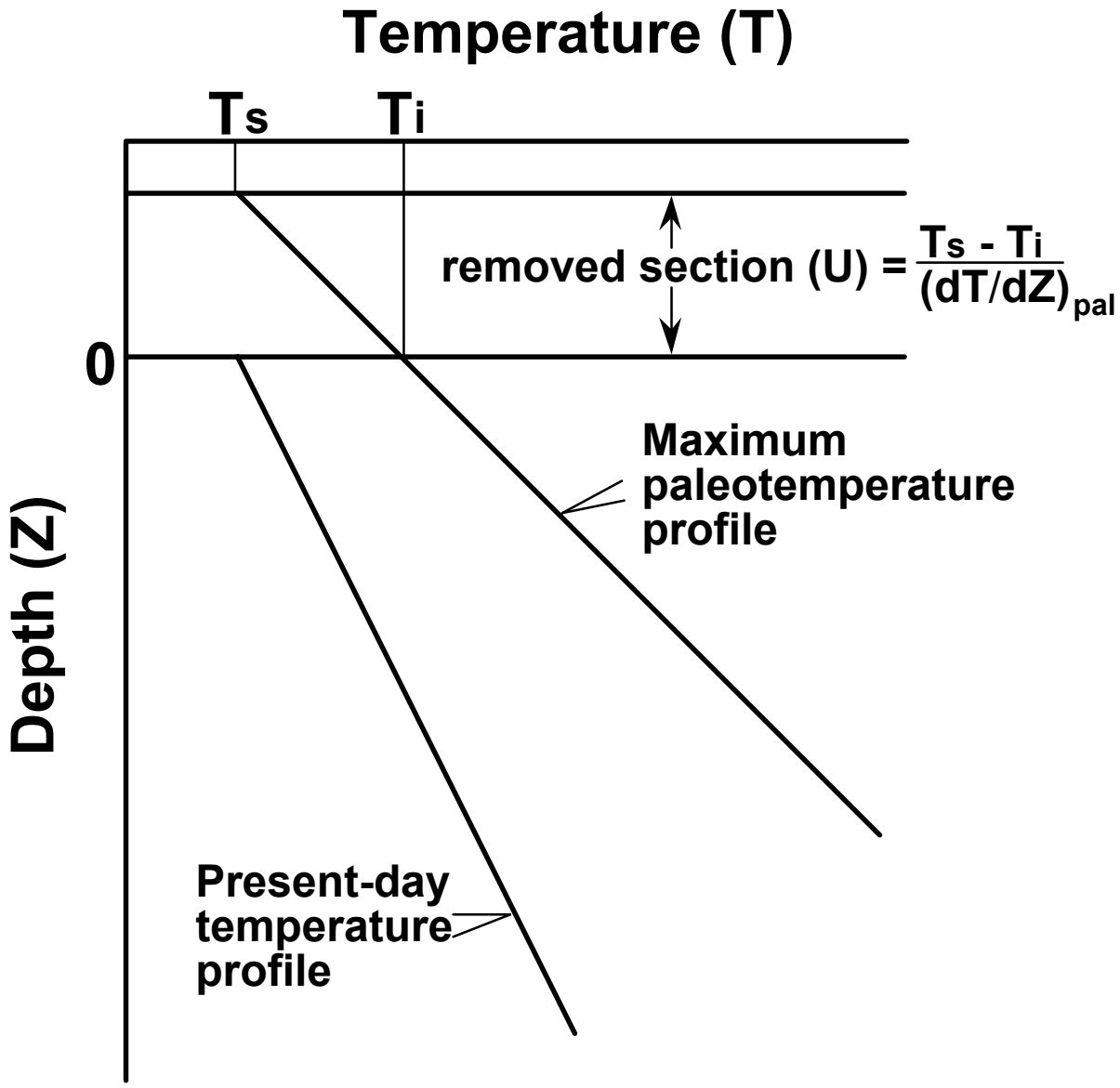

Figure C.10 If the paleogeothermal gradient can be constrained by AFTA and VR, as explained in the text, then for an assumed value of surface temperature, T_S, the amount of section removed can be estimated, as shown.

APPENDIX D

Vitrinite Reflectance Measurements

D.1 New vitrinite reflectance determinations

New vitrinite reflectance data were collected as part of this study, with details of determinations described in sections D.1 and D.2 below. In addition, further vitrinite reflectance data were supplied by the client, as summarised in section D.3.

Samples

Samples were submitted for vitrinite reflectance determination to Keiraville Konsultants, Australia. Results and sample details are summarised in Table D.2, while supporting data, including maceral descriptions and raw data sheets, are presented in the following pages.

Equipment

Leitz MPV1.1 photometer equipped with separate fluorescence illuminator, Swift point counter. Reflectance standards: spinel 0.42%, YAG 0.91%, GGG 1.72%, SiC standard for cokes and masked uranyl glass for measurement of intensity (I) in fluorescence mode. With the Keiraville Konsultants equipment, it is possible to alternate from reflectance to fluorescence mode to check for associated fluorescing liptinite, or importantly with some samples, to check for bitumen impregnation, or the presence, intensity, and source of oil-cut.

Sample preparation

Samples are normally mounted in cold setting polyester resin and polished using Cr_2O_3 and MgO polishing powders. Epoxy resins or araldite can be used if required. "Whole rock" samples are normally used but demineralisation can be undertaken. Large samples of coals and cokes can be mounted and examined.

Vitrinite Reflectance measurement

The procedure used generally follows Australian Standard (AS) 2486, but has been slightly modified for use with dispersed organic matter (DOM). For each sample, a minimum of 25 fields is measured (the number may be less if vitrinite is rare or if a limited number of particles of vitrinite is supplied, as may be the case with hand-picked

samples). If wide dispersal of vitrinite reflectances is found, the number of readings (N) is increased until a stable mean is obtained.

Vitrinite identification is made primarily on textural grounds, and this allows an independent assessment to be made of cavings and re-worked vitrinite populations. Histograms are only used for population definition when a cavings population significantly overlaps the range of the indigenous population. Where such data provides additional information, the mean maximum reflectance of inertinite and/or the mean maximum reflectance of liptinite (exinite) is reported. For each field, the maximum reflectance position is located and the reading recorded. The stage is then rotated by 180° which should give the same reading. In practice, the readings are seldom identical because of stage run-out and slight surface irregularities. If the readings are within ±5% relative, they are accepted. If not, the cause of the difference is sought and the results rejected. The usual source of differences is surface relief. The measurement of both maxima results in a total of 50 measurements being taken for the 25 fields reported. Thus, the 50 readings consist of 25 pairs of closely spaced readings which provide a check on the levelling of the surface and hence additional precision.

As the vitrinite reflectance measurements are being made, the various features of the samples are noted on a check sheet to allow a sample description to be compiled. When the reflectance measurements are complete, a thorough check is made of liptinite fluorescence characteristics. At the same time, organic matter abundance is estimated using a global estimate, a grain count method or point count method as required.

Data presentation

Individual sample results are reported in the following format:

KK No.	Depth (ft)	$\overline{R}_V$max*1	Range*2	N*3
x10324	3106	0.79	0.64 - 0.91	25

*1 Mean of all the maximum reflectance readings obtained.

*2 Lowest Rmax and highest Rmax of the population considered to represent the first generation vitrinite population.

*3 Number of fields measured (Number of measurements = 2N because 2 maximum values are recorded for each field)

Methods - Organic matter abundance and type.

After completion of vitrinite reflectance readings, the microscope is switched to fluorescence-mode and an estimate made of the abundance of each liptinite maceral. Fluorescence colours are also noted (BG 3 long UV excitation, TK400 dichroic mirror and a K490 barrier filter). The abundances are estimated using comparison charts. The categories used for liptinite (and other components) are:

Descriptor	%	Source potential
Absent	0	None
Rare	<0.1	Very poor
Sparse	0.1<x<0.5	Poor to fair
Common	0.5<x<2.0	Fair to good
Abundant	2.0<x<10.0	Good to very good
Major	10.0<x<40.0	Very good (excellent if algal)
Dominant	>40.0	Excellent

Dispersed Organic Matter (DOM) composition

At the same time as liptinite abundances are estimated, total DOM, vitrinite and inertinite abundances are estimated and reported in the categories listed above. Liptinite (exinite) fluorescence intensity and colour, lithology and a brief description of organic matter type and abundance are also recorded in a further column. Coal is described separately from dispersed organic matter (DOM). These data can be used to estimate the specific yield of the DOM and form a valuable adjunct to TOC data.

Lithological composition

The lithological abundances are ranked. For cuttings, these data can be useful in conjunction with geophysical logs in assessing the abundance and nature of cavings. For cores, it provides a record of the lithology examined and of the lithological associations of the organic matter.

Coal abundance and composition

Where coals are present, their abundance is recorded and their composition is reported as microlithotypes thus:

Coal major, **V**itrinite>**I**nertinite>**E**xinite, Clarodurite>vitrite>clarite>inertite.

These data give an approximate maceral composition and information about the organic facies of the coal. Where coal is a major or dominant component, and more precise maceral composition data are required, point count analyses should be requested. However, the precision of the original sampling is commonly a limiting factor in obtaining better quality data.

Abundance factor analysis

Especially where cuttings samples are used, abundance factor analyses are used to obtain an assessment of the maceral assemblages in the various lithologies. This can be done by a combination analysis using a point counter, but a large number of categories is required, and the precision is low if DOM is less than about 10%. For an abundance factor analysis (for core, 50 microscope fields of view) we assess the abundance of DOM, coal and shaly coal in 50 grains. The data can be used to plot DOM and coal abundance profiles.

Analyst/Advisor: Professor A.C. Cook

Prior to transmittal of final results, all samples are examined and checked by A.C. Cook who has more than 30 years' experience of work on coals, cokes, source rocks and source rock maturation.

D.2 Integration of vitrinite reflectance data with AFTA

Vitrinite reflectance is a time-temperature indicator governed by a kinetic response in a similar manner to the annealing of fission tracks in apatite as described in Appendix C. In this study, vitrinite reflectance data are interpreted on the basis of the distributed activation energy model describing the evolution of VR with temperature and time described by Burnham and Sweeney (1989), as implemented in the BasinMod™ software package of Platte River Associates. In a considerable number of wells from around the world, in which AFTA has been used to constrain the thermal history, we have found that the Burnham and Sweeney (1989) model gives good agreement between predicted and observed VR data, in a variety of settings.

As in the case of fission track annealing, it is clear from the chemical kinetic description embodied in equation 2 of Burham and Sweeney (1989) that temperature is more important than time in controlling the increase of vitrinite reflectance. If the Burham and Sweeney (1989) distributed activation energy model is expressed in the form of an Arrhenius plot (a plot of the logarithm of time versus inverse absolute temperature),

then the slopes of lines defining contours of equal vitrinite reflectance in such a plot are very similar to those describing the kinetic description of annealing of fission tracks in Durango apatite developed by Laslett et al. (1987), which is used to interpret the AFTA data in this report. This feature of the two quite independent approaches to thermal history analysis means that for a particular sample, a given degree of fission track annealing in apatite of Durango composition will be associated with the same value of vitrinite reflectance regardless of the heating rate experienced by a sample. Thus paleotemperature estimates based on either AFTA or VR data sets should be equivalent, regardless of the duration of heating. As a guide, Table D.1 gives paleotemperature estimates for various values of VR for two different heating times.

One practical consequence of this relationship between AFTA and VR is, for example, that a VR value of 0.7% is associated with total annealing of all fission tracks in apatite of Durango composition, and that total annealing of all fission tracks in apatites of more Chlorine-rich composition is accomplished between VR values of 0.7 and ~0.9%.

Furthermore, because vitrinite reflectance continues to increase progressively with increasing temperature, VR data allow direct estimation of maximum paleotemperatures in the range where fission tracks in apatite are totally annealed (generally above ~110°C) and where therefore AFTA only provides minimum estimates. Maximum paleotemperature estimates based on vitrinite reflectance data from a well in which most AFTA samples were totally annealed will allow constraints on the paleogeothermal gradient that would not be possible from AFTA alone. In such cases the AFTA data should allow tight constraints to be placed on the time of cooling and also the cooling history, since AFTA parameters will be dominated by the effects of tracks formed after cooling from maximum paleotemperatures. Even in situations where AFTA samples were not totally annealed, integration of AFTA and VR can allow paleotemperature control over a greater range of depth, e.g. by combining AFTA from sand-dominated units with VR from other parts of the section, thereby providing tighter constraint on the paleogeothermal gradient.

D.3 Client-supplied vitrinite reflectance

Vitrinite reflectance and other data (if applicable) supplied by the client is summarised in Table D.3. Unless specified, this vitrinite reflectance data has been treated at face value, as if it were collected in the same manner as described for the new data, because detailed information is usually not available.

References

Burnham, A.K. and Sweeney, J.J. (1989). A chemical kinetic model of vitrinite reflectance maturation. *Geochim. et Cosmochim. Acta,* 53, 2649-2657.

Laslett, G.M., Green, P.F., Duddy, I.R. and Gleadow, A.J.W. (1987). Thermal annealing of fission tracks in apatite 2. A quantitative analysis. *Chem. Geol. (Isot. Geosci.Sect.)*, 65, 1-13.

Table D.1: Paleotemperature - vitrinite reflectance nomogram based on Equation 2 of Burnham and Sweeney (1989)

Paleotemperature (°C / °*F*)	Vitrinite Reflectance (%) 1 Ma Duration of heating	10 Ma Duration of heating
40 / *104*	0.29	0.32
50 / *122*	0.31	0.35
60 / *140*	0.35	0.40
70 / *158*	0.39	0.45
80 / *176*	0.43	0.52
90 / *194*	0.49	0.58
100 / *212*	0.55	0.64
110 / *230*	0.61	0.70
120 / *248*	0.66	0.78
130 / *266*	0.72	0.89
140 / *284*	0.81	1.04
150 / *302*	0.92	1.20
160 / *320*	1.07	1.35
170 / *338*	1.23	1.55
180 / *356*	1.42	1.80
190 / *374*	1.63	2.05
200 / *392*	1.86	2.33
210 / *410*	2.13	2.65
220 / *428*	2.40	2.94
230 / *446*	2.70	3.23

Table D.2: Vitrinite reflectance sample details and results - well samples from Cape Sorell-1 (Geotrack Report #806)

Sample number	Depth (m)	Sample type	Stratigraphic Subdivision	Stratigraphic age (Ma)	Present temperature *1 (°C)	VR (Range) %	N
Cape Sorell-1							
GC806-4.1	485-494 *(1590-1620')*	cuttings	Nirranda Gp 2	47-37	28	-	
GC806-5.1	850-860 *(2790-2820')*	cuttings	Wangerripp 2	50-49	38	0.39 (0.31-0.52)	26
GC806-6	1216-1372 *(3990-4500')*	cuttings	Wangerripp 4 - Wangerripp 3	53-50	50	0.45 (0.34-0.58)	26
GC806-7	1500-1631 *(4920-5350')*	cuttings	Wangerripp 5 - Wangerripp 4	55-51	57	0.36 (0.33-0.40)	3
GC806-8	1929-2051 *(6330-6730')*	cuttings	Sherbrook 1	70-65	69	0.48 (0.35-0.61)	14
GC806-1	2198-2307 *(7210-7570')*	cuttings	Sherbrook 1	70-65	76	-	
GC806-9	2637-2752 *(8650-9030')*	cuttings	Sherbrook 2 - Sherbrook 1	73-65	88	-	
GC806-2	2899-3008 *(9510-9870')*	cuttings	Sherbrook 2	73-70	96	-	
GC806-10	3142-3249 *(10310-10660')*	cuttings	Sherbrook 3	78-73	102	0.54 (0.35-0.67)	30
GC806-10.1	3234-3237 *(10610-10620')*	cuttings	Sherbrook 3	78-73	103	0.56 (0.49-0.63)	27
GC806-3	3399-3501 *(11150-11485')*	cuttings	Sherbrook 5 - Sherbrook 4	80-78	109	0.60 (0.49-0.74)	26

Note: Some samples may contain both vitrinite and inertinite. Only vitrinite data is shown.

*1 See Appendix A for discussion of present temperature data.

Table D.3: Vitrinite reflectance sample details and results supplied by client - Cape Sorell-1 (Geotrack Report #806)

Depth (m)	Stratigraphic Subdivision	Stratigraphic age (Ma)	Present temperature *1 (°C)	VR (Range) %	FL
Cape Sorell-1					
1225	Wangerripp 3	51-50	48	0.40	3
1269	Wangerripp 3	51-50	49	0.48	2
1335	Wangerripp 4	53-51	51	0.55	2
1923	Sherbrook 1	70-65	67	0.44	3
2167	Sherbrook 1	70-65	74	0.45	3
2399	Sherbrook 1	70-65	80	0.42	3
2728	Sherbrook 1	70-65	89	0.47	3
3093	Sherbrook 2	73-70	99	0.60	4
3167	Sherbrook 3	78-73	102	0.45	2
3173	Sherbrook 3	78-73	102	0.54	3
3181	Sherbrook 3	78-73	102	0.46	1
3201	Sherbrook 3	78-73	102	0.90	0
3231	Sherbrook 3	78-73	103	0.45	2
3233	Sherbrook 3	78-73	103	0.47	1
3237	Sherbrook 3	78-73	103	0.57	3
3283	Sherbrook 3	78-73	105	0.54	1
3399	Sherbrook 4	79-78	108	0.61	3
3427	Sherbrook 4	79-78	109	1.00	0
3450	Sherbrook 4	79-78	109	0.56	3
3522	Sherbrook 5	80-79	111	0.66	3

Note: data with FL 3 is the most recent and most reliable

*1 See Appendix A for discussion of present temperature data.

GC806 KK # Ref #.	Depth (ft) /Type	$\overline{R}_{v}$max	Range	N	**CAPE SORRELL-1, p1** Sample description including liptinite fluorescence, maceral abundances, mineral fluorescence
					EOCENE - Nirranda Group
T7772 806-4.1 Ctgs	1590-1620	-	-	-	Rare sporinite orange to dull orange. (Sandstone with sideritic and pyrite cement. Dom rare, L only, I and L absent. Liptinite rare, inertinite and vitrinite absent. Mineral fluorescence weak, commonly absent within quartz grains but some weak patchy orange fluorescence from the matrix of some sandstone grains. Siderite major, Pyrite abundant to major.)
					EOCENE - Wangeripp Group
T7773 806-5.1 Ctgs	2790-2820	0.39	0.31-0.52	26	Rare sporinite yellowish orange to orange, rare cutinite orange to dull orange, rare liptodetrinite yellow to dull orange. (Sandstone >>silty claystone>sidereite. Dom sparse, V>L>I. Vitrinite and liptinite sparse, inertinite rare. Rare oil inclusions, yellow within quartz overgrowths. Mineral fluorescence weak, commonly absent within quartz grains but some weak patchy dull orange from claystone. Siderite abundant. Pyrite common to abundant.)
T7774 806-6 Ctgs	3990-4500	0.45	0.34-0.58	26	Rare sporinite yellowish orange to dull orange, rare cutinite orange to dull orange, rare liptodetrinite yellow to orange. (Sandstone with sideritic and marcasite cement>claystone> igneous rock fragments. Dom sparse, V>I>L. Vitrinite and inertinite sparse, liptinite rare. Mineral fluorescence absent within quartz grains but some weak patchy orange fluorescence from the matrix of some sandstone grains and patchy moderate orange to weak dull orange in claystone. The marcasite is coarsely crystalline and shows strong bireflectance. Siderite major. Marcasite abundant to major.)
T7775 806-7 Ctgs	4920-5350	0.36	0.33-0.40	3	Rare sporinite yellowish orange, rare liptodetrinite yellowish orange. (Sandstone some with calcite or marcasite cement> siderite. Dom rare, V>L, I absent. Vitrinite and liptinite rare, inertinite absent. Dom occurs within the siderite grains. Mineral fluorescence weak, absent within quartz grains but some weak patchy orange fluorescence from the calcite matrix of some sandstone grains and patchy weak dull orange within siderite. Siderite major, Marcasite abundant.)
					MAASTRICHTIAN - Sherbrook Group
T7776 806-8 Ctgs	6330-6730	0.48	0.35-0.61	14	Rare sporinite yellowish orange, rare liptodetrinite yellow, rare lamalginite yellow. (Sandstone with calcite and marcasite matrix>sideritic claystone. Dom rare, V>I>L. All maceral groups rare. Mineral fluorescence variable, commonly absent within quartz grains, moderate to bright orange from calcite, weak to absent from claystone. Some of the marcasite occurs as plant petrifactions. Siderite common. Marcasite abundant.)
T7777 806-1 Ctgs	7210-7570	-	-	-	Fluorescing liptinite absent. (Sandstone>igneous rock fragments >siltstone>silty claystone. Dom absent.. Mineral fluorescence generally weak to absent, but some possible oil contamination around some grains possibly from mud cake. Pyrite sparse.)

GC806 KK # Ref #.	Depth (ft) /Type	$\overline{R}_{v}$max	Range	N	**CAPE SORRELL-1, p2** Sample description including liptinite fluorescence, maceral abundances, mineral fluorescence
					MAASTRICHTIAN - Sherbrook Group
T7778 806-9 Ctgs	8650-9030	-	-	-	Fluorescing liptinite absent. (Sandstone>igneous rock fragments >siltstone>claystone. Dom absent.. Mineral fluorescence generally weak to absent. Pyrite sparse.)
T7779 806-2 Ctgs	9510-9870	-	-	-	Fluorescing liptinite absent. (Sandstone>igneous rock fragments >siltstone>claystone. Dom absent.. Mineral fluorescence generally weak to absent. Pyrite sparse.)
T7780 806-10 Ctgs	10310-10660	0.54	0.35-0.67	30	Sparse sporinite yellow to yellowish orange, sparse suberinite dull brown to non-fluorescing, sparse cutinite orange, sparse liptodetrinite yellow to orange sparse resinite yellow to orange. (Sandstone, silty>sandy siltstone>silty claystone>coal. Coal abundant, clarite>vitrite, approx maceral group composition of coal: vitrinite 95%, inertinite trace, liptinite 5%. Dom common, V>L>I. Vitrinite and liptinite common, inertinite rare. The lower reflecting fields are associated with bark tissues, and are probably not due to cavings. Rare to common oil inclusions in calcite. Mineral fluorescence patchy, bright orange to weak orange. Pyrite abundant.)
T7781 806- 10.1 Ctgs	10610-10620	0.56	0.49-0.63	27	Sparse suberinite dull brown to non-fluorescing, sparse cutinite yellow to dull orange, sparse sporinite yellow to yellowish orange, sparse liptodetrinite yellow to orange, sparse resinite yellow to orange. (Claystone>siltstone>sandstone>coal and shaly coal. Coal and shaly coal major, vitrite>clarite>clarodurite. Approx maceral group composition of coal: vitrinite 95%, inertinite 2, liptinite 3%. Most of the inertinite is associated with shaly coal, while vitrite occurs both in coal and shaly coal. Dom common, V>L>I. Vitrinite and liptinite common, inertinite rare. The vitrinite reflectance range is very small. Vitrinite fluorescence is distinct but weak, little or no evidence of oil cut from vitrinite initially, but oil haze develops on standing from coal and shaly coal. Exsudatinite vein, bright yellow. Rare to common oil inclusions in calcite. Mineral fluorescence patchy, bright orange to weak orange. Pyrite abundant.)
T7782 806-3 Ctgs	11150-11485	0.60	0.49-0.74	26	Sparse suberinite weak brown to non-fluorescing, sparse sporinite yellow to yellowish orange, sparse cutinite yellowish orange to orange, sparse liptodetrinite yellow to orange. (Igneous rock fragments>sandstone>siltstone>silty claystone. Dom common, V>L>I. Vitrinite and liptinite common, inertinite rare. Rare to common oil inclusions in calcite and rare oil inclusions within quartz overgrowths. Mineral fluorescence patchy, bright orange to weak orange. Pyrite abundant.)

The Wangeripp Group down to about 6730' is immature although it is close to the top of the oil window in the deepest sample. The upper part of the Sherbrook Group is barren and organic matter is not found again until 10310'. Most of the samples in the barren interval are dominated by igneous rock fragments. It is possible that these are reworked, but it seems likely that some represent a tuffaceous section or there are intrusions within the section. Igneous rock fragments are also present in the deeper samples but there is not evidence of contact alteration. The three deepest samples contain relatively abundant organic matter and coals are present in two of the samples. The coals are clarite and vitrite, and represent the vitrinite rich coal facies that is found within the Cretaceous (an inertinite-rich facies also occurs within the Cretaceous but is not evident in this well). The deepest part of the section is oil mature, the vitrinite may be marginally perhydrous, but the data provide a very precise measure of the level of maturation without any need for corrections. Oil occurs as inclusions associated with calcite in the three deeper samples and also occurs more rarely as "normal" inclusions in quartz overgrowths in the deepest sample (806-3) and in the shallowest Wangeripp Group sample, 806-5.1. Oil haze seeping from coal and shaly coal after sample left standing and a bright yellow exsudatinite vein are noted in 806-10.1.

ACC Friday, 28 September 2001

Keiraville Konsultants Pty. Ltd.
7 Dallas Street,
Keiraville, NSW 2500
Australia.

Telephone: (02) 42 299843
International: +61-2-42 299843
Fax: +61-(0)2-42 299624
Email: acc@ozemail.com.au

GC806-8, Cape Sorrell-1, 6630-6730', Ctgs (T7776)

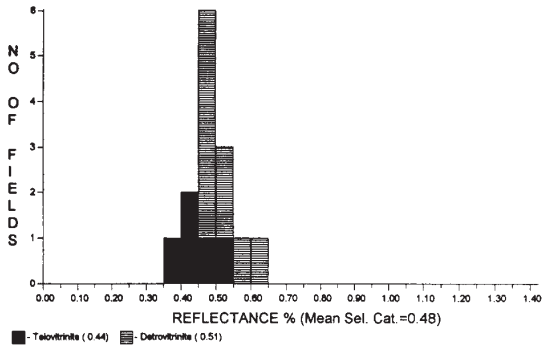

Category	No. of Readings	Mean	Standard Deviation
Telovitrinite	5	0.44	0.068
Detrovitrinite	9	0.51	0.049
Total:	14	0.48	0.066

Selected categories: Telovitrinite, Detrovitrinite.

No. of readings:	14
Mean of selected categories:	0.48
Standard deviation of selected categories:	0.066

Keiraville Konsultants Pty. Ltd.
7 Dallas Street,
Keiraville, NSW 2500
Australia.

Telephone: (02) 42 299843
International: +61-2-42 299843
Fax: +61-(0)2-42 299624
Email: acc@ozemail.com.au

GC806-5.1 Cape Sorrell-1, 2790-2820', Ctgs (T7773)

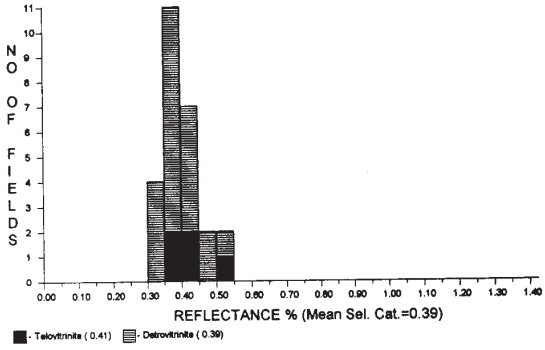

Category	No. of Readings	Mean	Standard Deviation
Telovitrinite	5	0.41	0.054
Detrovitrinite	21	0.39	0.049
Total:	26	0.39	0.050

Selected categories: Telovitrinite, Detrovitrinite.

No. of readings:	26
Mean of selected categories:	0.39
Standard deviation of selected categories:	0.050

Keiraville Konsultants Pty. Ltd.
7 Dallas Street,
Keiraville, NSW 2500
Australia.

Telephone: (02) 42 299843
International: +61-2-42 299843
Fax: +61-(0)2-42 299624
Email: acc@ozemail.com.au

GC806-6, Cape Sorrell-1, 3990-4500', Ctgs (T7774)

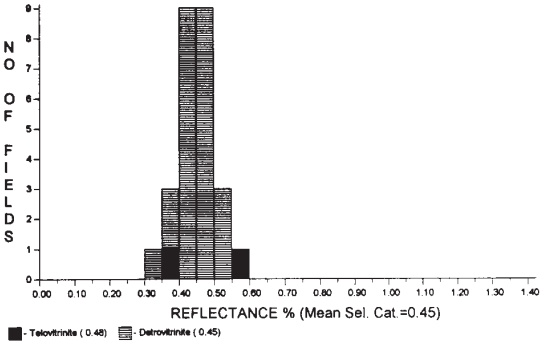

Category	No. of Readings	Mean	Standard Deviation
Telovitrinite	2	0.48	0.100
Detrovitrinite	24	0.45	0.048
Total:	26	0.45	0.054

Selected categories: Telovitrinite, Detrovitrinite.

No. of readings:	26
Mean of selected categories:	0.45
Standard deviation of selected categories:	0.054

Keiraville Konsultants Pty. Ltd.
7 Dallas Street,
Keiraville, NSW 2500
Australia.

Telephone: (02) 42 299843
International: +61-2-42 299843
Fax: +61-(0)2-42 299624
Email: acc@ozemail.com.au

GC806-7 Cape Sorrell-1, 4920-5350', Ctgs (T7775)

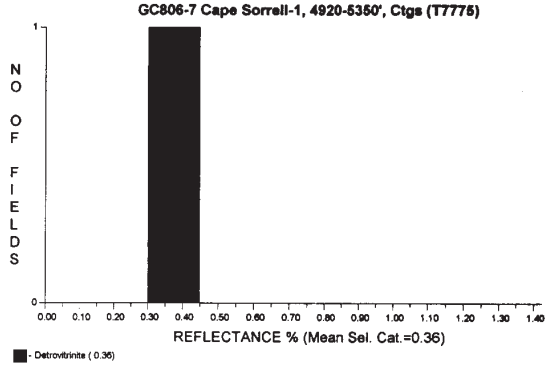

Category	No. of Readings	Mean	Standard Deviation
Detrovitrinite	3	0.36	0.029
Total:	3	0.36	0.029

Selected categories: Detrovitrinite.

No. of readings:	3
Mean of selected categories:	0.36
Standard deviation of selected categories:	0.029

Keiraville Konsultants Pty. Ltd.
7 Dallas Street,
Keiraville, NSW 2500
Australia.

Telephone: (02) 42 299843
International: +61-2-42 299843
Fax: +61-(0)2-42 299624
Email: acc@ozemail.com.au

GC806-10, Cape Sorrell-1, 10310-10660' Ctgs (T7780)

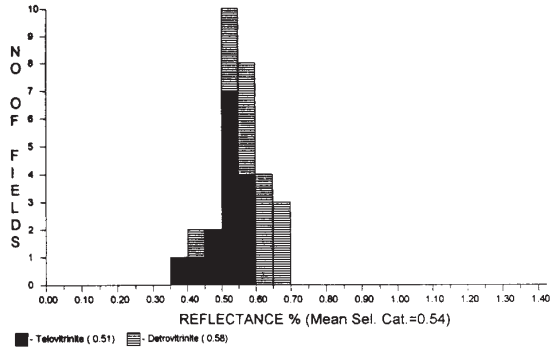

Category	No. of Readings	Mean	Standard Deviation
Telovitrinite	15	0.51	0.060
Detrovitrinite	15	0.58	0.067
Total:	30	0.54	0.074

Selected categories: Telovitrinite, Detrovitrinite.

No. of readings:	30
Mean of selected categories:	0.54
Standard deviation of selected categories:	0.074

Keiraville Konsultants Pty. Ltd.
7 Dallas Street,
Keiraville, NSW 2500
Australia.

Telephone: (02) 42 299843
International: +61-2-42 299843
Fax: +61-(0)2-42 299624
Email: acc@ozemail.com.au

GC806-10.1, Cape Sorrell-1 10610-10620', Ctgs (T7781)

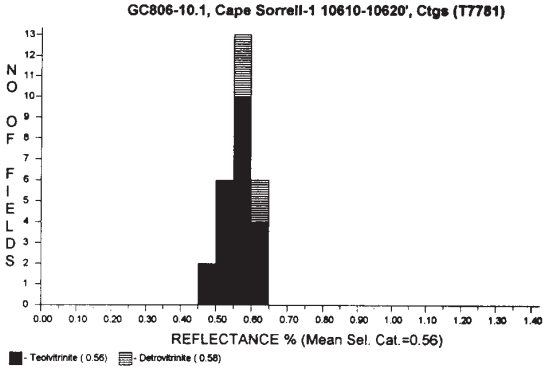

Category	No. of Readings	Mean	Standard Deviation
Teolvitrinite	22	0.56	0.037
Detrovitrinite	5	0.58	0.032
Total:	27	0.56	0.038

Selected categories: Teolvitrinite, Detrovitrinite.

No. of readings:	27
Mean of selected categories:	0.56
Standard deviation of selected categories:	0.038

Keiraville Konsultants Pty. Ltd.
7 Dallas Street,
Keiraville, NSW 2500
Australia.

Telephone: (02) 42 299843
International: +61-2-42 299843
Fax: +61-(0)2-42 299624
Email: acc@ozemail.com.au

GC806-3, Cape Sorrell-1, 11150-11485', Ctgs (T7782)

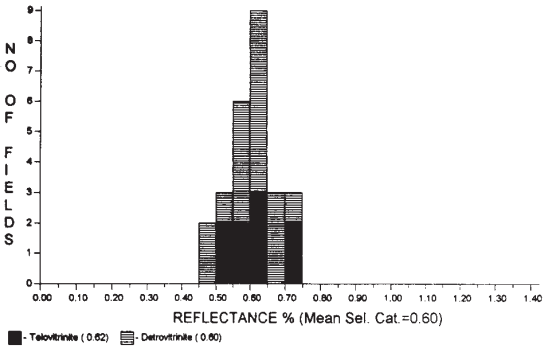

Category	No. of Readings	Mean	Standard Deviation
Telovitrinite	9	0.62	0.061
Detrovitrinite	17	0.60	0.061
Total:	26	0.60	0.062

Selected categories: Telovitrinite, Detrovitrinite.

No. of readings:	26
Mean of selected categories:	0.60
Standard deviation of selected categories:	0.062

R	No Read	Pop Range	R	No Read	Pop Range	R	No Read	Pop Range	R	No Read	Pop Range	R	No Read	Pop Range	R	No Read	Pop Range	R	No Read	Pop Range	R	No Read	Pop Range	R	No Read	Pop Range
0.10			0.40			0.70			1.00			1.30			1.60			1.90			2.20			2.50		
0.11			0.41			0.71			1.01			1.31			1.61			1.91			2.21			2.51		
0.12			0.42			0.72			1.02			1.32			1.62			1.92			2.22			2.52		
0.13			0.43			0.73			1.03			1.33			1.63			1.93			2.23			2.53		
0.14			0.44			0.74			1.04			1.34			1.64			1.94			2.24			2.54		
0.15			0.45			0.75			1.05			1.35			1.65			1.95			2.25			2.55		
0.16			0.46			0.76			1.06			1.36			1.66			1.96			2.26			2.56		
0.17			0.47			0.77			1.07			1.37			1.67			1.97			2.27			2.57		
0.18			0.48			0.78			1.08			1.38			1.68			1.98			2.28			2.58		
0.19			0.49			0.79			1.09			1.39			1.69			1.99			2.29			2.59		
0.20			0.50			0.80			1.10			1.40			1.70			2.00			2.30			2.60		
0.21			0.51			0.81			1.11			1.41			1.71			2.01			2.31			2.61		
0.22			0.52	No	FGV	0.82			1.12	No	Inert	1.42			1.72			2.02			2.32			2.62		
0.23			0.53			0.83			1.13			1.43			1.73			2.03			2.33			2.63		
0.24			0.54			0.84			1.14			1.44			1.74			2.04			2.34			2.64		
0.25			0.55			0.85			1.15			1.45			1.75			2.05			2.35			2.65		
0.26			0.56			0.86			1.16			1.46			1.76			2.06			2.36			2.66		
0.27			0.57			0.87			1.17			1.47			1.77			2.07			2.37			2.67		
0.28			0.58			0.88			1.18			1.48			1.78			2.08			2.38			2.68		
0.29			0.59			0.89			1.19			1.49			1.79			2.09			2.39			2.69		
0.30			0.60			0.90			1.20			1.50			1.80			2.10			2.40			2.70		
0.31			0.61			0.91			1.21			1.51			1.81			2.11			2.41			2.71		
0.32			0.62			0.92			1.22			1.52			1.82			2.12			2.42			2.72		
0.33			0.63			0.93			1.23			1.53			1.83			2.13			2.43			2.73		
0.34			0.64			0.94			1.24			1.54			1.84			2.14			2.44			2.74		
0.35			0.65			0.95			1.25			1.55			1.85			2.15			2.45			2.75		
0.36			0.66			0.96			1.26			1.56			1.86			2.16			2.46			2.76		
0.37			0.67			0.97			1.27			1.57			1.87			2.17			2.47			2.77		
0.38			0.68			0.98			1.28			1.58			1.88			2.18			2.48			2.78		
0.39			0.69			0.99			1.29			1.59			1.89			2.19			2.49			2.79		

VITRINITE - %		INERTINITE - %						LIPTINITE <0.1 %								OIL DROPS	BITUMEN
TV	DV	Sfus	Scler	Fus	Macr	ID	Micr	Spor <0.1	Cut	Sub	Res	Ld	Bituminite	Telalginite	Lamalginite	Oil cut	

Sample Number..T7772.....Well Name...GEOTRACK, GC806-4.1 Cape Sorrell-1..... Depth...1590-1620 ft... ..... SampleType....Ctgs....
Date. ..24/.09/ 2001.. Op..ACC..... FGV - First Generation Vitrinite, RV - Reworked Vitrinite, BTT - Bituminite, B - Bitumen, Inert - Inertinite, Cav - Cavings, DA - Drilling Mud Additives MICR D:\RWORK.ms6\806VRW.doc

R	No Read	Pop Range	R	No Read	Pop Range	R	No Read	Pop Range	R	No Read	Pop Range	R	No Read	Pop Range	R	No Read	Pop Range	R	No Read	Pop Range	R	No Read	Pop Range	R	No Read	Pop Range
0.10			0.40	4		0.70			1.00			1.30			1.60			1.90			2.20			2.50		
0.11			0.41	1		0.71			1.01			1.31			1.61			1.91			2.21			2.51		
0.12			0.42	1		0.72			1.02			1.32			1.62			1.92			2.22			2.52		
0.13			0.43	1		0.73			1.03			1.33			1.63			1.93			2.23			2.53		
0.14			0.44			0.74			1.04			1.34			1.64			1.94			2.24			2.54		
0.15			0.45			0.75			1.05			1.35			1.65			1.95			2.25			2.55		
0.16			0.46	2		0.76			1.06			1.36			1.66			1.96			2.26			2.56		
0.17			0.47			0.77			1.07			1.37			1.67			1.97			2.27			2.57		
0.18			0.48			0.78			1.08			1.38			1.68			1.98			2.28			2.58		
0.19			0.49			0.79			1.09			1.39			1.69			1.99			2.29			2.59		
0.20			0.50	1		0.80			1.10			1.40			1.70			2.00			2.30			2.60		
0.21			0.51		FGV	0.81			1.11			1.41			1.71			2.01			2.31			2.61		
0.22			0.52	1	↓	0.82			1.12			1.42			1.72			2.02			2.32			2.62		
0.23			0.53			0.83			1.13			1.43			1.73			2.03			2.33			2.63		
0.24			0.54			0.84			1.14			1.44			1.74			2.04			2.34			2.64		
0.25			0.55			0.85			1.15			1.45			1.75			2.05			2.35			2.65		
0.26			0.56			0.86			1.16			1.46			1.76			2.06			2.36			2.66		
0.27			0.57			0.87			1.17			1.47			1.77			2.07			2.37			2.67		
0.28			0.58			0.88			1.18			1.48			1.78			2.08			2.38			2.68		
0.29			0.59			0.89			1.19			1.49			1.79			2.09			2.39			2.69		
0.30			0.60			0.90			1.20			1.50			1.80			2.10			2.40			2.70		
0.31	1	↑	0.61			0.91			1.21			1.51			1.81			2.11			2.41			2.71		
0.32		FGV	0.62			0.92			1.22			1.52			1.82			2.12			2.42			2.72		
0.33	2		0.63			0.93			1.23			1.53			1.83			2.13			2.43			2.73		
0.34	1		0.64			0.94			1.24			1.54			1.84			2.14			2.44			2.74		
0.35	2		0.65			0.95			1.25			1.55			1.85			2.15			2.45			2.75		
0.36	5		0.66			0.96			1.26			1.56			1.86			2.16			2.46			2.76		
0.37			0.67			0.97			1.27			1.57			1.87			2.17			2.47			2.77		
0.38	3		0.68			0.98			1.28			1.58			1.88			2.18			2.48			2.78		
0.39	1		0.69			0.99			1.29			1.59			1.89			2.19			2.49			2.79		

VITRINITE 0.2 %		INERTINITE <0.1 %						LIPTINITE 0.1 %							OIL DROPS	BITUMEN
TV	DV	Sfus	Scler	Fus	Macr	ID	Micr	Spor <0.1	Cut <0.1	Sub	Res	Ld <0.1	Bituminite	Telalginite	Lamalginite	Oil cut

Sample Number..T7773.....Well Name...GEOTRACK, GC806-5.1 Cape Sorrell-1..... Depth...2790-2820 ft... ..... SampleType....Ctgs....
Date. ..24/.09/ 2001.. Op..ACC..... FGV - First Generation Vitrinite, RV - Reworked Vitrinite, BTT - Bituminite, B - Bitumen, Inert - Inertinite, Cav - Cavings, DA - Drilling Mud Additives MICR D:\RWORK.ms6\806VRW.doc

R	No Read	Pop Range	R	No Read	Pop Range	R	No Read	Pop Range	R	No Read	Pop Range	R	No Read	Pop Range	R	No Read	Pop Range	R	No Read	Pop Range	R	No Read	Pop Range	R	No Read	Pop Range
0.10			0.40	2		0.70			1.00			1.30			1.60			1.90			2.20			2.50		
0.11			0.41	2		0.71			1.01			1.31			1.61			1.91			2.21			2.51		
0.12			0.42	2		0.72			1.02			1.32			1.62			1.92			2.22			2.52		
0.13			0.43			0.73			1.03			1.33			1.63			1.93			2.23			2.53		
0.14			0.44	3		0.74			1.04			1.34			1.64			1.94			2.24			2.54		
0.15			0.45			0.75			1.05			1.35			1.65			1.95			2.25			2.55		
0.16			0.46	2		0.76			1.06			1.36			1.66			1.96			2.26			2.56		
0.17			0.47	2		0.77			1.07			1.37			1.67			1.97			2.27			2.57		
0.18			0.48	2		0.78			1.08			1.38			1.68			1.98			2.28			2.58		
0.19			0.49	3		0.79			1.09			1.39			1.69			1.99			2.29			2.59		
0.20			0.50			0.80			1.10			1.40			1.70			2.00			2.30			2.60		
0.21			0.51	1		0.81			1.11			1.41			1.71			2.01			2.31			2.61		
0.22			0.52	1		0.82			1.12			1.42			1.72			2.02			2.32			2.62		
0.23			0.53			0.83			1.13			1.43			1.73			2.03			2.33			2.63		
0.24			0.54	1		0.84			1.14			1.44			1.74			2.04			2.34			2.64		
0.25			0.55			0.85			1.15			1.45			1.75			2.05			2.35			2.65		
0.26			0.56			0.86			1.16			1.46			1.76			2.06			2.36			2.66		
0.27			0.57		FGV	0.87			1.17			1.47			1.77			2.07			2.37			2.67		
0.28			0.58	1	↓	0.88			1.18			1.48			1.78			2.08			2.38			2.68		
0.29			0.59			0.89			1.19			1.49			1.79			2.09			2.39			2.69		
0.30			0.60			0.90			1.20			1.50			1.80			2.10			2.40			2.70		
0.31			0.61			0.91			1.21			1.51			1.81			2.11			2.41			2.71		
0.32			0.62			0.92			1.22			1.52			1.82			2.12			2.42			2.72		
0.33			0.63			0.93			1.23			1.53			1.83			2.13			2.43			2.73		
0.34	1	↑	0.64			0.94			1.24			1.54			1.84			2.14			2.44			2.74		
0.35		FGV	0.65			0.95			1.25			1.55			1.85			2.15			2.45			2.75		
0.36			0.66			0.96			1.26			1.56			1.86			2.16			2.46			2.76		
0.37			0.67			0.97			1.27			1.57			1.87			2.17			2.47			2.77		
0.38	2		0.68			0.98			1.28			1.58			1.88			2.18			2.48			2.78		
0.39	1		0.69			0.99			1.29			1.59			1.89			2.19			2.49			2.79		

VITRINITE 0.3 %		INERTINITE 0.1 %						LIPTINITE <0.1 %							OIL DROPS	BITUMEN
TV	DV	Sfus	Scler	Fus	Macr	ID	Micr	Spor <0.1	Cut <0.1	Sub	Res	Ld <0.1	Bituminite	Telalginite	Lamalginite	Oil cut

Sample Number..T7774.....Well Name...GEOTRACK, GC806-6 Cape Sorrell-1..... Depth...3990-4500 ft... ..... SampleType....Ctgs....
Date. ..24/.09/ 2001.. Op..ACC..... FGV - First Generation Vitrinite, RV - Reworked Vitrinite, BTT - Bituminite, B - Bitumen, Inert - Inertinite, Cav - Cavings, DA - Drilling Mud Additives MICR D:\RWORK.ms6\806VRW.doc

R	No Read	Pop Range	R	No Read	Pop Range	R	No Read	Pop Range	R	No Read	Pop Range	R	No Read	Pop Range	R	No Read	Pop Range	R	No Read	Pop Range	R	No Read	Pop Range	R	No Read	Pop Range
0.10			0.40	1	↓	0.70			1.00			1.30			1.60			1.90			2.20			2.50		
0.11			0.41			0.71			1.01			1.31			1.61			1.91			2.21			2.51		
0.12			0.42			0.72			1.02			1.32			1.62			1.92			2.22			2.52		
0.13			0.43			0.73			1.03			1.33			1.63			1.93			2.23			2.53		
0.14			0.44			0.74			1.04			1.34			1.64			1.94			2.24			2.54		
0.15			0.45			0.75			1.05			1.35			1.65			1.95			2.25			2.55		
0.16			0.46			0.76			1.06			1.36			1.66			1.96			2.26			2.56		
0.17			0.47			0.77			1.07			1.37			1.67			1.97			2.27			2.57		
0.18			0.48			0.78			1.08			1.38			1.68			1.98			2.28			2.58		
0.19			0.49			0.79			1.09			1.39			1.69			1.99			2.29			2.59		
0.20			0.50			0.80			1.10			1.40			1.70			2.00			2.30			2.60		
0.21			0.51			0.81			1.11			1.41			1.71			2.01			2.31			2.61		
0.22			0.52			0.82			1.12			1.42			1.72			2.02			2.32			2.62		
0.23			0.53			0.83			1.13			1.43			1.73			2.03			2.33			2.63		
0.24			0.54			0.84			1.14			1.44			1.74			2.04			2.34			2.64		
0.25			0.55			0.85			1.15			1.45			1.75			2.05			2.35			2.65		
0.26			0.56			0.86			1.16			1.46			1.76			2.06			2.36			2.66		
0.27			0.57			0.87			1.17			1.47			1.77			2.07			2.37			2.67		
0.28			0.58			0.88			1.18			1.48			1.78			2.08			2.38			2.68		
0.29			0.59			0.89			1.19			1.49			1.79			2.09			2.39			2.69		
0.30			0.60			0.90			1.20			1.50			1.80			2.10			2.40			2.70		
0.31			0.61			0.91			1.21			1.51			1.81			2.11			2.41			2.71		
0.32			0.62			0.92			1.22			1.52			1.82			2.12			2.42			2.72		
0.33	1	↑	0.63			0.93			1.23			1.53			1.83			2.13			2.43			2.73		
0.34		FGV	0.64			0.94			1.24			1.54			1.84			2.14			2.44			2.74		
0.35	1		0.65			0.95			1.25			1.55			1.85			2.15			2.45			2.75		
0.36			0.66			0.96			1.26			1.56			1.86			2.16			2.46			2.76		
0.37			0.67			0.97			1.27			1.57			1.87			2.17			2.47			2.77		
0.38			0.68			0.98			1.28			1.58			1.88			2.18			2.48			2.78		
0.39			0.69			0.99			1.29			1.59			1.89			2.19			2.49			2.79		

VITRINITE <0.1 %		INERTINITE - %						LIPTINITE <0.1 %								OIL DROPS	BITUMEN
TV	DV	Sfus	Scler	Fus	Macr	ID	Micr	Spor <0.1	Cut	Sub	Res	Ld <0.1	Bituminite	Telalginite	Lamalginite	Oil cut	

Sample Number..T7775.....Well Name...GEOTRACK, GC806-7 Cape Sorrell-1..... Depth...4920-5350 ft... ..... SampleType....Ctgs....
Date. ..25/.09/ 2001.. Op..ACC..... FGV - First Generation Vitrinite, RV - Reworked Vitrinite, BTT - Bituminite, B - Bitumen, Inert - Inertinite, Cav - Cavings, DA - Drilling Mud Additives MICR D:\RWORK.ms6\806VRW.doc

R	No Read	Pop Range	R	No Read	Pop Range	R	No Read	Pop Range	R	No Read	Pop Range	R	No Read	Pop Range	R	No Read	Pop Range	R	No Read	Pop Range	R	No Read	Pop Range	R	No Read	Pop Range
0.10			0.40	1		0.70			1.00			1.30			1.60			1.90			2.20			2.50		
0.11			0.41	1		0.71			1.01			1.31			1.61			1.91			2.21			2.51		
0.12			0.42			0.72			1.02			1.32			1.62			1.92			2.22			2.52		
0.13			0.43			0.73			1.03			1.33			1.63			1.93			2.23			2.53		
0.14			0.44			0.74			1.04			1.34			1.64			1.94			2.24			2.54		
0.15			0.45	1		0.75			1.05			1.35			1.65			1.95			2.25			2.55		
0.16			0.46	1		0.76			1.06			1.36			1.66			1.96			2.26			2.56		
0.17			0.47			0.77			1.07			1.37			1.67			1.97			2.27			2.57		
0.18			0.48	1		0.78			1.08			1.38			1.68			1.98			2.28			2.58		
0.19			0.49	3		0.79			1.09			1.39			1.69			1.99			2.29			2.59		
0.20			0.50	1		0.80			1.10			1.40			1.70			2.00			2.30			2.60		
0.21			0.51			0.81			1.11			1.41			1.71			2.01			2.31			2.61		
0.22			0.52	1		0.82			1.12			1.42			1.72			2.02			2.32			2.62		
0.23			0.53			0.83			1.13			1.43			1.73			2.03			2.33			2.63		
0.24			0.54	1		0.84			1.14			1.44			1.74			2.04			2.34			2.64		
0.25			0.55			0.85			1.15			1.45			1.75			2.05			2.35			2.65		
0.26			0.56			0.86			1.16			1.46			1.76			2.06			2.36			2.66		
0.27			0.57	1		0.87			1.17			1.47			1.77			2.07			2.37			2.67		
0.28			0.58			0.88			1.18			1.48			1.78			2.08			2.38			2.68		
0.29			0.59			0.89			1.19			1.49			1.79			2.09			2.39			2.69		
0.30			0.60		FGV	0.90			1.20			1.50			1.80			2.10			2.40			2.70		
0.31			0.61	1	↓	0.91			1.21			1.51			1.81			2.11			2.41			2.71		
0.32			0.62			0.92			1.22			1.52			1.82			2.12			2.42			2.72		
0.33			0.63			0.93			1.23			1.53			1.83			2.13			2.43			2.73		
0.34			0.64			0.94			1.24			1.54			1.84			2.14			2.44			2.74		
0.35	1	↑	0.65			0.95			1.25			1.55			1.85			2.15			2.45			2.75		
0.36		FGV	0.66			0.96			1.26			1.56			1.86			2.16			2.46			2.76		
0.37			0.67			0.97			1.27			1.57			1.87			2.17			2.47			2.77		
0.38			0.68			0.98			1.28			1.58			1.88			2.18			2.48			2.78		
0.39			0.69			0.99			1.29			1.59			1.89			2.19			2.49			2.79		

VITRINITE <0.1 %		INERTINITE <0.1 %						LIPTINITE <0.1 %								OIL DROPS	BITUMEN
TV	DV	Sfus	Scler	Fus	Macr	ID	Micr	Spor <0.1	Cut	Sub	Res <0.1	Ld <0.1	Bituminite	Telalginite	Lamalginite <0.1	Oil cut	

Sample Number..T7776.....Well Name...GEOTRACK, GC806-8 Cape Sorrell-1..... Depth...6330-6730 ft... ..... SampleType....Ctgs....
Date. ..25/.09/ 2001.. Op..ACC..... FGV - First Generation Vitrinite, RV - Reworked Vitrinite, BTT - Bituminite, B - Bitumen, Inert - Inertinite, Cav - Cavings, DA - Drilling Mud Additives MICR D:\RWORK.ms6\806VRW.doc

R	No Read	Pop Range	R	No Read	Pop Range	R	No Read	Pop Range	R	No Read	Pop Range	R	No Read	Pop Range	R	No Read	Pop Range	R	No Read	Pop Range	R	No Read	Pop Range	R	No Read	Pop Range
0.10			0.40			0.70			1.00			1.30			1.60			1.90			2.20			2.50		
0.11			0.41			0.71			1.01			1.31			1.61			1.91			2.21			2.51		
0.12			0.42			0.72			1.02			1.32			1.62			1.92			2.22			2.52		
0.13			0.43			0.73			1.03			1.33			1.63			1.93			2.23			2.53		
0.14			0.44			0.74			1.04			1.34			1.64			1.94			2.24			2.54		
0.15			0.45			0.75			1.05			1.35			1.65			1.95			2.25			2.55		
0.16			0.46			0.76			1.06			1.36			1.66			1.96			2.26			2.56		
0.17			0.47			0.77			1.07			1.37			1.67			1.97			2.27			2.57		
0.18			0.48			0.78			1.08			1.38			1.68			1.98			2.28			2.58		
0.19			0.49			0.79			1.09			1.39			1.69			1.99			2.29			2.59		
0.20			0.50			0.80			1.10			1.40			1.70			2.00			2.30			2.60		
0.21			0.51			0.81			1.11			1.41			1.71			2.01			2.31			2.61		
0.22			0.52			0.82			1.12			1.42			1.72			2.02			2.32			2.62		
0.23			0.53			0.83			1.13			1.43			1.73			2.03			2.33			2.63		
0.24			0.54			0.84			1.14			1.44			1.74			2.04			2.34			2.64		
0.25			0.55			0.85			1.15			1.45			1.75			2.05			2.35			2.65		
0.26			0.56			0.86	Samp	le	1.16	barren	of	1.46	organ	ic	1.76	matter		2.06			2.36			2.66		
0.27			0.57			0.87			1.17			1.47			1.77			2.07			2.37			2.67		
0.28			0.58			0.88			1.18			1.48			1.78			2.08			2.38			2.68		
0.29			0.59			0.89			1.19			1.49			1.79			2.09			2.39			2.69		
0.30			0.60			0.90			1.20			1.50			1.80			2.10			2.40			2.70		
0.31			0.61			0.91			1.21			1.51			1.81			2.11			2.41			2.71		
0.32			0.62			0.92			1.22			1.52			1.82			2.12			2.42			2.72		
0.33			0.63			0.93			1.23			1.53			1.83			2.13			2.43			2.73		
0.34			0.64			0.94			1.24			1.54			1.84			2.14			2.44			2.74		
0.35			0.65			0.95			1.25			1.55			1.85			2.15			2.45			2.75		
0.36			0.66			0.96			1.26			1.56			1.86			2.16			2.46			2.76		
0.37			0.67			0.97			1.27			1.57			1.87			2.17			2.47			2.77		
0.38			0.68			0.98			1.28			1.58			1.88			2.18			2.48			2.78		
0.39			0.69			0.99			1.29			1.59			1.89			2.19			2.49			2.79		

VITRINITE - %		INERTINITE - %						LIPTINITE - %								OIL DROPS	BITUMEN
TV	DV	Sfus	Scler	Fus	Macr	ID	Micr	Spor	Cut	Sub	Res	Ld	Bituminite	Telalginite	Lamalginite	Oil cut	

Sample Number..T7777.....Well Name...GEOTRACK, GC806-1 Cape Sorrell-1..... Depth...7210-7570 ft... ..... SampleType....Ctgs....
Date. ..25/.09/ 2001.. Op..ACC..... FGV - First Generation Vitrinite, RV - Reworked Vitrinite, BTT - Bituminite, B - Bitumen, Inert - Inertinite, Cav - Cavings, DA - Drilling Mud Additives MICR D:\RWORK.ms6\806VRW.doc

R	No Read	Pop Range	R	No Read	Pop Range	R	No Read	Pop Range	R	No Read	Pop Range	R	No Read	Pop Range	R	No Read	Pop Range	R	No Read	Pop Range	R	No Read	Pop Range	R	No Read	Pop Range
0.10			0.40			0.70			1.00			1.30			1.60			1.90			2.20			2.50		
0.11			0.41			0.71			1.01			1.31			1.61			1.91			2.21			2.51		
0.12			0.42			0.72			1.02			1.32			1.62			1.92			2.22			2.52		
0.13			0.43			0.73			1.03			1.33			1.63			1.93			2.23			2.53		
0.14			0.44			0.74			1.04			1.34			1.64			1.94			2.24			2.54		
0.15			0.45			0.75			1.05			1.35			1.65			1.95			2.25			2.55		
0.16			0.46			0.76			1.06			1.36			1.66			1.96			2.26			2.56		
0.17			0.47			0.77			1.07			1.37			1.67			1.97			2.27			2.57		
0.18			0.48			0.78			1.08			1.38			1.68			1.98			2.28			2.58		
0.19			0.49			0.79			1.09			1.39			1.69			1.99			2.29			2.59		
0.20			0.50			0.80			1.10			1.40			1.70			2.00			2.30			2.60		
0.21			0.51			0.81			1.11			1.41			1.71			2.01			2.31			2.61		
0.22			0.52			0.82			1.12			1.42			1.72			2.02			2.32			2.62		
0.23			0.53			0.83			1.13			1.43			1.73			2.03			2.33			2.63		
0.24			0.54			0.84			1.14			1.44			1.74			2.04			2.34			2.64		
0.25			0.55			0.85			1.15			1.45			1.75			2.05			2.35			2.65		
0.26			0.56			0.86	Samp	le	1.16	barren	of	1.46	organ	ic	1.76	matter		2.06			2.36			2.66		
0.27			0.57			0.87			1.17			1.47			1.77			2.07			2.37			2.67		
0.28			0.58			0.88			1.18			1.48			1.78			2.08			2.38			2.68		
0.29			0.59			0.89			1.19			1.49			1.79			2.09			2.39			2.69		
0.30			0.60			0.90			1.20			1.50			1.80			2.10			2.40			2.70		
0.31			0.61			0.91			1.21			1.51			1.81			2.11			2.41			2.71		
0.32			0.62			0.92			1.22			1.52			1.82			2.12			2.42			2.72		
0.33			0.63			0.93			1.23			1.53			1.83			2.13			2.43			2.73		
0.34			0.64			0.94			1.24			1.54			1.84			2.14			2.44			2.74		
0.35			0.65			0.95			1.25			1.55			1.85			2.15			2.45			2.75		
0.36			0.66			0.96			1.26			1.56			1.86			2.16			2.46			2.76		
0.37			0.67			0.97			1.27			1.57			1.87			2.17			2.47			2.77		
0.38			0.68			0.98			1.28			1.58			1.88			2.18			2.48			2.78		
0.39			0.69			0.99			1.29			1.59			1.89			2.19			2.49			2.79		

VITRINITE - %		INERTINITE - %						LIPTINITE - %								OIL DROPS	BITUMEN
TV	DV	Sfus	Scler	Fus	Macr	ID	Micr	Spor	Cut	Sub	Res	Ld	Bituminite	Telalginite	Lamalginite	Oil cut	

Sample Number..T7778.....Well Name...GEOTRACK, GC806-9 Cape Sorrell-1..... Depth...8650-9030 ft... ..... SampleType....Ctgs....
Date. ..25/.09/ 2001.. Op..ACC..... FGV - First Generation Vitrinite, RV - Reworked Vitrinite, BTT - Bituminite, B - Bitumen, Inert - Inertinite, Cav - Cavings, DA - Drilling Mud Additives MICR D:\RWORK.ms6\806VRW.doc

R	No Read	Pop Range	R	No Read	Pop Range	R	No Read	Pop Range	R	No Read	Pop Range	R	No Read	Pop Range	R	No Read	Pop Range	R	No Read	Pop Range	R	No Read	Pop Range	R	No Read	Pop Range
0.10			0.40			0.70			1.00			1.30			1.60			1.90			2.20			2.50		
0.11			0.41			0.71			1.01			1.31			1.61			1.91			2.21			2.51		
0.12			0.42			0.72			1.02			1.32			1.62			1.92			2.22			2.52		
0.13			0.43			0.73			1.03			1.33			1.63			1.93			2.23			2.53		
0.14			0.44			0.74			1.04			1.34			1.64			1.94			2.24			2.54		
0.15			0.45			0.75			1.05			1.35			1.65			1.95			2.25			2.55		
0.16			0.46			0.76			1.06			1.36			1.66			1.96			2.26			2.56		
0.17			0.47			0.77			1.07			1.37			1.67			1.97			2.27			2.57		
0.18			0.48			0.78			1.08			1.38			1.68			1.98			2.28			2.58		
0.19			0.49			0.79			1.09			1.39			1.69			1.99			2.29			2.59		
0.20			0.50			0.80			1.10			1.40			1.70			2.00			2.30			2.60		
0.21			0.51			0.81			1.11			1.41			1.71			2.01			2.31			2.61		
0.22			0.52			0.82			1.12			1.42			1.72			2.02			2.32			2.62		
0.23			0.53			0.83			1.13			1.43			1.73			2.03			2.33			2.63		
0.24			0.54			0.84			1.14			1.44			1.74			2.04			2.34			2.64		
0.25			0.55			0.85			1.15			1.45			1.75			2.05			2.35			2.65		
0.26			0.56			0.86	Samp	le	1.16	barren	of	1.46	organ	ic	1.76	matter		2.06			2.36			2.66		
0.27			0.57			0.87			1.17			1.47			1.77			2.07			2.37			2.67		
0.28			0.58			0.88			1.18			1.48			1.78			2.08			2.38			2.68		
0.29			0.59			0.89			1.19			1.49			1.79			2.09			2.39			2.69		
0.30			0.60			0.90			1.20			1.50			1.80			2.10			2.40			2.70		
0.31			0.61			0.91			1.21			1.51			1.81			2.11			2.41			2.71		
0.32			0.62			0.92			1.22			1.52			1.82			2.12			2.42			2.72		
0.33			0.63			0.93			1.23			1.53			1.83			2.13			2.43			2.73		
0.34			0.64			0.94			1.24			1.54			1.84			2.14			2.44			2.74		
0.35			0.65			0.95			1.25			1.55			1.85			2.15			2.45			2.75		
0.36			0.66			0.96			1.26			1.56			1.86			2.16			2.46			2.76		
0.37			0.67			0.97			1.27			1.57			1.87			2.17			2.47			2.77		
0.38			0.68			0.98			1.28			1.58			1.88			2.18			2.48			2.78		
0.39			0.69			0.99			1.29			1.59			1.89			2.19			2.49			2.79		

VITRINITE - %		INERTINITE - %						LIPTINITE - %								OIL DROPS	BITUMEN
TV	DV	Sfus	Scler	Fus	Macr	ID	Micr	Spor	Cut	Sub	Res	Ld	Bituminite	Telalginite	Lamalginite	Oil cut	

Sample Number..T7779.....Well Name...GEOTRACK, GC806-2 Cape Sorrell-1..... Depth...9510-9870 ft... ..... SampleType....Ctgs....
Date. ..25/.09/ 2001.. Op..ACC..... FGV - First Generation Vitrinite, RV - Reworked Vitrinite, BTT - Bituminite, B - Bitumen, Inert - Inertinite, Cav - Cavings, DA - Drilling Mud Additives MICR D:\RWORK.ms6\806VRW.doc

R	No Read	Pop Range	R	No Read	Pop Range	R	No Read	Pop Range	R	No Read	Pop Range	R	No Read	Pop Range	R	No Read	Pop Range	R	No Read	Pop Range	R	No Read	Pop Range	R	No Read	Pop Range
0.10			0.40			0.70			1.00			1.30			1.60			1.90			2.20			2.50		
0.11			0.41	1		0.71			1.01			1.31			1.61			1.91			2.21			2.51		
0.12			0.42	1		0.72			1.02			1.32			1.62			1.92			2.22			2.52		
0.13			0.43			0.73			1.03			1.33			1.63			1.93			2.23			2.53		
0.14			0.44			0.74			1.04			1.34			1.64			1.94			2.24			2.54		
0.15			0.45			0.75			1.05			1.35			1.65			1.95			2.25			2.55		
0.16			0.46	1		0.76			1.06			1.36			1.66			1.96			2.26			2.56		
0.17			0.47			0.77			1.07			1.37			1.67			1.97			2.27			2.57		
0.18			0.48			0.78			1.08			1.38			1.68			1.98			2.28			2.58		
0.19			0.49	1		0.79			1.09			1.39			1.69			1.99			2.29			2.59		
0.20			0.50	3		0.80			1.10			1.40			1.70			2.00			2.30			2.60		
0.21			0.51	2		0.81			1.11			1.41			1.71			2.01			2.31			2.61		
0.22			0.52	3		0.82			1.12			1.42			1.72			2.02			2.32			2.62		
0.23			0.53	1		0.83			1.13			1.43			1.73			2.03			2.33			2.63		
0.24			0.54	1		0.84			1.14			1.44			1.74			2.04			2.34			2.64		
0.25			0.55	1		0.85			1.15			1.45			1.75			2.05			2.35			2.65		
0.26			0.56	2		0.86			1.16			1.46			1.76			2.06			2.36			2.66		
0.27			0.57	1		0.87			1.17			1.47			1.77			2.07			2.37			2.67		
0.28			0.58	3		0.88			1.18			1.48			1.78			2.08			2.38			2.68		
0.29			0.59	1		0.89			1.19			1.49			1.79			2.09			2.39			2.69		
0.30			0.60	1		0.90			1.20			1.50			1.80			2.10			2.40			2.70		
0.31			0.61			0.91			1.21			1.51			1.81			2.11			2.41			2.71		
0.32			0.62	1		0.92			1.22			1.52			1.82			2.12			2.42			2.72		
0.33			0.63			0.93			1.23			1.53			1.83			2.13			2.43			2.73		
0.34			0.64	2		0.94			1.24			1.54			1.84			2.14			2.44			2.74		
0.35	1	↑	0.65	1		0.95			1.25			1.55			1.85			2.15			2.45			2.75		
0.36		FGV	0.66	1	FGV	0.96			1.26			1.56			1.86			2.16			2.46			2.76		
0.37			0.67	1	↓	0.97			1.27			1.57			1.87			2.17			2.47			2.77		
0.38			0.68			0.98			1.28			1.58			1.88			2.18			2.48			2.78		
0.39			0.69			0.99			1.29			1.59			1.89			2.19			2.49			2.79		

VITRINITE 4.1%		INERTINITE <0.1 %						LIPTINITE 0.7 %								OIL DROPS	BITUMEN
TV	DV	Sfus	Scler	Fus	Macr	ID	Micr	Spor 0.2	Cut 0.1	Sub 0.2	Res 0.1	Ld 0.1	Bituminite	Telalginite	Lamalginite	Oil cut	

Sample Number..T7780.....Well Name...GEOTRACK, GC806-10 Cape Sorrell-1..... Depth...10,310-10,660' ..... SampleType....Ctgs....
Date. ..25/.09/ 2001.. Op..ACC..... FGV - First Generation Vitrinite, RV - Reworked Vitrinite, BTT - Bituminite, B - Bitumen, Inert - Inertinite, Cav - Cavings, DA - Drilling Mud Additives MICR D:\RWORK.ms6\806VRW.doc

R	No Read	Pop Range	R	No Read	Pop Range	R	No Read	Pop Range	R	No Read	Pop Range	R	No Read	Pop Range	R	No Read	Pop Range	R	No Read	Pop Range	R	No Read	Pop Range	R	No Read	Pop Range
0.10			0.40			0.70			1.00			1.30			1.60			1.90			2.20			2.50		
0.11			0.41			0.71			1.01			1.31			1.61			1.91			2.21			2.51		
0.12			0.42			0.72			1.02			1.32			1.62			1.92			2.22			2.52		
0.13			0.43			0.73			1.03			1.33			1.63			1.93			2.23			2.53		
0.14			0.44			0.74			1.04			1.34			1.64			1.94			2.24			2.54		
0.15			0.45			0.75			1.05			1.35			1.65			1.95			2.25			2.55		
0.16			0.46			0.76			1.06			1.36			1.66			1.96			2.26			2.56		
0.17			0.47			0.77			1.07			1.37			1.67			1.97			2.27			2.57		
0.18			0.48			0.78			1.08			1.38			1.68			1.98			2.28			2.58		
0.19			0.49	2	↑	0.79			1.09			1.39			1.69			1.99			2.29			2.59		
0.20			0.50		FGV	0.80			1.10			1.40			1.70			2.00			2.30			2.60		
0.21			0.51	3		0.81			1.11			1.41			1.71			2.01			2.31			2.61		
0.22			0.52			0.82			1.12			1.42			1.72			2.02			2.32			2.62		
0.23			0.53			0.83			1.13			1.43			1.73			2.03			2.33			2.63		
0.24			0.54	3		0.84			1.14			1.44			1.74			2.04			2.34			2.64		
0.25			0.55	6		0.85			1.15			1.45			1.75			2.05			2.35			2.65		
0.26			0.56			0.86			1.16			1.46			1.76			2.06			2.36			2.66		
0.27			0.57			0.87			1.17			1.47			1.77			2.07			2.37			2.67		
0.28			0.58	5		0.88			1.18			1.48			1.78			2.08			2.38			2.68		
0.29			0.59	2		0.89			1.19			1.49			1.79			2.09			2.39			2.69		
0.30			0.60	3		0.90			1.20			1.50			1.80			2.10			2.40			2.70		
0.31			0.61	1		0.91			1.21			1.51			1.81			2.11			2.41			2.71		
0.32			0.62	1	FGV	0.92			1.22			1.52			1.82			2.12			2.42			2.72		
0.33			0.63	1	↓	0.93			1.23			1.53			1.83			2.13			2.43			2.73		
0.34			0.64			0.94			1.24			1.54			1.84			2.14			2.44			2.74		
0.35			0.65			0.95			1.25			1.55			1.85			2.15			2.45			2.75		
0.36			0.66			0.96			1.26			1.56			1.86			2.16			2.46			2.76		
0.37			0.67			0.97			1.27			1.57			1.87			2.17			2.47			2.77		
0.38			0.68			0.98			1.28			1.58			1.88			2.18			2.48			2.78		
0.39			0.69			0.99			1.29			1.59			1.89			2.19			2.49			2.79		

VITRINITE 10.5 %		INERTINITE 0.5 %						LIPTINITE 1.0 %								OIL DROPS	BITUMEN
TV	DV	Sfus	Scler	Fus	Macr	ID	Micr	Spor 0.2	Cut 0.3	Sub 0.3	Res 0.1	Ld 0.2	Bituminite	Telalginite	Lamalginite	Oil cut	

Sample Number..T7781.....Well Name...GEOTRACK, GC806-10.1 Cape Sorrell-1..... Depth...10,610-10,620' ..... SampleType....Ctgs....
Date. ..26/.09/ 2001.. Op..ACC..... FGV - First Generation Vitrinite, RV - Reworked Vitrinite, BTT - Bituminite, B - Bitumen, Inert - Inertinite, Cav - Cavings, DA - Drilling Mud Additives MICR D:\RWORK.ms6\806VRW.doc

R	No Read	Pop Range	R	No Read	Pop Range	R	No Read	Pop Range	R	No Read	Pop Range	R	No Read	Pop Range	R	No Read	Pop Range	R	No Read	Pop Range	R	No Read	Pop Range	R	No Read	Pop Range
0.10			0.40			0.70			1.00			1.30			1.60			1.90			2.20			2.50		
0.11			0.41			0.71	2		1.01			1.31			1.61			1.91			2.21			2.51		
0.12			0.42			0.72			1.02			1.32			1.62			1.92			2.22			2.52		
0.13			0.43			0.73		FGV	1.03			1.33			1.63			1.93			2.23			2.53		
0.14			0.44			0.74	1	↓	1.04			1.34			1.64			1.94			2.24			2.54		
0.15			0.45			0.75			1.05			1.35			1.65			1.95			2.25			2.55		
0.16			0.46			0.76			1.06			1.36			1.66			1.96			2.26			2.56		
0.17			0.47			0.77			1.07			1.37			1.67			1.97			2.27			2.57		
0.18			0.48			0.78			1.08			1.38			1.68			1.98			2.28			2.58		
0.19			0.49	2	↑	0.79			1.09			1.39			1.69			1.99			2.29			2.59		
0.20			0.50		FGV	0.80			1.10			1.40			1.70			2.00			2.30			2.60		
0.21			0.51			0.81			1.11			1.41			1.71			2.01			2.31			2.61		
0.22			0.52	1		0.82			1.12			1.42			1.72			2.02			2.32			2.62		
0.23			0.53	1		0.83			1.13			1.43			1.73			2.03			2.33			2.63		
0.24			0.54	1		0.84			1.14			1.44			1.74			2.04			2.34			2.64		
0.25			0.55	1		0.85			1.15			1.45			1.75			2.05			2.35			2.65		
0.26			0.56			0.86			1.16			1.46			1.76			2.06			2.36			2.66		
0.27			0.57	2		0.87			1.17			1.47			1.77			2.07			2.37			2.67		
0.28			0.58	2		0.88			1.18			1.48			1.78			2.08			2.38			2.68		
0.29			0.59	1		0.89			1.19			1.49			1.79			2.09			2.39			2.69		
0.30			0.60	3		0.90			1.20			1.50			1.80			2.10			2.40			2.70		
0.31			0.61	1		0.91			1.21			1.51			1.81			2.11			2.41			2.71		
0.32			0.62	2		0.92			1.22			1.52			1.82			2.12			2.42			2.72		
0.33			0.63	2		0.93			1.23			1.53			1.83			2.13			2.43			2.73		
0.34			0.64	1		0.94			1.24			1.54			1.84			2.14			2.44			2.74		
0.35			0.65	3		0.95			1.25			1.55			1.85			2.15			2.45			2.75		
0.36			0.66			0.96			1.26			1.56			1.86			2.16			2.46			2.76		
0.37			0.67			0.97			1.27			1.57			1.87			2.17			2.47			2.77		
0.38			0.68			0.98			1.28			1.58			1.88			2.18			2.48			2.78		
0.39			0.69			0.99			1.29			1.59			1.89			2.19			2.49			2.79		

VITRINITE 1.2 %		INERTINITE 0.1 %						LIPTINITE 0.5 %								OIL DROPS <0.1	BITUMEN
TV	DV	Sfus	Scler	Fus	Macr	ID	Micr	Spor 0.1	Cut 0.1	Sub 0.2	Res	Ld <0.1	Bituminite	Telalginite	Lamalginite	Oil cut	

Sample Number..T7782.....Well Name...GEOTRACK, GC806-3 Cape Sorrell-1..... Depth...11,150-11,485' ..... SampleType....Ctgs....
Date. ..26/.09/ 2001.. Op..ACC..... FGV - First Generation Vitrinite, RV - Reworked Vitrinite, BTT - Bituminite, B - Bitumen, Inert - Inertinite, Cav - Cavings, DA - Drilling Mud Additives MICR D:\RWORK.ms6\806VRW.doc